TAMPERE UNIVERSITY OF TECHNOLOGY

DIEGO TORRES LOBERA

MEASURING ACTUAL OPERATING CONDITIONS OF A PHOTOVOLTAIC POWER GENERATOR

Master of Science Thesis

Examiner: Professor Seppo Valkealahti
Examinor and topic approved in the
Computing and Electrical Engineering
Faculty Council meeting on 03 March 2010

ABSTRACT

TAMPERE UNIVERSITY OF TECHNOLOGY
Master's Degree Programme in Electrical Engineering
Diego Torres Lobera: Measuring actual operating conditions of a photovoltaic power generator
Master of Science Thesis, 81 pages, 27 Appendix pages
November 2010
Major: Electrical Energy
Examiner: Professor Seppo Valkealahti
Keywords: Photovoltaic, power generation, measurement system, climatic measurements, operating measurements, performance of PV modules.

Photovoltaic (PV) modules are composed by PV cells, normally connected in series, which convert the energy of solar radiation (direct and diffuse) into electrical energy. However, many factors affect the output power of photovoltaic devices that are operating such as module temperature, incident irradiance and spectral irradiance distribution. Subsequently, the climatic parameters involved on the module temperature, such as ambient temperature, relative humidity and wind speed and direction, must be studied too.

In this thesis a state-of-the-art climatic measurement facility is designed and built to measure the climatic and operating conditions of the TUT solar PV power test plant. This climatic measurement system contains an accurate weather station that also includes solar radiation measurements in parallel to a comprehensive mesh of irradiance and module temperature measurements all around the solar facility. First the climatic instruments and possible data-acquisition architectures are introduced in order to understand the measuring methods and the different possible solutions for the system. A market study is needed as well to gather the most suitable devices for the system.

In this thesis also a thermal model of the modules is developed using Matlab™ Simulink software to analyze the influence of the environmental parameters on the operating conditions and the performance of the PV modules and strings. Simulations show a clear dependence of the module temperature on the ambient temperature, wind speed and irradiance conditions. Regarding the generated power and string efficiency, increasing ambient temperature and wind speed causes a negative and positive influence, respectively.

Measurements of module temperature and irradiance show the appearance of a delay between the curves caused by the thermal inertia of the modules. This phenomenon was not considered in the model, which is meant to predict the module temperature in a stationary state. Small error appears between the measured module temperature and the simulated one as well as with the string performance results. However, the results confirm the right performance of the thermal model and measuring system.

PREFACE

This Master of Science Thesis has been developed in the Deparment of Electric Energy Engineering of the Tampere University of Technology (TUT). The supervisors and examiners of the thesis have been Prof. Seppo Valkealahti and Dr. Tommi Keikko.

First of all, I would like to thank Prof. Seppo Valkealahti for providing me this interesting topic and for his guidance and ideas. I also want to thank Dr. Tommi Keikko and Ansi Mäkki for their help because it wouldn't have been possible to make it without them. Great thanks also to all my colleagues of the Department, they have made me feel like at home despite the language and cultural differences.

I would like to thank all the great friends I met in Tampere for supporting and cheering me up during these 13 months and, specially, in the hard times: my roomtmates from Lukonmäki and Mikontalo, Imanol, Modesto, Tuukka, Adèle, Quique, Juha, Jenni, Marcos, Freddy, Pepa, Riccardo, Elina, Fernando, Debbie, Javi, Elena, Lucía, Jan, Ana, Luis, Ugur, the whole Roxbury Team, etc; it is impossible to name all of them because many pages would be needed.

My last gratitude goes to my parents and my brother, to whom I am very grateful for the sacrifice they have made in allowing me to study abroad and for supporting and encouraging me in every decision.

Gracias, thank you, kiitos!

Tampere, November 2010

Diego Torres Lobera
dtorreslobera@gmail.com

CONTENTS

ABBREVIATIONS AND NOTATION

Notation

A	Diode ideality factor
A_{bypass}	Bypass diode ideality factor
B	Temperature independent constant of saturation current
c	Speed of light
E	Energy of a photon
E_G	Energy gap
E_{G0}	The linearly extrapolated zero temperature band gap of the semiconductor
G	Irradiance
G_0	Reference irradiance
h	Planck's constant
Id	Diode current
Io	Saturation current of the diode in one-diode model of photovoltaic cell
$Io1$	Saturation current of the diode 1 in a photovoltaic cell model
I_{PV}	Photocurrent
$I_{PV,STC}$	Photocurrent in standard test conditions
I_{SC}	Short-circuit current
$I_{SC,REF}$	Short-circuit current in a reference temperature
$I_{SC,STC}$	Short-circuit current in standard test conditions
k	Boltzmann constant
K_I	Temperature coefficient of short-circuit current
K_U	Temperature coefficient of open-circuit voltage
K_T	Temperature-rise coefficient of photovoltaic module
n	Number of bypass diodes in series connection of photovoltaic modules
N_s	Number of series connected photovoltaic cells in a photovoltaic module
P_M, P_{max}	Maximum power
R_S	Series resistance
R_{SH}	Shunt resistance
T	Temperature
T_{AMB}	Ambient temperature
T_{bypass}	Bypass diode temperature
T_{MOD}	Module temperature

T_0, T_{REF}	Reference temperature
T_{STC}	Temperature in standard test conditions
q	Elementary charge
V_{bypass}	Voltage of bypass diode
V	Voltage
V_{OC}	Open-circuit voltage
$V_{OC,STC}$	Open-circuit voltage in standard test conditions
V_T	Thermal voltage in photovoltaic module
$V_{T,bypass}$	Thermal voltage in bypass diode
γ	Temperature dependence of parameters of the dark saturation current
λ	Wavelength of a photon

Abbreviations

AC	Alternating current
AM	Air mass
AM1.5	Air mass 1.5
AWS	Automatic weather station
CPU	Central processing unit
DAQ	Data acquisition system
DC	Direct current
FF	Fill factor
MPP	Maximum power point
NOC	Normal operating conditions
NOCT	Normal operating conditions temperature
PV	Photovoltaic
RTD	Electrical resistance thermometer
Si	Silicon
STC	Standard test conditions
TUT	Tampere University of Technology
VB	Valence band
WMO	World Meteorological Organization
WS	Weather station

1. INTRODUCTION

Mankind has always needed energy sources and several times it has been provided by the Sun. Coal, oil and gas, that are widely used as energy sources, come from production plants that needed the Sun to carry out their function. Especially in these days, when the whole World is concerned by the exhaustion of the non-renewable energy sources besides to the pollution generated by the use of them, the scientific and technological community is focussed on finding renewable energy sources to replace the oil with atomic energy, wind generation and solar energy.

Using solar energy presents several advantages in comparison to other energy sources. The Sun is a practically inexhaustible source of light and heat and it is relatively easy to use it. Solar technology is a wide field and its development is still growing. It is possible to produce power electricity from solar energy and some materials present a suitable behaviour to provide the power needs of small facilities with relatively small solar stations. It is possible, as well, to build solar energy collectors to produce steam that makes power generators to work.

The photovoltaic (PV) effect was discovered by Alexandre-Edmond Becquerel in 19th century but PV systems are still producing very small portion of the electrical energy. [22] Photovoltaic cells transform the energy from any global, direct and diffuse solar radiation into electrical energy and, normally, they are connected in series or parallel as PV modules. Photovoltaic generators are not economically competitive for large scale applications yet. Thus, just during the last years, and thank to financial support, several facilities have been built. It is important, therefore, to make PV systems more efficient. [20]

Department of Electrical Energy Engineering of Tampere University of Technology has designed and built a PV power station test plant composed by 69 solar NP195GKg photovoltaic modules [29] on the rooftop of the department. This plant is meant to be a grid connected system with research purposes and to study the effects of environmental parameters in the performance of the generator or to test and evaluate different power electronic components or systems

The output power of photovoltaic devices operating outdoors under real working conditions is influenced by many factors, such as module temperature, incident irradiance and spectral irradiance distribution. [28] The operating temperature of the solar module plays a central role in the photovoltaic process. Hence, the electrical efficiency and the power output of a PV module depend on the operating temperature, decreasing with it. [34] Subsequently, the climatic parameters involved on the module temperature as well as the operating conditions must be studied.

In order to analyze the influence of the environmental parameters on the operating conditions and the performance of the modules and strings, a thermal model of the modules has been made using Matlab™ Simulink software. Several simulations have been run varying the different involved climatic parameters. This model has been integrated to an already developed model of the generator to complete it. In this way, simulations studying the string performances have been run as well. However, in order to test the influence of these climatic and operating parameters on the real generator, a measuring system has been designed and built. This system contains a state-of-the-art climatic measurement system in parallel with a comprehensive mesh of radiation and temperature measurements around the power station test plant. The climatic measurement system consists in an accurate automatic weather station that provides ambient temperature, relative humidity, wind speed and direction and global and diffuse solar radiation measurements. On the other hand, the operating conditions of each string of the plant are obtained by the mesh of irradiance and module temperature measurements.

To design the measuring systems, several specific literatures have been studied such as the Guide to Meteorological Instruments and Methods of Observation [42], among others. In this guide, the accuracy level of the used instruments is well established as well as the measuring methods. Also many operating facilities have been studied and a deeply extensive market study is basis to find the most suitable instruments for the system. Regarding the data-acquisition system, different architectures that may suit for the system have been considered and analyzed.

This thesis is organized as follows: first the characteristics of photovoltaic systems and the semiconductor physics behind the operation of the PV cell are introduced to understand how the PV cells convert energy of the solar radiation into electrical energy. After that, climatic measurement systems are introduced in Chapter 3, especially focussing on automatic weather stations. The climatic parameters involved in the module operating temperature are described and the techniques to measure them are presented. At last, different possible data-acquisition architectures are discussed. In Chapter 4, a study of the effects of those climatic conditions on the operating module temperature and the PV generator performance characteristics is carried out. A simulation model of the PV generator with a Simulink thermal model of the PV modules is exploited to realize a set of simulations meant to analyze those effects. After that, Chapter 5 describes in detail the designing process of the TUT climatic measurement system and presents the final design of it. In Chapter 6, the obtained results after testing the photovoltaic modules and sensors are presented. Several measurements and simulations have been carried out and the results of them are compared and discussed. Finally, in Chapter 7, the conclusions of the thesis are presented.

This thesis also contains 3 appendixes which are meant to present in detail the market study carried out, the TUT solar PV power test plant and the ordering bills of the sensors and data-acquisition systems.

2. PHOTOVOLTAIC POWER SYSTEMS

2.1. Introduction

A photovoltaic (PV) system is a system which converts light into electricity by mean of PV cells. In this chapter this type of systems and their components are described, as well as some typical configurations.

In Section 2, photovoltaic systems are described giving an overview about the modular nature of PV generators and the different PV systems. Later on, the text focuses on the main energy source of PV systems: the photovoltaic cell. Its physical properties are studied and, also, its construction and electrical characteristics. Finally, the different module and array configurations are proposed and discussed.

Section 3 describes the grid-connected PV systems, focussing on the different possible configurations of a photovoltaic generator and the advantages and problems that they present.

Finally, in Section 4, the influence of temperature and irradiance over the PV cell and module behaviour is studied. Also a brief description on the effects of varying these operating parameters on the system performance is carried out in this chapter.

2.2. Photovoltaic systems

The modular nature of photovoltaic generators allows us to accomplish specific goals ranging from powering small devices up to systems of kilowatts power to feed electricity into the main distribution grid or generating megawatts power in large central photovoltaic stations.

An overview on the PV systems allows classifying them as stand-alone and grid connected systems [25] as depicted in Figure 2.1. The main difference between both systems is that in the stand-alone system the generated energy is matched with the load while the grid-connected system is connected with the existent electrical utility grid.

Since PV modules produce power only when illuminated, PV systems often make use of energy storage mechanisms such as batteries. In this manner, the energy yielded by the modules may be made available at a later time. On the other hand, using storage batteries provides other advantages as system voltage regulation or a source of current that can exceed the PV configuration capacities.

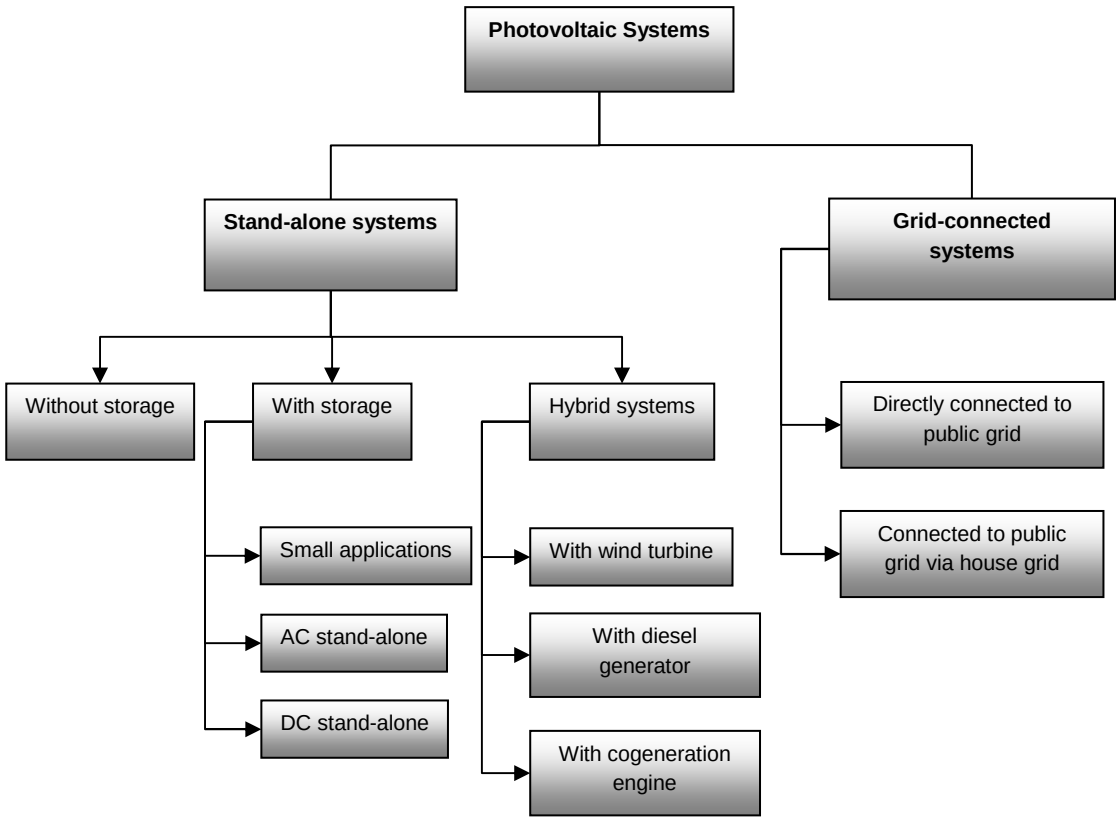

Figure 2.1. *Classification of PV systems. [8]*

When using battery storage it is common to employ a charge controller, thus it can prevent reaching possible battery levels of overcharged or over discharged. An inverter may also be needed in case of serving alternating current (AC) loads. The functions of an inverter will be converting direct current (DC) power from the solar modules into AC.

Another possible configuration for the photovoltaic system is to be connected to a utility grid. Such systems may operate bidirectional delivering excess PV energy to the grid or using it as a backup system when lacking PV generation. Figure 2.2 shows the components of several types of photovoltaic systems. [25]

It is possible to affirm that the basic structure of PV systems consists of arrays of photovoltaic modules, energy storage batteries, backup generators, battery charge controllers and inverters. Obviously, it is possible to vary certain components and designs depending on each particular system.

In the following subsections some of these PV system components are described and studied. Since this Master Thesis is focussed on the TUT PV Power Generation Plant, just the expected components of this particular system are studied. Specifically the next subsections describe the PV modules and the inverters, specially focussing on the PV cell.

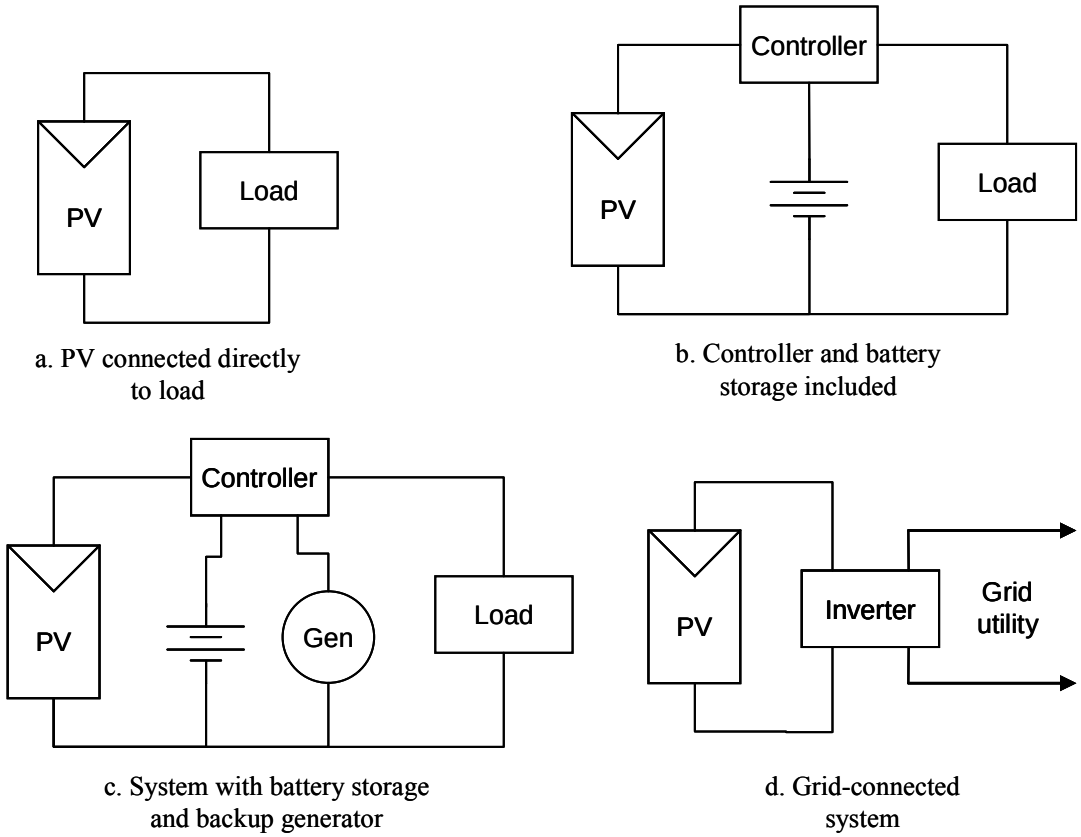

Figure 2.2. *Examples of PV systems. [25]*

2.2.1. Photovoltaic cell

The solar module is the main energy source of any photovoltaic system. However, the PV module results from the combination of solar cells connected in series and parallel, plus additional protections. Therefore, before studying the solar module, the photovoltaic cell has to be studied as the true nucleus of light conversion into electrical current. [13]

A photovoltaic cell is a device that generates electric power when illuminated by sunlight or artificial light by means of the photoelectric effect. [4] The PV effect was first observed in a solid material, in the selenium metal, in 1877. This material was used for many years for light meters, which need a very small quantity of energy. The silicon-PV cells currently available offer an energy conversion efficiency ratio near to 18% of the light that illuminate them. Nowadays the main studies referring to this field are focussed on the development of new photovoltaic cells based on other semiconductor materials such as titanium dioxide. Its efficiency is around 7%, that is approximately a third part of the efficiency of current silicon cells, but the production process of the titanium dioxide cells is easier and much more inexpensive.

Modern solar cells base their operation in the properties of semiconductor materials. These materials present different energy bands for electrons. The last ones with smallest binding energy define the electronic properties of a crystal. The last two bands, which can be totally or partially occupied by electrons, are called conduction and valence

bands as seen in Figure 2.3. There is an energy gap between them, E_g, which is the energy needed by an electron to be able to jump from the valence to the conduction band.

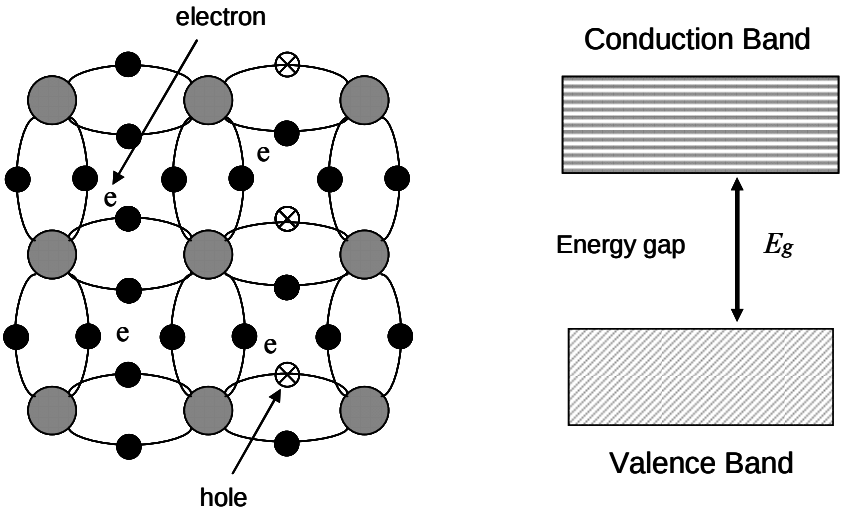

Figure 2.3. *Silicon crystal structure and energy band levels.*

There are two types of semiconductor materials: n-type and p-type. The former have extra electrons in the conduction band, while the latter have extra holes in the valence band. Photovoltaic cells contain a pn-junction in the way that the absorption of photons that have greater energy than the band gap energy of the semiconductor drives electrons from the valence to the conduction band. This is known as creating hole-electron pairs. [4] The flowing of holes and electrons in opposite directions across the junction generates DC power.

The basic cell construction is shown in Figure 2.4. The metallic contacts are provided on both sides of the junction to collect electrical current induced by the photons received on one side. The most common material used in PV cells is mono-crystalline or poly-crystalline silicon.

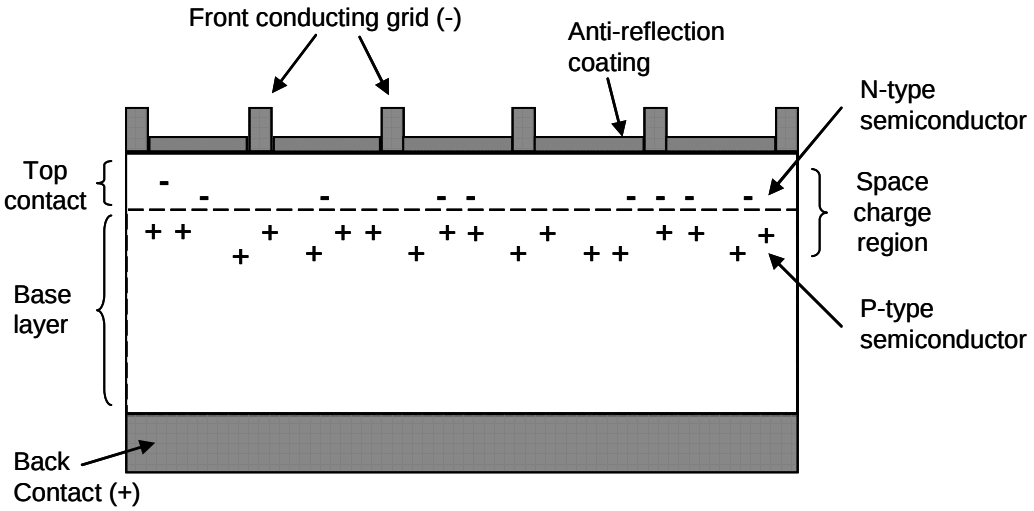

Figure 2.4. *Structure of a PV cell. [8]*

A solar cell generates electron-hole pairs when exposed to sunlight. These electrons travel through the circuit. Associated to this process there is a process of recombination. Every time that the electrons reach the p-type semiconductor, they recombine with holes which were created during the formation of electron-hole pairs.

To explain the operation of a solar cell, a connected circuit with a resistance R is shown in Figure 2.5. If admitted that a current, I, is flowing through the exterior resistive circuit, this current will cause a voltage drop in the resistance. That means that the solar cell is operating at a current I and voltage V. This voltage affects to the recombination process, since this process depends on V exponentially. Hence if the load is too high also the tension will be high and the voltage will rise. Consequently, the recombination process will take place before the electrons can reach the exterior circuit and will avoid the current flowing.

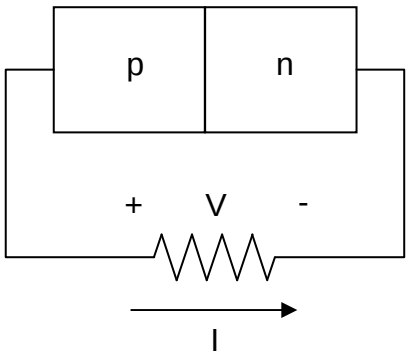

Figure 2.5. *Operation scheme of a photovoltaic cell.*

The electrical characteristic of a PV cell in sunlight and in the useful operation range is represented by the I-V curve. Another typical curve used to study the working performance of a solar cell is the power-voltage (P-V) curve. The I-V characteristics of a PV cell is

$$I = I_{SC} - I_O\left(e^{\frac{qV}{AkT}} - 1\right), \tag{2.1}$$

where I is the current at the PV cell, I_{sc} is the short circuit current, V is the voltage of the PV cell, I_o is the saturation current of the diode, k is the Boltzmann constant, q is the elementary charge, T is the temperature of the cell and A is the ideality factor of the diode. Figure 2.6 illustrates the equivalent circuit of the diode model of a photovoltaic cell.

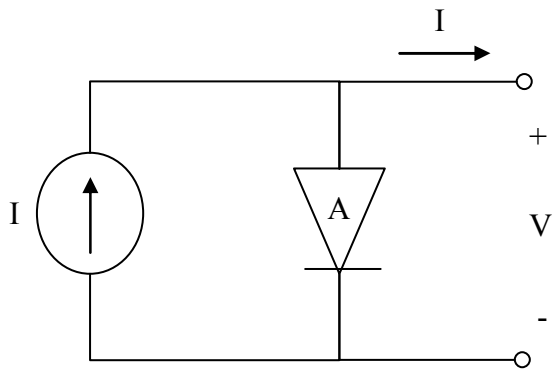

Figure 2.6. *Equivalent circuit diagram of the diode model of photovoltaic cell. [19]*

The open-circuit voltage can be written as

$$V_{OC} = \frac{AkT}{q} \ln\left(\frac{I_{SC} + I_o}{I_o}\right), \tag{2.2}$$

Hence, the three most important parameters widely used for describing the electrical performance of a cell are the short circuit current, I_{SC}; the open circuit voltage, V_{OC}; and the maximum power, P_{MAX}. The former, is measured by shorting the output terminals, and measuring the terminal current under full illumination. The current under this condition is the maximum current the cell can deliver. The maximum voltage produced by the solar cell is produced under the open circuit voltage. P_{MAX} is just the maximum value of the product of the voltage and the current outputs at various load conditions. At uniform illumination conditions P_{MAX} takes place at voltages around 80% of the V_{OC}.

Last but not least, there is one important parameter which must be mentioned, the fill factor *FF*. It describes the quality and function of the PV cell. It is the ratio of maximum power to the product of the I_{SC} and V_{OC} and is written as

$$FF = \frac{P_{MAX}}{I_{SC} V_{OC}}. \tag{2.3}$$

PV cells have also parasitic elements: series resistance R_S and shunt resistance R_{SH}. The former is due to the bulk resistance of the semiconductor, metallic contacts, etc. The latter is due to the non-idealities near the pn-junction. Thus, the I-V characteristics change to

$$I = \frac{R_{SH}\left\{I_{PV} - I_O\left[\exp\left(\frac{q(V + IR_S)}{AkT}\right) - 1\right]\right\} - V}{R_S + R_{SH}}, \tag{2.4}$$

where I_{PV} is the photocurrent of the cell. Figure 2.7 illustrates the equivalent circuit of the PV cell including the parasitic resistances.

Parasitic resistances affect the performance of the PV cell and indicate the cell quality. Higher shunt resistance and smaller series resistance indicate a better photovoltaic cell. [20]

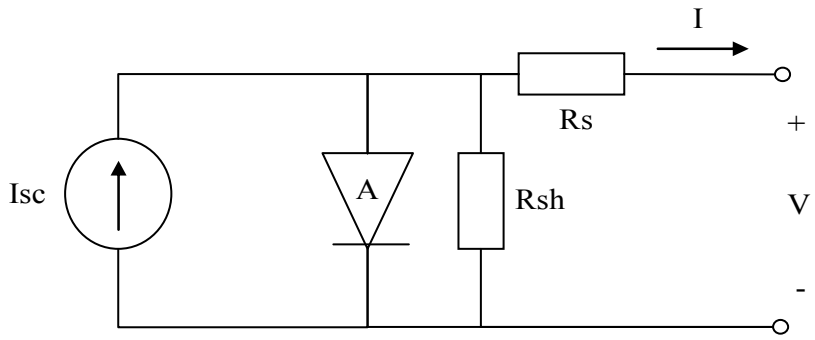

Figure 2.7. *Equivalent circuit diagram of the diode model of photovoltaic cell with parasitic elements. [19]*

2.2.2. Photovoltaic modules

A typical photovoltaic cell produces less than 3 W at 0.5 V DC. For the majority of applications, multiple PV cells need to be connected in series-parallel configurations to produce the suitable voltage and power. PV modules result after this solar cells connection. Within a module the different cells are typically mounted on a base substrate and connected into a series string of 36 or 72 cells to achieve the desired output voltage.

Figure 2.8 shows a typical layout of how 36 cells are connected in series into a module. In this type of connection the same current flows through all the cells but the voltage generated by the module is the sum of the individual cell voltages. When cells are connected in parallel the voltage at the module terminals will be equal to that of a single cell, while the output current results the sum of the individual cell currents.

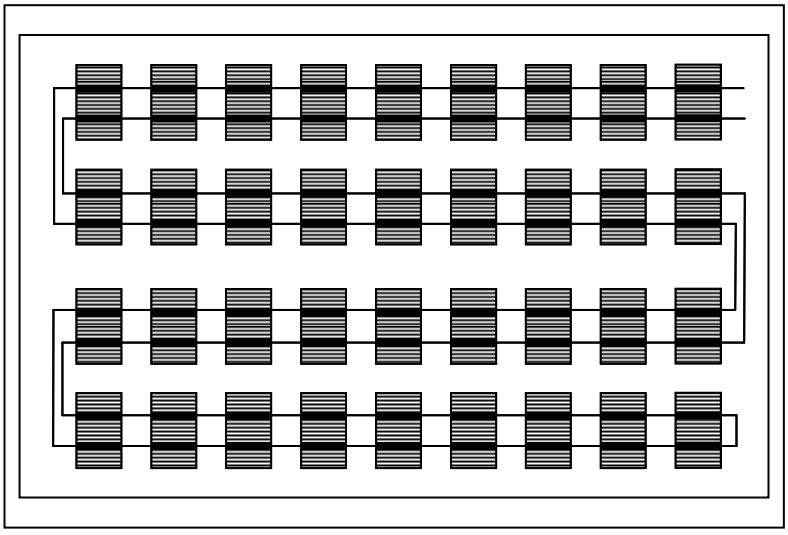

Figure 2.8. *Structure of a PV module with 36 cells connected in series. [8]*

Cells are connected in series in order to achieve the adequate module output voltage. However, an important observation relating to this connection type refers to shading of individual PV cells. If any cell operates shaded, the performance of this cell will be

degraded. It is possible that the shaded cell may become reverse biased if other non-shaded modules are connected in series. The cell acts as a load, which will produce cell heating and a cell failure. To protect the system against this type of fail, the solar modules are protected with bypass diodes, as shown in Figure 2.9. If a PV current cannot flow through one or various cells in the solar module, it will do it through the diode instead. [25]

Finally, it is important to consider that the module efficiency is established by the weakest link. Since the solar cells are connected in series, it is important that they have closest possible connections to each other. In other case, there will be cells operating at peak power and others will not. As a result, the module power will be lower than the theoretical power given by multiplying the power of each cell by the number of cells.

The maximum current in the module is affected by the cell with least current under specific load conditions at the operating irradiance level. If 30 or more series-connected cells don't perform with the same I-V curve, when the module is short-circuit, some cells will generate power while others will dissipate it. If all cells match perfectly, no power will be dissipated and the module efficiency will be equivalent to the cell efficiency. [25]

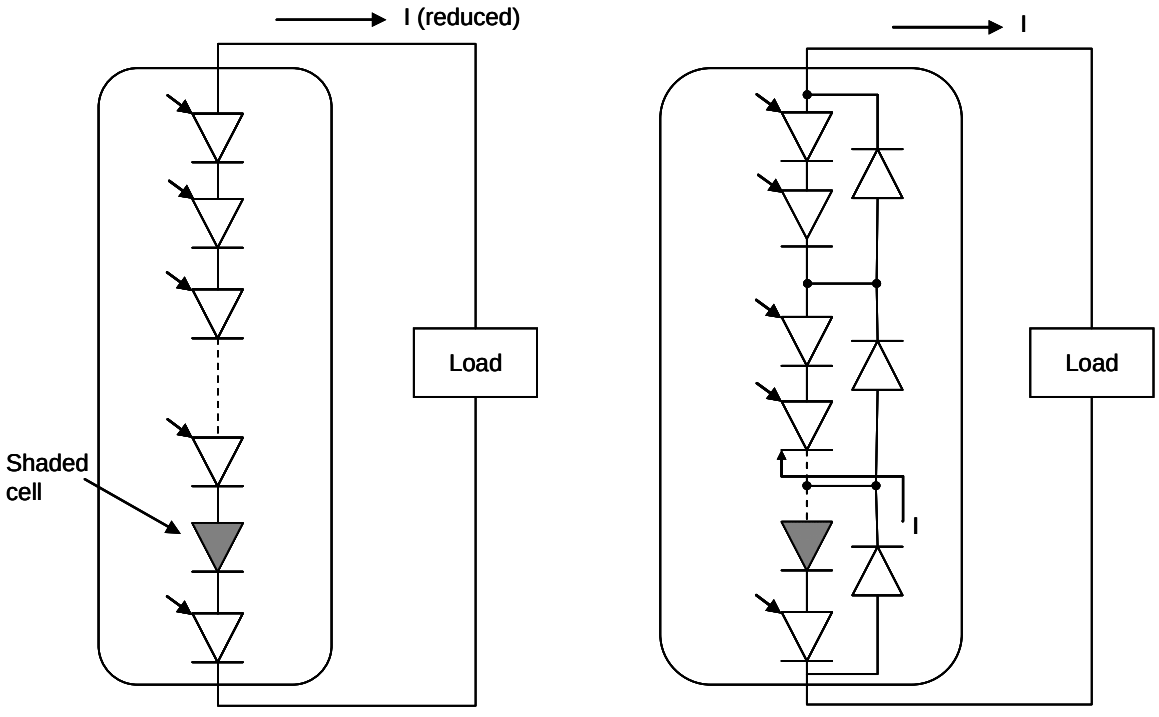

(a) Module without Bypass Diodes (b) Module with Bypass Diodes

Figure 2.9. *Protection of shaded PV cells with bypass diodes. [25]*

2.2.3. Photovoltaic array

A photovoltaic array is a structure that consists of a number of PV modules, mounted on the same plane with proper electrical connections to provide enough electrical power for a specific application. The same as for PV cells, when connecting modules in series, higher voltages are reached. When modules are connected in parallel, higher currents are obtained. When modules are connected in series, it is desirable that the modules operate at the maximum power and same current. While for parallel connections, it is desirable to have a system with the modules working at the maximum power and same voltage.

Figure 2.10 shows two typical array configurations. In Figure 2.10a, modules are connected in series-parallel configuration with series-connected fuses in each series string. In Figure 2.10b, the modules are connected to produce positive and negative voltages with respect to ground. [25]

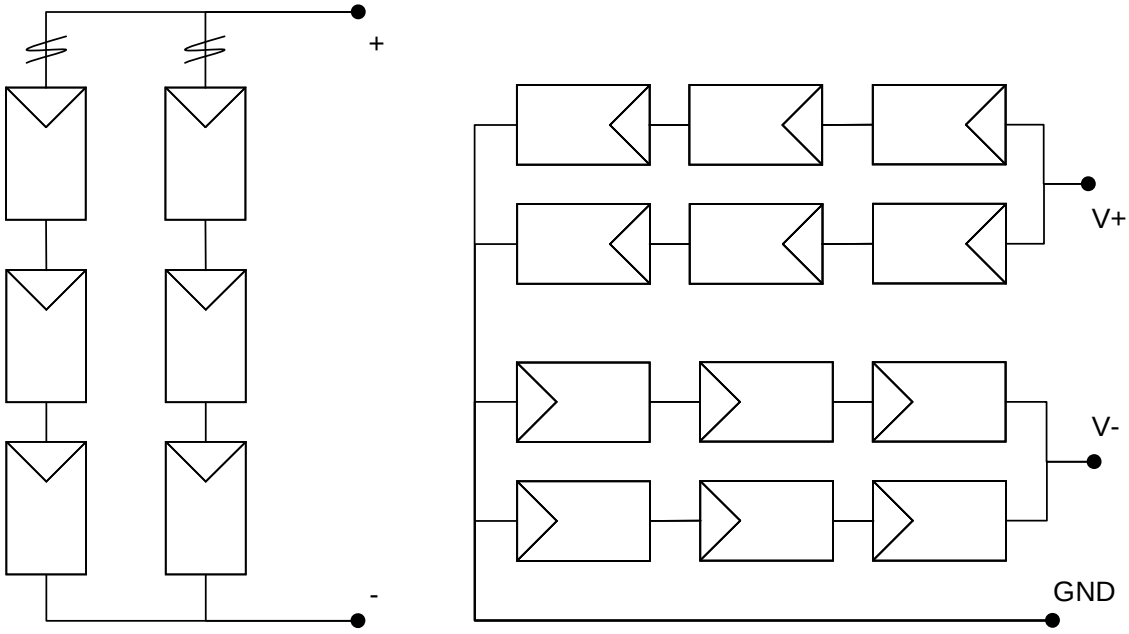

(a) Series-Parallel with internal bypass diodes and series fuses

(b) Series-Parallel with centre grounded to provide + and – supplies (fuses and diodes not shown)

Figure 2.10. *Examples of PV arrays. [25]*

2.2.4. DC/AC inverter

Inverters are power electronic devices which convert direct current into alternating current, which may be single or multi-phase. These devices are used in various photovoltaic system configurations as grid-connected systems, stand-alone systems with rechargeable batteries and pumping systems without storage batteries. In the former and last configurations, the inverter performs as interface between the photovoltaic

generator and the utility grid or pumping systems. For the stand-alone systems, the inverter operates as the grid administrator and feeds the loads. [13]

Depending on the requirements of the load, a number of different types of inverters are available. Selecting the proper inverter for each system depends on the waveform requirements of the load and on the efficiency of the inverter. It will also depend on the type of system where the inverter will operate. As commented, inverters for stand-alone systems have different requirements than for grid-connected systems. [25]

2.3. Grid-connected photovoltaic systems

As told before, grid-connected photovoltaic systems can be meant from relatively small units, for distributed power generation by systems installed on roofs; to big centralized power generation plants. Several configurations can be used to build the PV generator, as well as several technologies are available to connect this generator to the utility grid. Depending on the modularity of the system, centralized inverter, string inverter, AC module or multi-string inverter technologies will be chosen. As known, the interface equipments to connect the PV generator to the utility grid are converters and inverters. [20]

Centralized inverter technology, illustrated in Figure 2.11a, interfaces a large number of PV modules to the grid. Modules are connected in series connections assembling strings to achieve high voltages and avoid amplification. In order to reach high power, several photovoltaic strings can be connected in parallel through protection diodes. Even though this technology has the advantage that high voltage inverters have low price per power ratio, it has also some disadvantages: power losses due to centralized maximum power point tracking (*MPPT*), extra power losses in the string diodes and a very nonflexible design. [17]

While centralized inverters are rather the past technology, string inverters and ac modules are the presently used technology. String inverters just interface an individual string to the grid. Hence it is possible to improve the MPPT efficiency through a better string control. On the other hand, since no string diode is needed to connect several strings in parallel the system results to be more efficient by reducing power losses. [17] Finally, flexibility is also increased since it is possible to add strings one at a time. A string inverter configuration is shown in Figure 2.11b.

The AC module is the integration of the inverter and the PV module in the same device as shown in Figure 2.11d. This is the most modular solution available to build a photovoltaic system. Since there is just one PV module there are no mismatching losses. Thus, there is an optimal adjustment between the inverter and the module. [17]

Multi-string inverter technology, depicted in Figure 2.11c, is the further development of the string inverter. This technology is the combination of centralized and string inverter technologies. In this way, the advantages of both technologies are achieved. On one hand, the system is modular since it is possible to add strings afterwards and, to have an individual MPPT for every PV string; a high efficiency

system is achieved. On the other hand, this technology makes use of a large inverter where all the strings are connected. This leads to a low price per power ratio inverter.

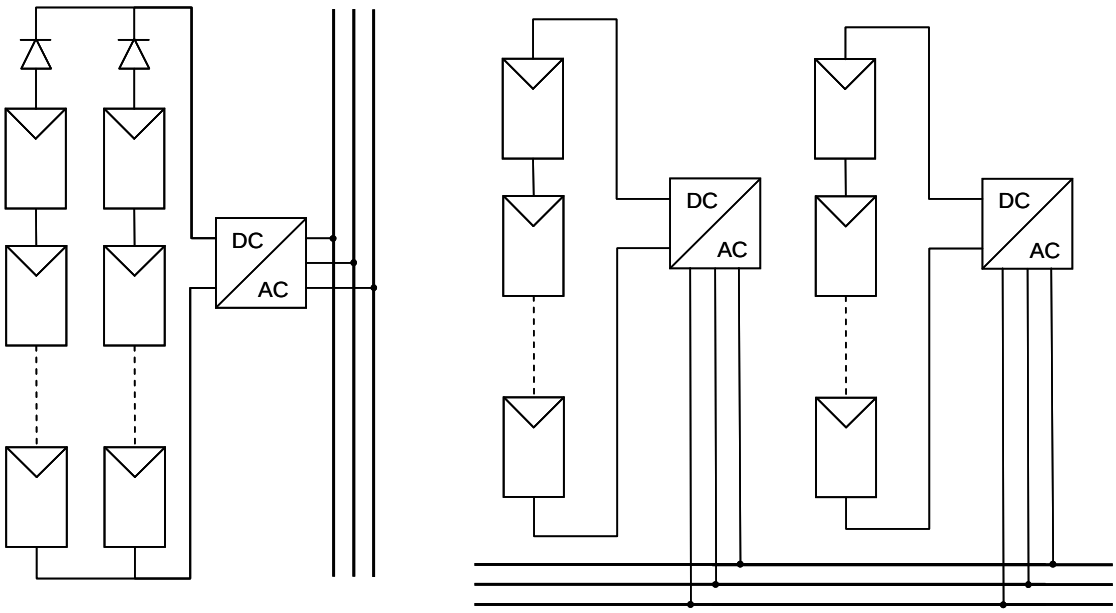

(a) Centralized technology (b) String technology

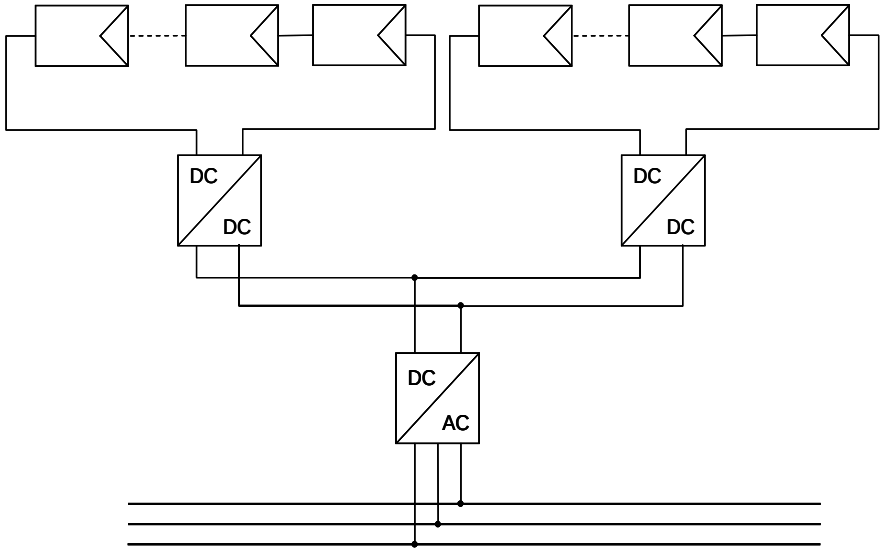

(c) Multi-string technology

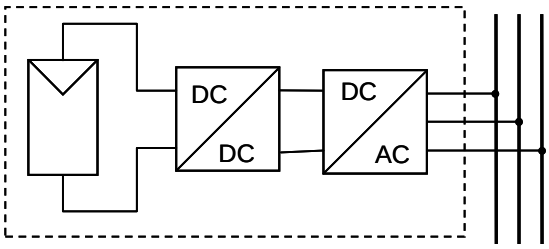

AC module

(d) AC module technology

Figure 2.11. *Configurations of photovoltaic generators. [17]*

All the configurations of PV generators shown in this section are suitable in different situations. For a PV generator located in a place where all the modules have the same operating conditions the most suitable configuration may be the centralized inverter technology. On the other hand, string and multi-string inverter configurations may be the best choices to place several module strings in different locations with variation of the operating conditions. Finally, the ac modules are the best solution for a user who wants to build a system a module at a time.

2.4. The dependence of PV module performance on temperature and irradiance

It is well established that the operating temperature plays a central role in the PV systems affecting to basic electrical quantities, such as voltage and current of the photovoltaic module. [34] However, PV cell's behaviour is not only affected by the pn-junction temperature but also by the value of the irradiance on the cell. Accordingly, the combined effects of irradiance and other operation conditions on the module performance deserve careful consideration. [25] However, this section is meant to study the dependence of the module performance on the operating temperature of the panel and the irradiance received by it. The temperature dependence of the operating module on the climatic conditions will be studied later on.

Referring to the irradiance, the short-circuit current I_{SC} is directly proportional to the value of irradiance reaching a PV cell as [25]

$$I_{SC}(G) = (G / G_0) \cdot I_{SC}(G_0), \tag{2.5}$$

where G is the irradiance yielded over the modules and G_0 the reference level of irradiance. Thus, the I-V characteristic of a PV cell shifts down at lower irradiance on the cell. On the other hand, the open-circuit voltage of the cell (Equation 2.2) is logarithmically dependent on the cell illumination. [25] The irradiance dependence of a PV cell is illustrated in Figure 2.12.

On the other hand, temperature increases due to increased irradiance. Short-circuit current increases due to increased temperature, whereas the open circuit voltage decreases. For a crystalline silicon based cell, the short-circuit current is dependent on temperature as following

$$I_{SC}(T) \approx I_{SC,REF} + 0.0006 \frac{A}{K}(T - T_{REF}), \tag{2.6}$$

where I_{SC} is the short circuit current at temperature T and $I_{SC,REF}$ is the short circuit current at the reference temperature T_{REF}.

The open-circuit voltage is dependent on temperature as following [19, p. 106]

$$V_{OC}(T) \approx \frac{E_{G0}}{q} - \frac{kT}{q} \ln\left(\frac{BT^{\gamma}}{I_{SC}}\right), \tag{2.7}$$

where E_{G0} is the linearly extrapolated zero temperature band gap of the semiconductor, B the temperature independent constant of saturation current and γ the temperature

dependence of parameters of the dark saturation current Since the decrease in voltage due to temperature increase is much higher than the increase of current, the net effect is the decrease in power. [31] It can be roughly said that for every degree centigrade risen in the operating temperature, the silicon cell power output decreases by 0.50 %. [31, p.156] Figure 2.13 illustrates the effects of varying temperature on the I-V characteristics of a photovoltaic module.

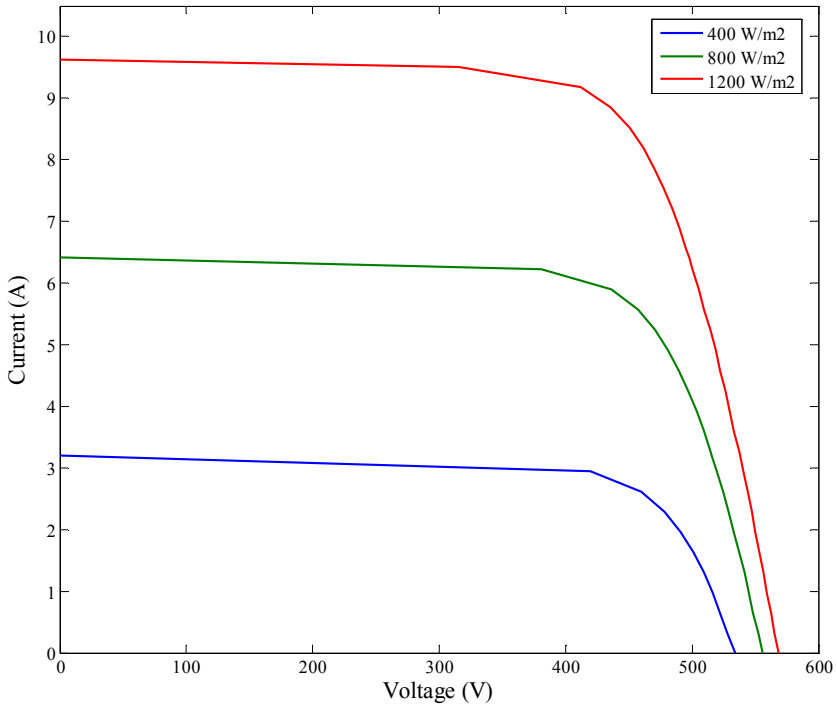

Figure 2.12. *The effect of irradiance on the I-V characteristics of a PV module.*

Consequently, for the best performance of a PV cell, it is necessary to work under conditions of low temperature and the highest level of irradiance possible. However, it is well know that most of the solar radiation absorbed by a PV panel is not converted to electricity but contributes to increase the temperature of the module. [34, 24, 2] This is especially important if regarding to the module efficiency η_C, which is the generated power P_m divided by the area of the module A and the received irradiance G as following

$$\eta_C = \frac{P_m}{A \cdot G}. \tag{2.8}$$

As seen, the operating conditions have a great influence in the behaviour of PV cells and modules. For this reason, there has been a need to define the operating conditions in which the PV modules are tested and rated. Two of the most typical test conditions are standard test conditions (STC) and nominal operating conditions (NOC). The former includes irradiance of 1000 Wm^{-2}, spectral irradiance of AM1.5 and cell temperature of

25 ºC [33]. However, it has to be mentioned that these conditions are very rare in practice.

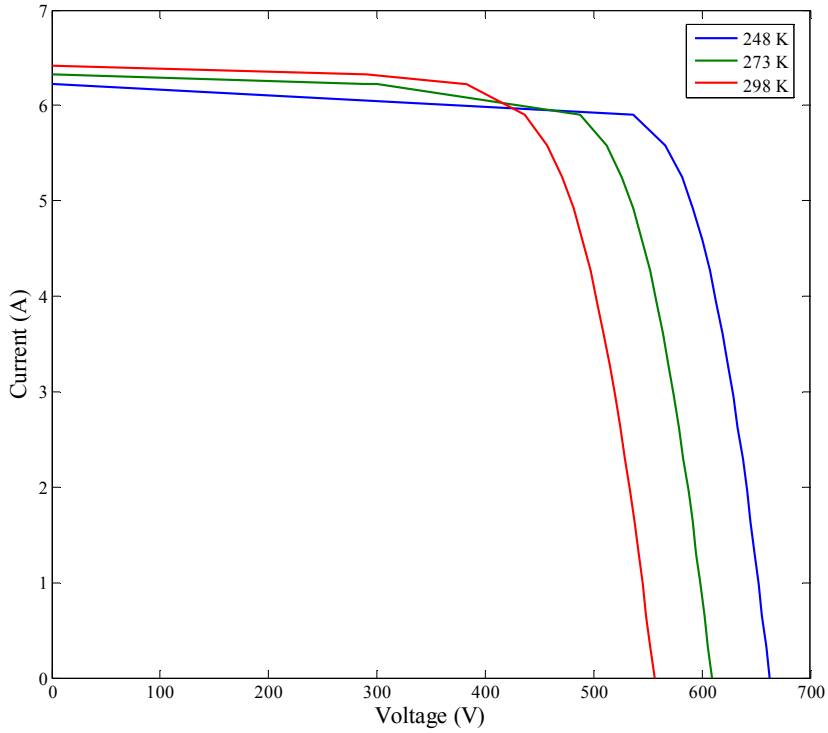

Figure 2.13. *The effect of temperature on the I-V characteristics of a PV module with irradiance of 800 W/m^2.*

The latter, NOC, is a set of reference conditions which includes irradiance of 800 W/m^2 and spectral irradiance of AM1.5. It is important to highlight that the module temperature is not defined in NOC, but the ambient temperature is defined to be 20 ºC. A typical value for the module temperature at NOC is 46 ºC. [29] NOC provide more reasonable testing conditions than STC but NOC parameter values are not always provided by the manufacturers.

3. CLIMATIC MEASUREMENT SYSTEMS

3.1. Introduction

Meteorological measurements are processes of measuring of the physical properties of the atmosphere. [11] A weather station is a facility with measuring instruments and equipment for observing the atmospheric conditions. Typical quantities measured are: temperature, pressure, humidity, wind speed and direction, cloud opacity, solar radiation, sunshine duration, etc. Many sensors are needed to measure them.

The output power of photovoltaic devices operating outside under real working conditions is influenced by many factors, such as temperature, incident irradiance, and spectral irradiance distribution. [28] The operating temperature of the solar module plays a central role in the photovoltaic process. The electrical efficiency and the power output of a PV module depend linearly on the operating temperature, decreasing with it. [34]

According to that, the atmospheric conditions involved on the operating temperature dependence of photovoltaic modules and the necessary sensors to observe and measure each of them will be discussed in this chapter. These properties are temperature, solar radiation, wind speed and direction as well as humidity.

Especially important it is the radiation received by the PV modules, which is directly involved on the generation of electricity in the photovoltaic effect of solar cells, thus the types of radiation and the different sensors to measure them will be more carefully analyzed.

It must be highlighted that any type of monitoring system based on sensor monitoring needs a data-collection system. This system shall be capable to manage and process the signals coming from the sensors.

Hence, this chapter is organized as following. Section 2 provides a brief description about automatic weather stations. Sections 3 to 5 describe the main aspects of several climatic properties as ambient temperature, humidity and wind direction and speed. The commonly used sensors to measure these properties are presented as well. Section 6 first provides a brief description of the main features of the solar radiation, the different types of solar radiation that reach the Earth's surface and the importance of them. Later on, it focuses on the sensors needed to measure the different components of solar radiation. Finally, Section 6 describes the basis of data-acquisition systems, presents several data-acquisition system architectures found in the literature and studies the advantages and disadvantages of them.

3.2. Automatic Weather Station

According to Word Meteorological Organization (WMO), an automatic weather station (AWS) is defined as a "meteorological station at which observations are made and transmitted automatically". At an AWS, the instrument measurements are received by a central data-acquisition unit. The collected data from the measuring devices can be processed afterwards, for instance, at the central processor. Automatic weather stations may be designed as an integrated concept of various measuring devices in combination with the data-acquisition and processing units. However, it has become common practice to refer to them as weather stations.

The development and installation of an AWS should be the result of a definite, coordinated plan for getting data to users in the format required. To achieve this, the functional requirements must be clearly specified to develop practical means of fulfilling them. Specifications for a standardized climatological AWS should be developed in a way that would record a basic set of climate variables such as temperature, humidity and wind. However, concerning the weather station of this Master's Thesis, radiation measurements will be included due to their relevance to the topic of the performance of photovoltaic modules. The meteorological sensors used must be robust and fairly maintenance-free. In general, all sensors with an electrical output are suitable. A large number of sensors of varying performance and quality (and price) are suitable for use with automatic data-acquisition systems. Depending on their output characteristics, sensors can be classified as analogue or digital sensors. The most common types of electrical sensors used in AWS are shown in Table 3.1.

Table 3.1. *Common sensors used in an automatic weather station. [42]*

Property	**Sensor type**
Temperature	Metal resistance thermometers Thermistors
Humidity	Low-cost resistance and capacitive sensors Dew-point meters
Wind	Cup or propeller anemometers Wind-direction vanes Sonic sensors
Radiation	Photodiodes Pyranometers Pyrheliometers

The core of an AWS is its central processing unit (CPU). Its hardware configuration depends on the complexity and magnitude of the functions that it has to perform. In general, the main functions of this CPU are data acquisition, processing, storage and data transmission. Depending on the local circumstances and requirements, the different functions may be executed by different units. They operate in a dependency relation, the data-processing unit being the independent unit. An example is the installation of one or more data-acquisition units in the field close to the sensors that are connected to the data processing or transmission unit.

In general, the data-acquisition hardware is composed of signal-conditioning hardware for prevention and adapting signals to make them suitable for further processing and data-acquisition electronics, which scans the output of the sensors or the sensor-conditioning modules. The data-processing hardware is basically a microprocessor, which allows the designer to perform technical functions to make the measurements easier, faster and more reliable. Finally, the data transmission part of the CPU forms the link with the "outside world".

3.3. Temperature

Temperature is a physical quantity characterizing the mean random motion of molecules in a physical body and represents the thermodynamic state of it. [42] The mean temperature of the atmosphere at each time and in a single place has a fairly regular annual value and a diurnal fluctuation when this temperature is the average of many years for each time and every day of the year. The temperature in a place and time is the addition of that mean temperature and the fluctuations caused by the wind and cloud conditions. [11]

The temperature units are divided in two categories: absolutes and relatives. The former have the lowest theoretical possible temperature: the absolute zero, as the reference and Kelvin degrees are the units. The latter compare a fixed physical-chemical process that always happens at the same temperature; the most used relative unit is Celsius degrees. It is the most used unit for meteorological purposes. This measurement unit is defined by choosing the water freezing point to be 0ºC and the water boiling point to be 100ºC.

As it has been said before, the operating temperature dependence of a solar module has some atmospheric properties involved in it. However, generally speaking, this operating temperature is practically insensitive to the atmospheric temperature. [34] Nevertheless, the environmental temperature is related to the module temperature, as it will be studied later on, and it will be necessary to measure it. This aspect is especially important here, in Finland, due to the significant temperature differences among the different seasons during the year, from -30ºC in winter to +30ºC in summer approximately.

For routine meteorological observations there is no advantage in using thermometers with a very small time-constant, since the temperature of the air continually fluctuates.

Thus, obtaining a representative reading by taking the mean of a number of readings may be a suitable solution. A recommended time-constant could be 20 s.

Temperature is one of the meteorological quantities whose measurements are particularly sensitive to exposure. Therefore, in order to ensure that the thermometer is at true air temperature, it is necessary to protect the instrument from radiation by a shield that also may serve to support it. The shield should completely surround the thermometer and exclude the radiant heat, precipitation and other phenomena that might influence the measurement. [42]

The thermometer should be located at 1.2 – 2 m above the ground. Temperature observations on the top of buildings are of doubtful significance and use because of the variable vertical temperature gradient and the effect of the building itself on the temperature distribution.

Electrical instruments are in widespread use in meteorology for measuring temperatures. Their main virtue lies in their ability to provide an output signal suitable for use in remote indication, recording, storage or transmission of temperature data. The most frequently used sensors are electrical resistance elements, semiconductor thermometers (thermistors) and thermocouples.

Electrical Resistance Thermometers (RTD) are based on the variation of the resistance of a metal to temperature and this variation is expressed as

$$R_T = R_0\left(1 + \alpha(T - T_0) + \beta(T - T_0)^2\right), \tag{3.1}$$

where R_T is the resistance of the metal, R_0 is the reference resistance at the reference temperature T_0, T is the temperature and α and β are temperature coefficients of resistance of the metal. The change of resistance is used to cause a variation in the current passing through the resistance or the voltage across it. An electric circuit is used for the measurement of temperature. Once the instrument is calibrated, it is expected to keep that calibration. With a good calibration and a good measuring circuit, platinum RTDs can measure temperature to a small fraction of a degree, much better than the accuracy needed for meteorological measurements. An RTD is shown in Figure 3.1.

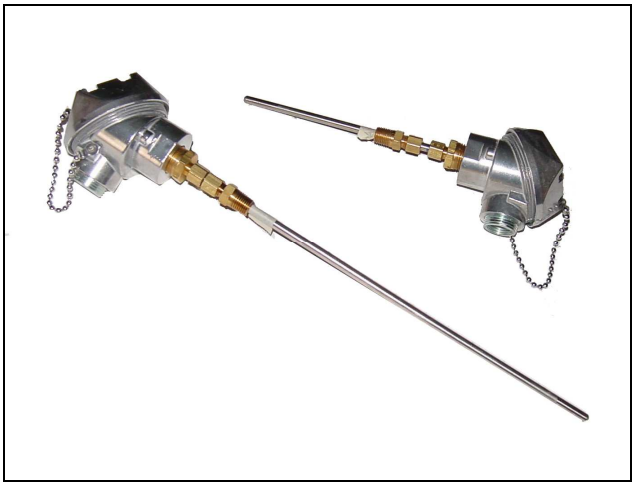

Figure 3.1. *Electrical Resistance Thermometer sensor.*

Semiconductor thermometers are another type of resistance elements. In this case, the semiconductor presents a relatively large temperature coefficient of resistance. This coefficient may be positive or negative depending upon the actual material. The general expression for the temperature dependence of the resistance, R, of the thermistor is:

$$R = a\exp\left(b/T\right), \tag{3.2}$$

where a and b are constants and T is the temperature in Kelvin. The advantages of thermistors are the large temperature coefficient of resistance and that the elements can be made very small. The former enables the voltage applied across a resistance bridge to be reduced. The latter allows the thermistors to be very small with low thermal capacities leading to reduced time-constant of the instrument.

Thermocouples are based on the electromotive forces set up by two different metals at different contact temperatures. The expression of the contact electromotive force is represented by the expression:

$$\left(E_T - E_S\right) = \alpha\left(T - T_S\right) + \beta\left(T - T_S\right)^2, \tag{3.3}$$

where E_T is the contact electromotive force at a temperature T and E_S is the electromotive force at some standard temperature T_S. α and β are constants. In meteorology, thermocouples are mostly used when a thermometer of very small-time constant, 1 or 2 s, and capable of remote reading and recording is required.

Electrical resistances and thermistors may be connected to a variety of electrical measurement circuits, many of which are variations of resistance bridge circuits in either balanced or unbalanced form. In the case of remote measuring, it should be taken into consideration that the wire between the instrument and the bridge also forms a resistance that alters depending on the temperature.

There are two main methods of measuring the electromotive force produced by thermocouples. By measuring the current produced in the circuit with a sensitive galvanometer or by balancing the electromotive force with a known force so that no current actually flows through the thermocouples themselves. [42]

According to the WMO, acceptable values for thermometers covering a typical measuring station are: span of scale from -40 to 40 ºC, range of calibration from -30 to 30 ºC and maximum error smaller than 0.3 ºC.

3.4. Humidity

Humidity is the amount of water vapour in the air; it depends also on temperature, since hot air can contain more water than cold air. The pressure of water vapour just above a liquid water surface in equilibrium is the saturated vapour pressure of the water. This saturated vapour pressure increases with temperature and equals atmospheric pressure at the boiling temperature of water.

Relative humidity is defined as the ratio of the partial pressure of water vapour to the saturated vapour pressure of water at a given temperature and it is expressed as a percentage (%). Humidity may also be expressed as specific humidity, which is the ratio

of water vapour to air in a particular air mass. Specific humidity is expressed as kilograms of water vapour per kilogram of humid air. Dew-point temperature (i.e.: frozen point below freezing) is the temperature at which water vapour saturates from an air mass into liquid or solid. It is associated with relative humidity since dew point occurs when the relative humidity of a mass of air is 100%.

Humidity measurements at the Earth's surface are required for meteorological analysis and forecasting. They are particularly important because of their relevance to the changes of state of water in the atmosphere. In fact, knowledge of water vapour density is used in weather prediction and in global climate modelling: relative humidity affects atmospheric light-transmission and the difference between temperature and dew point is an indicator of fog formation related with height of clouds. [11]

Any instrument that determines pressure of water vapour in the atmosphere is known as hygrometer and, generally, measure relative humidity and dew-point temperature. There are many methods of measuring the vapour density in the atmosphere; three common methods are given bellow.

The chilled mirror method consists in a mirror cooled by a solid-state thermoelectric cooler until water vapour just gets the dew-point and starts condensing. This mirror dew-point temperature is controlled to keep that point. Consequently, the ambient and block temperatures are measured by two RTDs and they allow us to calculate the relative humidity. This method is of higher cost than other methods of measuring the amount of water vapour in the atmosphere.

Thin film polymer capacitance method is a method in which the capacitance is formed by a thin polymer film as dielectric placed between the electrodes. The water vapour in air changes the dielectric constant and, consequently, the capacitance which can be measured electrically. Measuring the capacitance change is possible by comparing it to the fixed reference capacitance and it is related to the relative humidity by calibration. These sensors are low in cost and can measure relative humidity between 0 and 100% at a temperature range between -40ºC and +60ºC.

Psychometric method is based on the difference of temperature measurement of dry and wet bulb thermometers. Relative humidity is computed from the ambient temperature as shown by the dry-bulb thermometer and the difference between the two thermometers. However, in extremely dry environments, it can be difficult to keep the bulb wet. Accuracy is affected by air blowing the wet bulb. Therefore, psychrometers are generally replaced by more convenient methods.

The World Meteorological Organization provides the standards to follow to carry out measurements of humidity. They are shown in Table 3.2.

Table 3.2. *Standard instruments for the measurement of humidity. [42]*

Standard instrument	Dew-point temperature (ºC)		Relative humidity (%)	
	Range	Uncertainty	Range	Uncertainty
Primary standard				
Requirement	-60 to -15	0.3	5 to 100	0.2
	-15 to 40	0.1	5 to 100	0.2
Standard two-temperature humidity generator	-75 to -15	0.25		
	-15 to 30	0.1		
	30 to 80	0.2		
Secondary standard				
Requirement	-80 to -15	0.75	5 to 100	0.5
	-15 to 40	0.25		
Chilled-mirror hygrometer	-60 to 40	0.15		
Reference psychrometer			5 to 100	0.6
Working standard				
Requirement	-15 to 40	0.5	5 to 100	2
Chilled-mirror hygrometer	-10 to 30	0.5		

3.5. Wind speed and wind direction

Wind is the flow of gases on a large scale. On the Earth, wind consists of the mass movement of air. Moreover, in meteorology, wind is often referred according to the strength and the direction that the wind is blowing from. According to WMO, wind velocity is “a three-dimensional vector quantity with small-scale random fluctuations in space and time superimposed upon a larger-scale organized flow”.

Wind is caused by differences in pressure. When there is a pressure difference, the air is accelerated from higher to lower pressure areas and wind speed is directly proportional to the pressure gradient. However, on a rotating planet, except on the exact equator, the air will be deflected by the Coriolis Effect, which affects the direction of wind. Globally, the most important driving factor of large scale winds is the differential heating between the equator and the poles, which is due to the difference in absorption of solar energy and the rotation of the planet.

Most users of wind data require the averaged horizontal wind, usually expressed in polar coordinates as speed and direction. Wind direction is reported by the direction from which it originates. For example, at airports, windsocks are mainly used to indicate wind direction, but they can also be used to estimate wind speed. The latter is measured by anemometers; the most commonly used are rotating cups or propellers. When a high

measurement frequency is needed such as in research applications, wind speed can be measured by ultrasound signals or by the effect of ventilation on the resistance of a heated wire.

Concerning the operating temperature of PV modules; on one hand, wind direction hardly has an influence on it. However, generally speaking, the operating temperature is extremely related to the wind speed due to the important convection coefficient. Thus, it is important to be able to measure wind properties, especially wind speed. The most common digital instruments for measuring wind speed and direction include the cup and propeller sensors, the wind-direction vanes and sonic anemometers.

Anemometers are commonly used in weather stations, especially the 3-cup anemometers. It consists of a vertical axis rotating collar with three vanes in the form of cups. The rotation speed is directly proportional to wind speed. There are several ways to obtain an electrical signal indicating the speed but the most used is a rotating shaft interrupting a light beam and generating an electric pulse in a photo-detector. Rotating anemometers can measure wind velocities from 0 up to 70 m/s.

Ultrasonic wind sensors do not have moving parts. An ultrasonic pulse emitted by a transducer is received and returned by a nearby detector and the transit time is calculated. The presence of wind affects transit times. Typically there are three such pairs of transducers and detectors mounted 120° apart as shown in Figure 3.2.a. Moreover, heaters in the transducer heads minimize problems with ice and snow and the absence of moving parts eliminates the need for periodic maintenance.

Wind-direction vane sensors are based on an electronic read-out which can be achieved using a potentiometer. The resistance between the contact and one end of the wire resistor indicates the position of the vane. Also optical and magnetic position sensors are methods to get electronic signal.

A combination of wind speed and direction sensors can be made with a rotating anemometer and a weather vane, mounting the anemometer on the vane as seen in Figure 3.2.b. Thus, the vane keeps the device into wind direction and the anemometer measures its speed. Alternatively, two anemometers can be used to determine wind speed and direction when they are mounted in a mutually perpendicular structure. Propeller anemometers and weather vanes are susceptible to ice and snow buildup and can be purchased with heaters. Anyhow, periodic maintenance is needed with this kind of sensors.

(a) (b)

Figure 3.2. *(a) Ultrasonic wind sensor. (b) Combination of wind speed and direction sensors.*

3.6. Solar radiation

The total frequency spectrum of electromagnetic radiation emitted by the Sun is known as solar radiation. To calculate the amount of solar radiation reaching the ground of the Earth, both the elliptical orbit of the Earth and the attenuation by the Earth's atmosphere have to be taken into account.

Sun provides energy to the Earth and behaves similar as a black body emitting energy according to Planck's law at approximately 5777 K of temperature. [11] A black body is an ideal absorber and emitter of radiation. The spectral irradiance of a blackbody is given by Plank's radiation law as

$$G_\lambda(\lambda,T)=\frac{2\pi hc^2\cdot\lambda^{-5}}{[\exp(hc/(\lambda kT))-1]}, \tag{3.4}$$

where G_λ is power per unit area per unit wavelength, T is the temperature of a black body, k is the Boltzmann's constant, c the light speed, h the Plank's constant and λ the wavelength of a photon. [25, p 22] The spectral irradiance dependence on the temperature can be observed in Figure 3.3. The frequency spectrum is distributed from infrared to ultraviolet radiation.

The mean annual intensity of solar radiation above the earth atmosphere, named solar constant, is 1367 W/m^2 approximately, but it varies due to the distance of the Earth and the Sun. However, not the whole radiation reaches the Earth's surface. Solar radiation is attenuated by scattering, absorption and reflection. [11] Solar radiation is partially depleted and attenuated as it traverses the atmospheric layers, preventing a substantial portion of it from reaching the Earth's surface. This phenomenon is due to a thin layer of ozone in the upper atmosphere (stratosphere) and to the cloud formations in the lower atmosphere (troposphere).

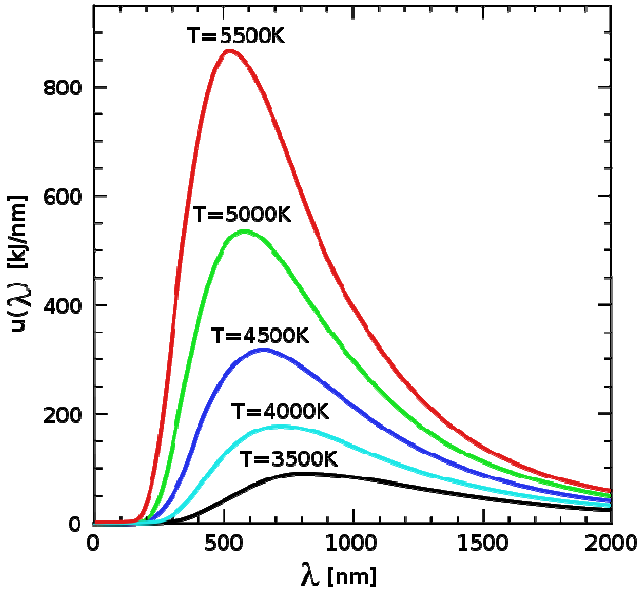

Figure 3.3. *Spectral irradiance for different black body temperatures.*

Consequently, the total solar radiation received at surface level consists of a direct and indirect, or diffuse, radiation. The intensity of sunlight at ground level varies with latitude, geographic position, elevation, season, etc. Moreover, the angle of incidence of solar radiation is affected by the 23.5º tilt of the Earth's axis causing seasonal and latitudinal variations during the day length. The spectral distribution of the received solar energy is approximately 3% in UV, 44% in visible and 53% in infrared regions. Therefore, with regard to measure solar energy, these variables need to be considered. [15]

The magnitude which measures the solar radiation received by the Earth is the irradiance. It measures the power per unit area and its SI units are watts per square meter (W/m^2). However, commonly both terms, solar radiation and irradiance, are used in the same way. On the other hand, solar irradiation should not be confused with irradiance, because it is the total power yielded by the Sun in an area over time. The units are watts-hour per square meter (Wh/m^2). [12]

For solar based renewable energy technologies such as solar thermal or photovoltaic (PV) conversion systems, the basic resource is solar radiation. Concerning PV generation systems the irradiance received by the modules is directly related to the energy yield by them according to the photoelectric effect. This photoelectric effect is a phenomenon in which electrons are emitted from different materials. It happens as a consequence of the absorption of energy from short wavelengths of electromagnetic radiation, as visible light or UV.

Therefore, knowledge of solar radiation received in an area is essential to predict, study and design the economic viability of any system which use solar energy. In spite of the importance of solar radiation measurements, this information is not readily available due to the cost and maintenance and calibration requirements of the measuring equipment. However, solar radiation data is not only needed in advanced for designing

issues for solar radiation based systems. Solar irradiance measurements are crucial in order to test and calibrate the right operation behaviour of already installed solar modules. On the other hand, the radiance level has a strong influence on the operating temperature of PV modules. [34]

Solar radiation measurements are based on pyranometers and pyrheliometers. The former respond to the incident radiation from the hemisphere (global radiation) and the latter are narrow field of view instruments that are only sensitive to the beam radiation (direct radiation). Diffuse radiation can be measured using a shadowed pyranometer. In this case, the beam radiation is blocked out by the shadow band and the pyranometer responds only to the diffuse component. The total hemispherical radiation, G, on a horizontal surface is calculated as follows

$$G = I\cos h + D, \tag{3.5}$$

where I is the direct beam, h is the angle between the solar disk and the normal to the horizontal surface and D is the sky radiation. This theoretical relationship shows that measuring two of the radiation quantities allows calculating the third one. Moreover, outdoor calibration of photometric instruments is based on Equation 3.5. [15] Because of that pyranometers and pyrheliometers are essential instruments to measure solar radiation parameters and are described in the following subsections. Both sensors are shown in Figure 3.4.

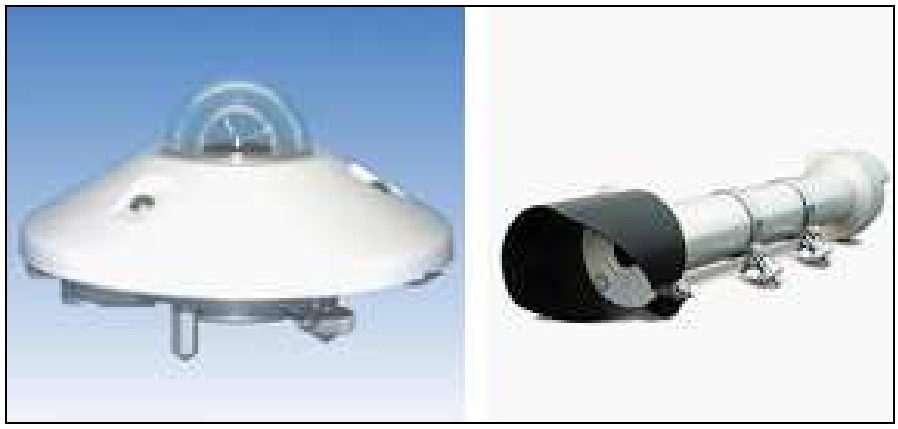

(a) (b)

Figure 3.4. *(a) Pyranometer. (b) Pyrheliometer.*

3.6.1. Pyranometer

Pyranometers are sensors that measure broadband solar irradiance. These sensors measure flux density, or global radiation, from the hemisphere. Moreover, pyranometers respond fairly linearly to the total solar radiation's frequency spectrum (from 300 to 2800nm), as illustrated in Figure 3.5. On The unit of intensity of solar radiation measurement is watts per square meter (W/m^2).

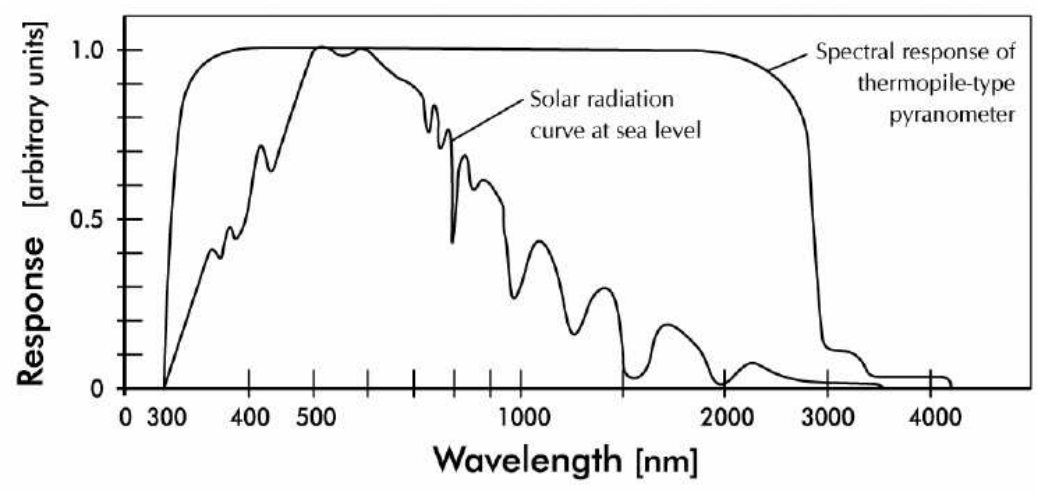

Figure 3.5. *Thermopile-based pyranometer spectral response.*

Roughly, pyranometers are based on two different technologies: thermopiles and solar cells. Both of them are described as following.

Thermopile-based pyranometers rely on the variation of temperature between junctions of different metals in contact with surfaces that absorb solar radiation, called hot junctions, and reference, or cold junctions, which does not receive solar radiation and are near the ambient temperature. The bottom unit has thermopile hot junctions in contact with a matte black absorbing surface and reference cold junctions protected by with non absorbing surface. [15] This type of sensors presents smaller thermal offsets in the voltage signal than pyranometers with all black receivers. Figure 3.6 illustrates the diagram of a thermopile-based pyranometer.

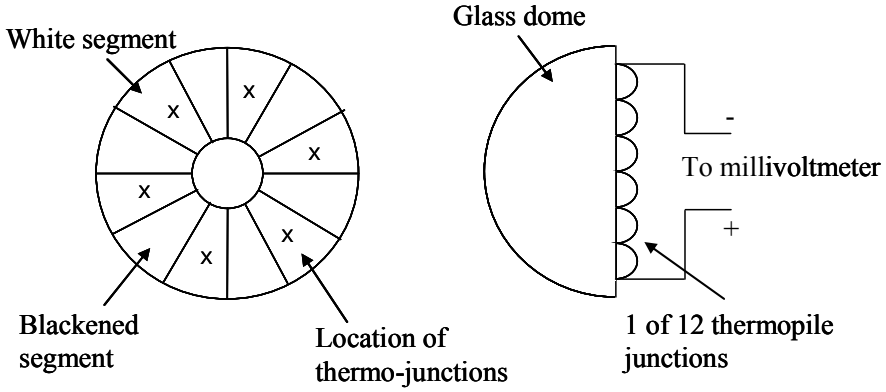

Figure 3.6. *Thermopile-based pyranometer diagrams.*

Solar cell-based pyranometers use silicon photovoltaic cells that produce a shot-circuit current that is directly proportional to the intensity of the incident solar radiation. It may be commented that this type of sensors perform well under clear skies but not so accurate in cloudy conditions. Furthermore, the former, thermopile based pyranometers, have a rather uniform spectral response over all significant wavelength as seen in Figure 3.5.

Pyranometers are standardized according to ISO 9060 standard, which is also adopted by the World Meteorological Organization (WMO). Thus, the standard

establishes three classes of sensors: secondary standard, first class and second class pyranometers. This classification is based on several specifications of the sensor as, for instance, response time, non-linearity, spectral selectivity, tilt error or non-stability. [38] Commonly, the secondary standard and first class sensors are thermopile-based pyranometers, while the second class type may be solar cell-based pyranometers. Table 3.3 [42] describes the characteristics of pyranometers of various levels of performance. The "Secondary standard" column refers to pyranometers near state-of-the-art, which are suitable for use as working standard; maintainable only at stations with special facilities and staff. "First class" refers to acceptable pyranometers for network operations.

Table 3.3. *Standard requirements for operational characteristics of pyranometers. [42]*

Characteristic	**Secondary standard**	**First class**
Response time (95% response)	< 15 s	< 30 s
Zero offset	7 W/m^2	15 W/m^2
Resolution (smallest detectable change)	1 W/m^2	5 W/m^2
Stability (percentage of full scale, change/year)	0.8	1.5
Temperature response (percentage maximum error due to change of ambient temperature within an interval of 50 K)	2.0	4.0
Non-linearity	0.5	1.0
Spectral sensitivity	2.0	5.0
Tilt response	0.5	2.0
Achievable uncertainly, 95% confidence level		
Hourly totals	3.0%	8.0%
Daily totals	2.0%	5.0%

As said before, pyranometers are commonly used to measure global radiation. However, diffuse radiation can be measured by shading a pyranometer with a disk located to prevent the direct beam.

3.6.2. Pyrheliometer

Pyrheliometers are instruments that measure direct beam or direct solar radiation. This radiation is coming direct from the sun without scattering or any other change produced by the atmospheric layers.

Pyrheliometers are based on the same technologies than pyranometers. There are thermopile- and solar cell-based types of sensor. However, for pyrheliometers, the sensor is placed at the bottom of an internally blackened, diaphragmed, collimator tube that limits the angular acceptance for solar radiation to be in the range of about 5º or 6º total acceptance angle. Moreover, the pyrheliometer must be mounted on an equatorial mount tracker that keeps the direct radiation from the sun parallel to the axis of the collimator tube. [40] Figure 3.7 shows the diagram of a thermopile-based pyrheliometer. Referring to the classification, pyrheliometers are also standardized according to ISO 9060. Some of the characteristics of operational pyrheliometers (other than primary standards) are given in Table 3.4.

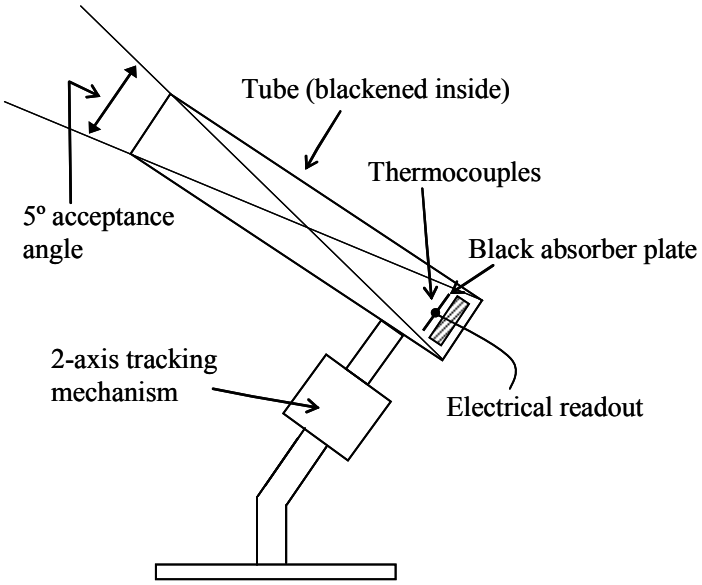

Figure 3.7. *Diagram of a thermopile-based pyrheliometer.*

Table 3.4. *Standard requirements for operational characteristics of pyrheliometers. [42]*

Characteristic	**High quality**	**Good quality**
Response time (95% response)	< 15 s	< 30 s
Zero offset	2 W/m^2	4 W/m^2
Resolution	0.51 W/m^2	1 W/m^2
Stability (percentage of full scale, change/year)	0.1 %	0.5 %
Temperature response (percentage maximum error due to change of ambient temperature within an interval of 50 K)	1.0	2.0
Non-linearity	0.2	0.5
Spectral sensitivity	0.5	1.0
Tilt response	0.2	0.5
Achievable uncertainly, 95% confidence level		
1 min totals	0.9%	1.8%
1 h totals	0.7%	1.5%
Daily totals	0.5%	1.0%

3.7. Architecture of a data-acquisition system

Data-acquisition systems are widely used in renewable energy source (RES) applications in order to collect and evaluate data concerning the installed system. [18] The aim of this section is to describe several data-acquisition system architectures capable to manage and process data coming from the sensors for evaluation purposes.

Data-acquisition (DAQ) is the process of sampling from the real world (analogical system) and generating the digital signals up to be processed by a digital system, e.g. a computer. The process involves several stages. A general example of the stages involved in a data-acquisition process is shown in Figure 3.8.

Different data-acquisition systems have been developed, as in [10] and [41], to collect and process meteorological data. Several DAQ system architectures are proposed as following.

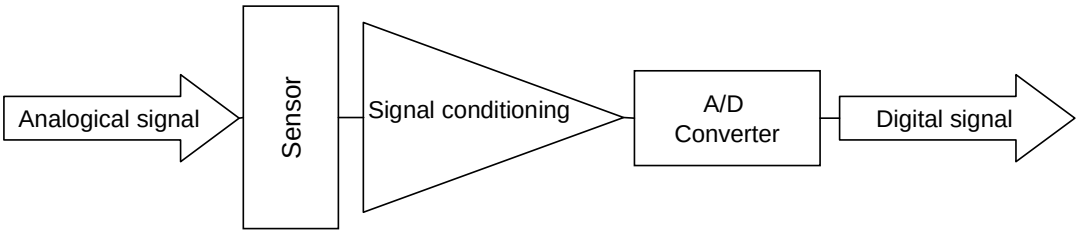

Figure 3.8. *Stages involved in a data-acquisition process.*

A data-acquisition system developed for solar radiation and meteorological measurements by, for instance, [27] and [5] is shown in Figure 3.9(a). An A/D converter connects the measuring sensors, converting analogical to digital signals, with the microcontroller (MC) unit which collects the sensor data. These data are transmitted to a PC, with a serial connection RS-232, and processed. [18] A different approach consists in substituting the A/D converter and the microcontroller by a commercial data-logging unit as seen in Figure 3.9(b). The collected data are transmitted, as in the previous case, with a RS-232 serial connection to the computer for further data processing.

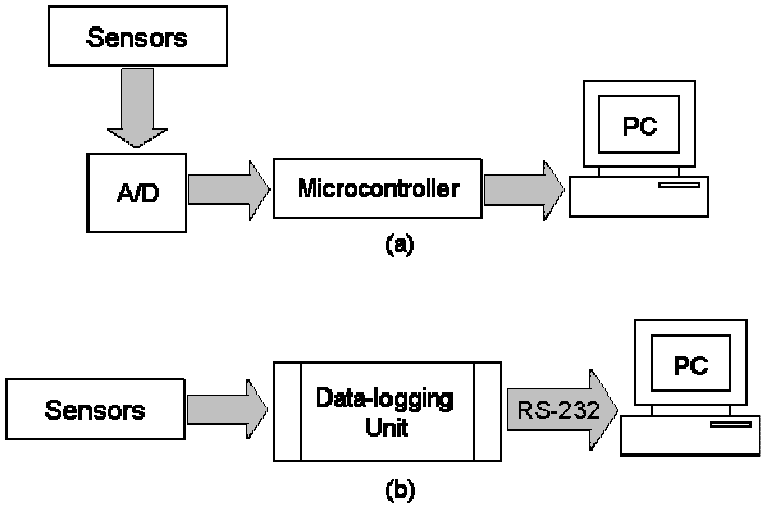

Figure 3.9. *Data-acquisition system architectures. (a) Microcontroller-based architecture system. (b) Data-logging unit connected to PC.*

Both options described have a common characteristic that is the transmitting RS-232 serial connection from the microcontroller and data-logging unit to the PC. However, for advanced controlling, the RS-232 transmission is not enough and it is necessary the use of specifically designed buses as, for instance, the PCI ones designed by National Instruments. [30] However, using a commercial data-logging unit lacks flexibility compared with a data-acquisition card-based system which allows total control for advanced controlling and data managing.

Consequently, a computer-based data-acquisition system e.g., as shown in Figure 3.10, will be more suitable and desirable. Several monitoring sensors, as, for instance, climatic sensors; are used to measure the most relevant conditions. The sensor signals are well conditioned by precision filters and amplifiers and interfaced to a PC.

Interfacing is carried out by a commercial data-acquisition card (DAQ card) through a PCI or USB bus. The collected data will be managed, processed, monitored and stored, for instance, using LABVIEW software.

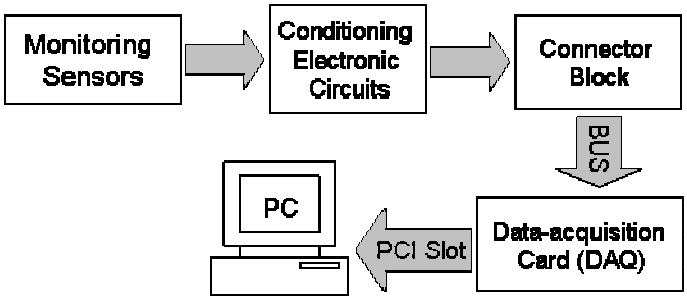

Figure 3.10. *Architecture of a computer-based data acquisition system.*

The proposed system in Figure 3.10 shows the advantages of high-speed data-acquisition system for advanced controlling up to academic research and flexibility in case of need of future changes.

4. CLIMATIC SENSITIVITY OF A PHOTOVOLTAIC GENERATOR

4.1. Introduction

Changing operating conditions affects the operation of a PV generator. These operating conditions are affected by several climatic variables as well. Hence, the aim of this chapter is to study the effects of those climatic conditions on the operating module temperature and the PV generator performance characteristics. A Simulink model of the PV generator with a Simulink thermal model of the PV modules is exploited to realize a set of simulations meant to analyze those effects. This chapter is organized as following.

Section 4.1 presents the photovoltaic generator Simulink model developed by [20] and adapted to study the climatic effects on a PV string composed by 17 modules. This model calculates the string performance characteristics using the irradiance received, operating module temperature and string current as inputs. Then, Section 4.2 describes the Simulink operating module temperature model developed. It calculates the operating temperature of a PV module from the climatic parameters of ambient temperature, irradiance and wind speed affecting the solar panel. [34] Section 4.3 presents the simulations that were used to study the effect of climatic parameters on the operating module temperature. The influence of each individual parameter, as well as the combination of them, on the operating temperature is analyzed. Finally, in Section 4.4, the influence of the climatic parameters on the photovoltaic string generator performance is studied. The characteristic curves and the generated power and system efficiency for each simulation case are presented.

4.2. Modelling of a photovoltaic generator

4.2.1. MATLAB^{TM} Simulink model of a photovoltaic generator

The model of the photovoltaic generator used in here is based on the model developed by Anssi Mäki in his Master of Science Thesis “Topology of a Silicon-Based Grid-Connected Photovoltaic Generator”. [20] In this section, the model is briefly presented as well as the particular characteristics of the PV generator model used in the simulations later on.

The model is made up with PV modules connected in series modelled according to the equations presented by Villalva et al. [39] These modules are modelled using the one-diode model of a photovoltaic cell, with a bypass diode connected in parallel (as

shown in Figure 2.7 in Section 2.2.1 Photovoltaic cell). The Simulink model of a PV module with bypass diode in parallel is shown in Figure 4.1.

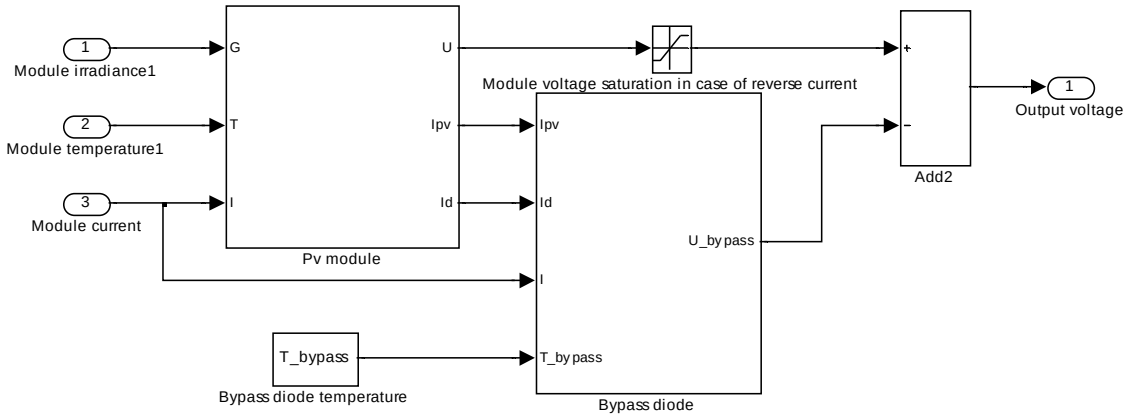

Figure 4.1. *Simulink model of a photovoltaic module and bypass diode. [20]*

Due to the bypass diode connected in parallel with the photovoltaic module, the diode conducts current when the module is reverse biased. This happens when the photocurrent (I_{PV}) is less than the sum of the module current (I) and diode saturation current (I_d). On the other hand, the module's output voltage is saturated to zero when the bypass diode conducts current.

As seen in Figure 4.1 the Simulink model has three inputs out of which two are operating conditions, module temperature and module irradiance. The third is the module current, which is used to obtain the module's I-V characteristics. It is done by changing the input current from zero to short-circuit current value and calculating the voltage value at every point. [20]

The block model illustrated in Figure 4.1 is one of the highest layers of the entire photovoltaic module model, which is composed by several subsystems. More detailed information about the complete model is presented and explained in [20]. Now it is possible to construct the photovoltaic generator model by interconnecting individual modules, as shown in Figure. 4.2.

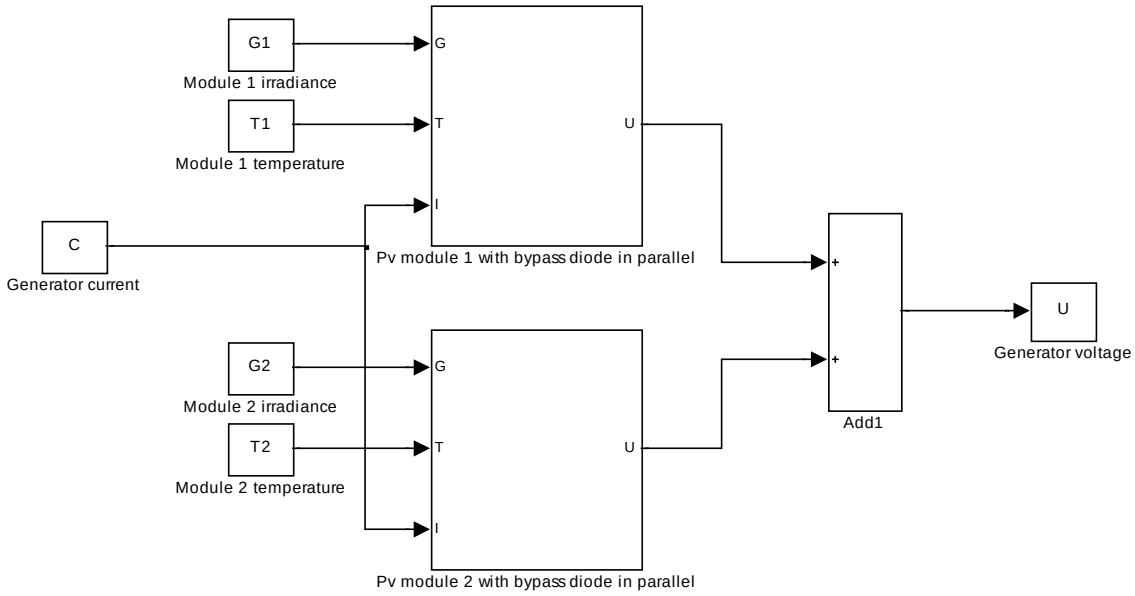

Figure 4.2. *Simulink model of a photovoltaic generator with 2 modules in series. [20]*

The model used for simulations has been designed accordingly to the system constructed in the Department of Electrical Engineering in Tampere University of Technology, which is located at the rooftop of the department. The system consists of a string of 17 modules connected in series. Modules are made up from 54 series connected polycrystalline silicon photovoltaic cells. The maximum power point of a module is 190 W and the short circuit-current and open-circuit voltage are 8.02 A and 33.1 V, respectively. [29] Figure 4.3 illustrates the photovoltaic generator model used for simulation.

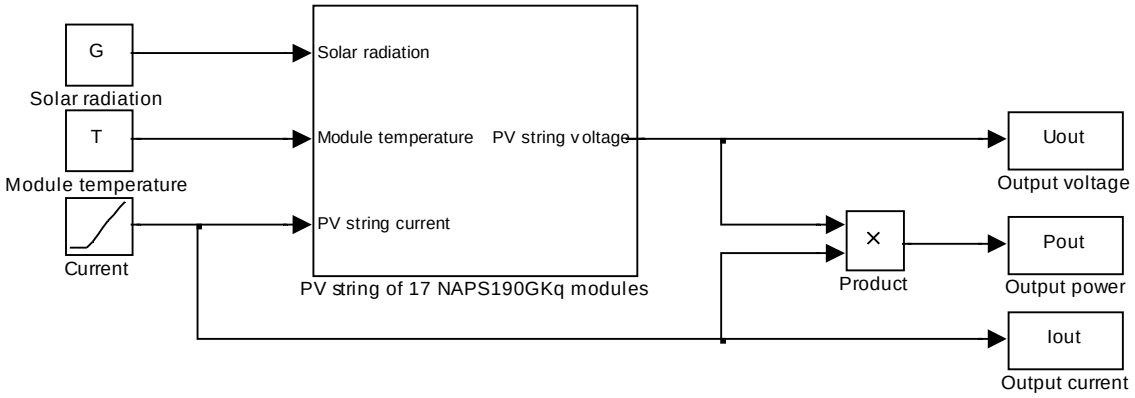

Figure 4.3. *Simulink model of a photovoltaic string system composed by 17 modules connected in series.*

Figures 4.4 depicts the simulated I-V and P-V characteristics of a string of 17 modules in conditions of 1000 W/m^2 and 25 ºC (standard test conditions).

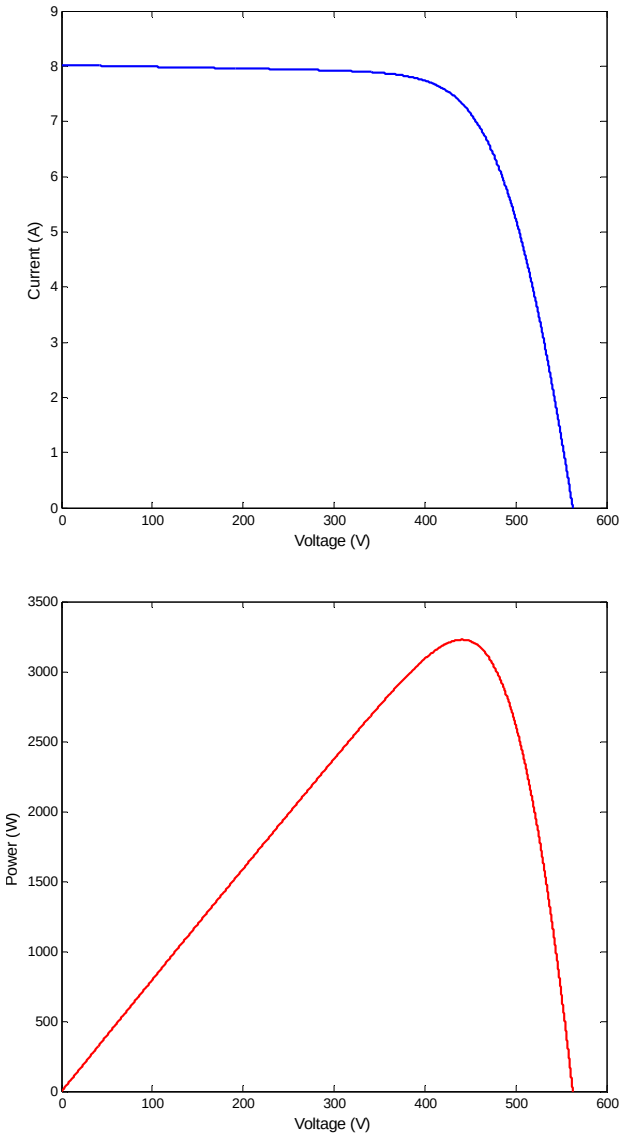

Figure 4.4. *Simulated I-V and P-V characteristics in STC of a PV string of 17 NP190Kg modules connected in series.*

4.2.2. MATLAB™ Simulink operating module temperature model

As seen in Section 2.4, the operating conditions affect the solar module performance, especially the irradiance and the operating module temperature. [34] Hence, both factors are input parameters in the model described in the previous section.

Thus, due to the strong module temperature influence on the generated power and the module efficiency, the purpose of this section is to propose a thermal model of the PV panel. The aim of it is to predict, as accurate as possible, the operating temperature of the module based on a fixed climatic conditions. In this way, based on information about radiation level, wind speed, ambient temperature, etc., it will be possible to calculate the PV system operating condition.

There is a wide literature [2, 3, 14, 23] about the thermal transfer processes in PV modules. However, the design of the thermal model is based on a 3-parameter model of

Skoplaki et al. [34] that considers solar radiation, ambient temperature and wind speed as relevant parameters regarding the PV module performance. Other parameters as wind direction and humidity do not have an important influence over the operating condition of a solar panel [37]. Skoplaki et at. [34] base their development of the model on studying the thermal transfer produced by the processes of conduction and convection in the front and back sides of the PV module. After some approximations and presuming some methodological approaches, the authors involve the NOC temperature NOCT to formulate the module operating temperature T_C dependence on the solar radiation, ambient temperature and wind as following

$$T_c = \frac{T_a + \left(\frac{G_T}{G_{NOCT}}\right)\left(\frac{h_{w,NOCT}}{h_w}\right)\left(T_{NOCT} - T_{a,NOCT}\right)\left[1 - \frac{\eta_{ref}}{(\tau\alpha)}\left(1 + \beta_{ref} T_{ref}\right)\right]}{1 - \left(\frac{\beta_{ref}\eta_{ref}}{(\tau\alpha)}\right)\left(\frac{G_T}{G_{NOCT}}\right)\left(\frac{h_{w,NOCT}}{h_w}\right)\left(T_{NOCT} - T_{a,NOCT}\right)}, \tag{4.1}$$

where, T_a is the ambient temperature, T_{NOCT} is the operating module temperature at NOCT conditions, T_{ref} is the reference temperature, $T_{a,NOCT}$ is the ambient temperature at NOCT conditions, G_{NOCT} is the irradiance at NOCT conditions, G_T is the irradiance on the module plane, h_w is the wind-convection heat transfer coefficient at a temperature, $h_{w,NOCT}$ is the wind-convection heat transfer coefficient at NOCT conditions, τ is the transmittance of glazing, α is the solar absorption of PV layer, η_{ref} is the electrical efficiency at T_{ref} and β_{ref} is the efficiency correction coefficient for temperature.

Equation 4.1 represents a general expression for the PV module operating temperature considering that radiation losses are negligible. Taking into account the forced convection (wind) as

$$h_w = 8.91 + 2.0 v_f , \tag{4.2}$$

where v_f is the free wind speed hitting the PV module in m/s, Equation 4.1 can be reduced to simple semi-empirical equation as following

$$T_c = T_a + \left(\frac{0.32}{8.91 + 2.0\, v_f}\right) G_T \qquad \left(V_f > 0\right). \tag{4.3}$$

where v_f is in m/s and G_T in W/m^2. This equation relates the three basic environmental variables of wind speed, irradiance and ambient temperature. Two more parameters must be taken into account to normalize the equation (4.3) with respect to the free-standing case. The mounting effect (ω) can be defined as

$$\omega = \frac{k_{mt}}{k_{fsa}}, \tag{4.4}$$

where k_{mt} is the mounting type coefficient and the k_{fsa} is the free standing array coefficient.

The values for the different types of PV array mounting are listed in Table 4.1. On the other hand, it is necessary to comment that V_f is the wind speed measured by a mast-mounted anemometer above the PV array. If considering the TUT PV power plant in

which several arrays are installed in different locations at the rooftop of Department of Electrical Energy Engineering, it is a better solution to study the effect of local wind speed or wind speed near the PV array, v_w. The transformation from v_f to v_w is done using the relation

$$v_f = \frac{v_w}{0.67}. \tag{4.5}$$

Table 4.1. *Values of the mounting coefficient, ω, for several PV array mounting situations. [34]*

PV array mounting type	ω
Free standing	1.0
Flat roof	1.2
Sloped roof	1.8 (1.0-2.7)
Façade integrated	2.4 (2.2-2.6)

Hence, Equation 4.3 is written as

$$T_c = T_a + \omega\left(\frac{0.32}{8.91 + 2.0\frac{v_w}{0.67}}\right)G_T, \tag{4.6}$$

for any type of mounting and for local wind speeds greater than 0 m/s. In the present case of the system installed at the rooftop of the department, the solar panels have been mounted free-standing on a flat roof, thus the mounting coefficient value is 1. Figure 4.5 illustrates the Simulink block diagram of a PV module thermal model based on Equation 4.6 with ω=1.

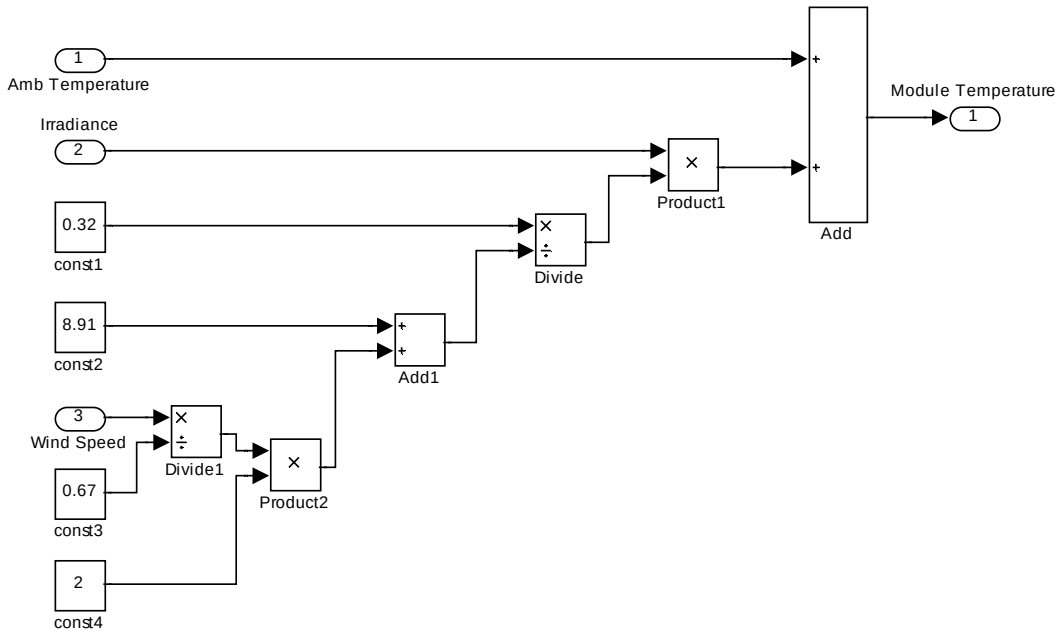

Figure 4.5. *Simulink bloc diagram of the PV module thermal model.*

As seen in Figure 4.5, the model has 3-input parameters that are irradiance, ambient temperature and wind speed. The mask of the model is shown in Figure 4.6.

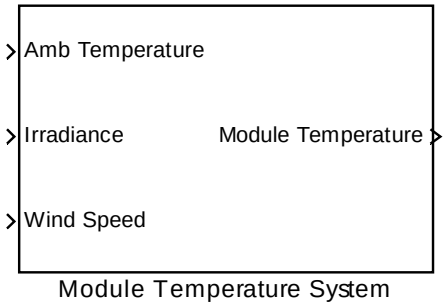

Figure 4.6. *Simulink thermal model of a PV module.*

The effects of climatic conditions on the operating module temperature are shown in Figure 4.7 and Figure 4.8. The measurement data has been obtained from a measurement system of the Department of Electronics. The system is located at the rooftop of the department and consists of a polycrystalline silicon module with power rating of 125 W. Module temperature is monitored, as well as some climatic measurements such as ambient temperature, irradiance and wind. The dataset used for this analysis was taken the 1St of June, 2008 acquiring data every 20 seconds.

In Figure 4.7, irradiance, ambient temperature and the calculated module temperature are presented. It is possible to notice that the module temperature peak values are in accord with the irradiance values.

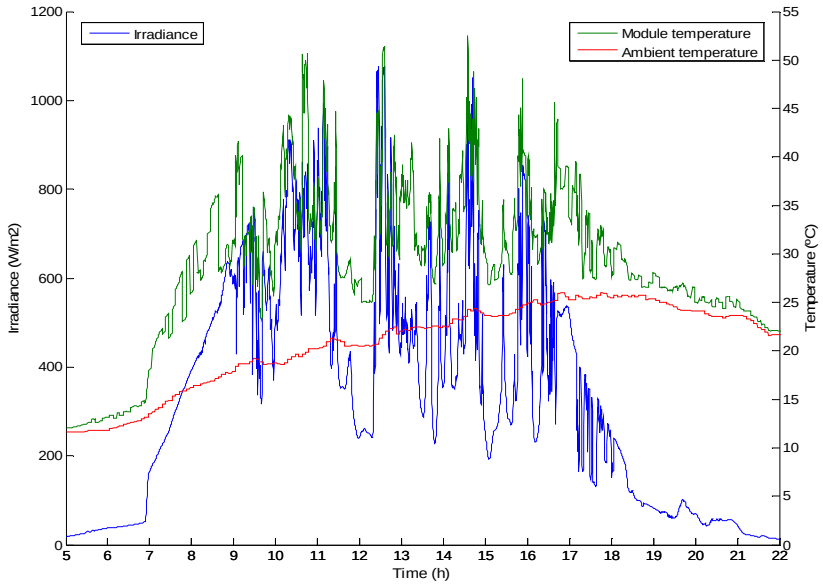

Figure 4.7. *The effect of irradiance and ambient temperature on the calculated module temperature.*

The monitored signals of wind speed and module temperature with the calculated temperature are represented in Figure 4.8. This figure verifies the correct performance

of the correlation used to calculate the operating module temperature, since the deviation should be around 3 ºC. [34]

It has to be mentioned that, according to the obtained results, the thermal model performs better under wind speeds higher than 3 m/s. For lower wind speed conditions the error of the measured operating temperature increases several degrees. This is due to the fact that the proposed correlation in [34] ignores the free-convection, which is small for high wind speeds, and radiation, which is important for small wind speeds. Finally, the connection of the PV module thermal model with the PV generator proposed in the previous section is shown in Figure 4.9.

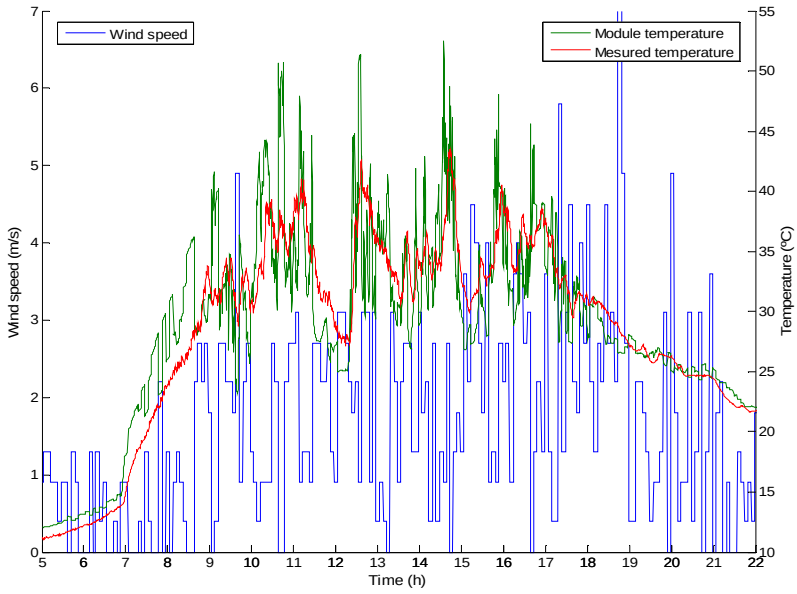

Figure 4.8. *Comparison of the module temperature calculated by the thermal model, the measured module temperature and the wind speed.*

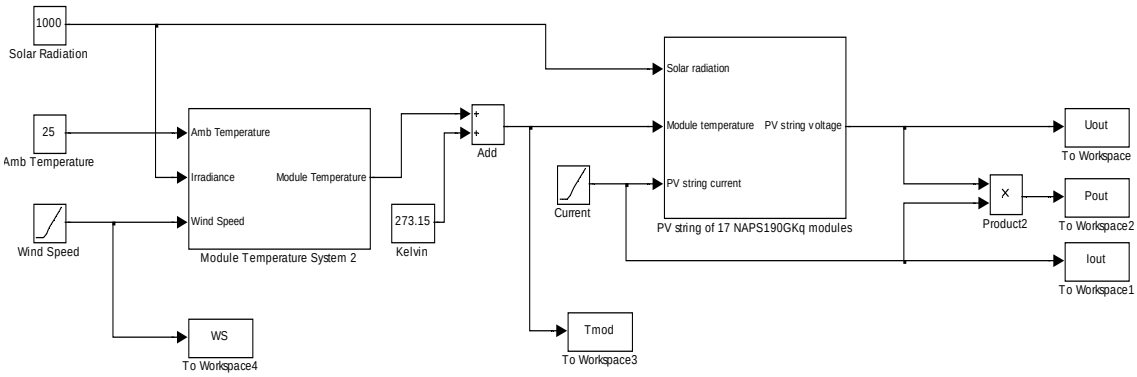

Figure 4.9*. Simulink model of a PV string generator including the PV module thermal model.*

4.3. The effect of climatic parameters on the operating module temperature

Changing operating conditions affect the operation of a PV generator significantly. The effect of the climatic parameters on the operating conditions is studied by simulations using the thermal model introduced in the previous section. The aim of this set of simulations is to know the operating module temperature limits for several typical values of ambient temperature, irradiance and wind speed in Finland. On the other hand, the thermal model dependence on the different climatic parameters is studied.

Furthermore, the effect of the climatic parameters on the PV module's performance is carried out by studying the characteristics of the Simulink model of the generator introduced in Section 4.2.1, including the thermal model as shown in Figure 4.9. The IV and PV characteristics are studied in three different cases, as well as the generated power and the system efficiency.

The results of the simulations studying the effect of climatic parameters on the operating module temperature are shown as graphs in Figures 4.10, 4.11 and 4.12. The effect of ambient temperature on the module temperature is presented in Figure 4.10. As extracted from Equation 4.6, the thermal model is directly proportional with the ambient temperature. Thus, the difference between module and ambient temperature is always greater than 0 and depends on the wind speed and irradiance conditions. The ambient temperature values vary from -5 ºC to +15 ºC, which are rather normal in Finland.

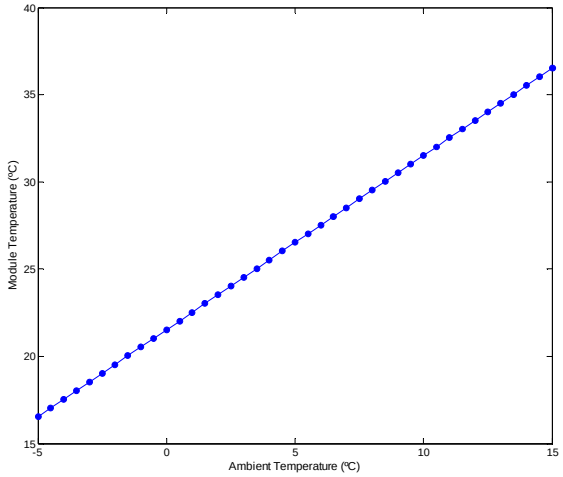

***Figure 4.10**. Simulated effect of ambient temperature on the operating module temperature for given values of wind speed of 1 m/s and irradiance of 800 W/m^2.*

To study the effect of wind speed on the operating temperature two different simulations are presented. First fixing the ambient temperature value to 5 ºC and simulating with irradiance values of 400 W/m^2, 600 W/m^2 and 800 W/m^2. Secondly, fixing the irradiance value to 600 W/m^2 and varying the ambient temperature to values of -5 ºC, 5 ºC and 15 ºC. The value range of wind speed varies from 1 m/s to 12 m/s. The results are shown in Figure 4.11.

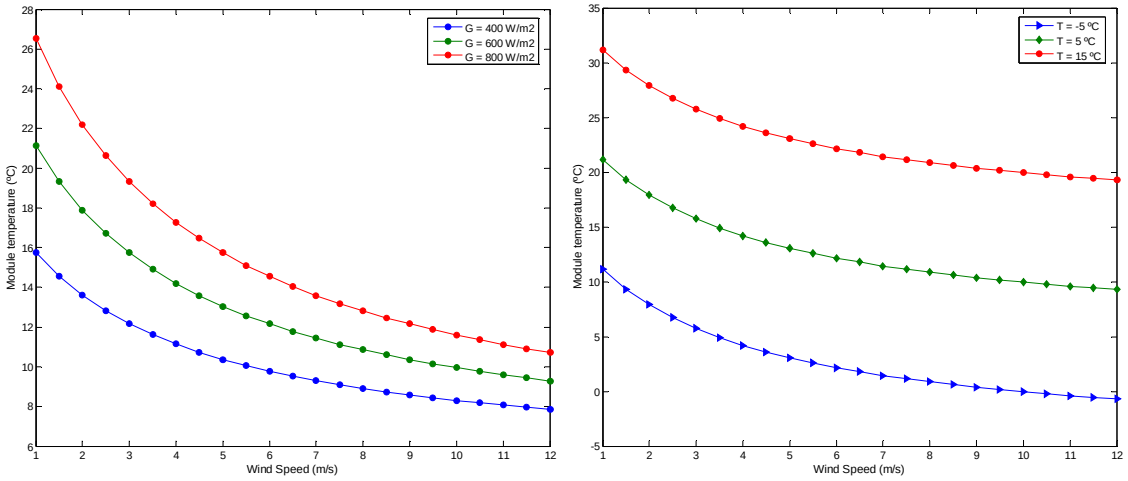

Figure 4.11. *Simulated effect of wind speed on the operating module temperature for given values of irradiance and ambient temperature.*

As expected, the wind speed is in inverse proportion to the operating temperature due to the fact that it increases the convection process in the module. Thus, in both cases the module temperature decreases with the wind speed. In the study of the influence of wind speed and ambient temperature, the simulated T_{MOD} curves are parallel and with the same difference as the ambient temperature values have. However, regarding to the analysis of the influence of wind speed and irradiance, the influence is greater at higher levels of irradiance. Thus, for 400 W/m^2 the module temperature variation is approximately 8 ºC in the range from 1 to 11 m/s; while for 800 W/m^2, the temperature variation is 16 ºC.

The effect of irradiance on the operating temperature is presented in Figure 4.12. As in the previous case, two simulations are available. In the first one the ambient temperature value is fixed to 5 ºC while in the second one the wind speed value is fixed to 3 m/s. The former studies the influence of irradiance and wind speed for values of 3 m/s, 6 m/s and 9 m/s. On the other hand, the latter studies the influence of irradiance and ambient temperature. The irradiance values range goes from 200 W/m^2 to 1200 W/m^2 in both simulations.

The module temperature is directly proportional to irradiance due to the effect of radiation process in the module. It is possible to notice that the module temperature decreases with wind speed increasing. The difference of operating temperature can reach a value of 16 ºC in a 1000 W/m^2 difference (200 – 1200 W/m^2) with low wind speed condition (3 m/s). On the other hand, as in the previous analysis, when fixing the wind speed, the difference between module temperature and ambient temperature remains constant.

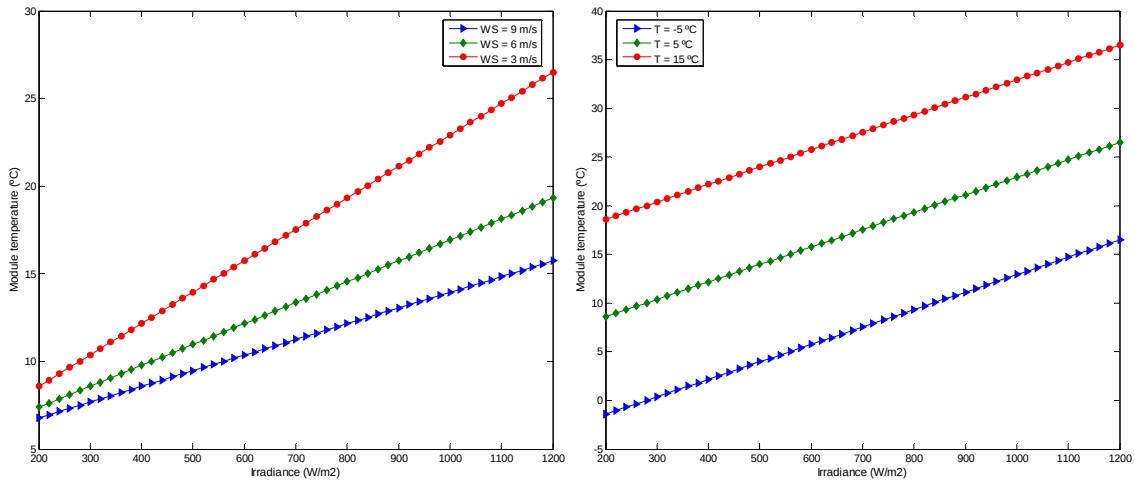

***Figure 4.12**. Simulated effect of irradiance on the operating module temperature for given values of wind speed and ambient temperature.*

4.4. The effect of climatic parameters on photovoltaic module efficiency

In order to study the effect of climatic parameters on the performance of 17-photovoltaic modules string three different cases are analysed. These "representative" cases are meant to reproduce three possible climatic conditions that are usual in Finland. Table 4.2 presents the values of the climatic parameters for each study case. Due to the variability of the Finnish climate, it is hard to determine the most common climatic condition during a season. Thus, as said, the selected values are just possible conditions given during those seasons.

***Table 4.2**. Values of climatic parameters used to simulate the performance of 17-pannels photovoltaic string.*

"Winter" conditions:		
	Ambient temperature	-5 ºC
	Irradiance	300 W/m^2
	Wind Speed	9 m/s
"Spring" conditions:		
	Ambient temperature	+5 ºC
	Irradiance	600 W/m^2
	Wind Speed	6 m/s
"Summer" conditions:		
	Ambient temperature	+15 ºC
	Irradiance	900 W/m^2
	Wind Speed	3 m/s

The simulation results studying the effect of climatic parameters on the photovoltaic string performance under the climatic conditions specified in Table 4.2 are shown as

graphs in Figure 4.13. The operating module temperature, maximum generated power and system efficiency are calculated for each simulation case as well. The latter are presented in Table 4.3 as well as the string characteristic values of V_{OC} and I_{SC}. The module efficiency is calculated as

$$\eta = \frac{P_M}{AG}, \tag{4.7}$$

where P_M is the maximum generated power and A the area of the modules and its value is 22.84 m^2 for the 17-PV modules string.

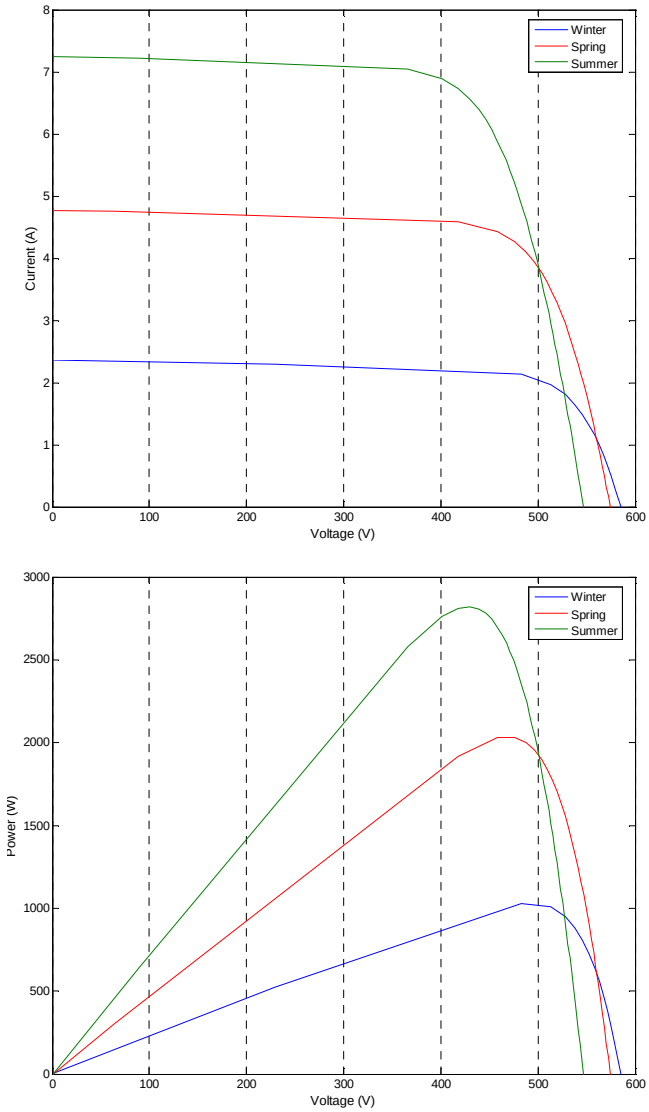

Figure 4.13. *I-V and P-V performance characteristics of the 17 PV modules string under "winter", "spring" and "summer" conditions.*

Figure 4.13 clearly illustrates the effect of climatic conditions on the PV modules characteristics performance. On one hand, the irradiance is fairly proportional to the short-circuit current. Thus, as increasing the irradiance level in the simulated cases, I_{SC}

increases accordingly. On the other hand, the open-circuit voltage is influenced by module temperature and decreases with it.

Table 4.3. *Values of the I_{SC}, V_{OC}, operating module temperature, generated maximum power and system efficiency for the 17-pannels photovoltaic string performance simulations.*

"Winter" conditions:		"Summer" conditions:	
I_{SC}	2.37 A	I_{SC}	7.24 A
V_{OC}	585.20 V	V_{OC}	546.4 V
T_{OP}	-2.32 ºC	T_{OP}	31.12 ºC
P_M	1010 W	P_M	2820 W
η	14.73 %	η	13.72 %
"Spring" conditions:			
I_{SC}	4.78 A		
V_{OC}	574.30 V		
T_{OP}	12.16 ºC		
P_M	2030 W		
η	14.81 %		

The generated power clearly seems to increase proportional to the irradiance received by the photovoltaic string. Though, module temperature has a negative effect on generated power.

Moreover, efficiency is less affected by irradiance since it is divided by the irradiance received by the solar modules. Hence, the system efficiency leads us to compare the overall effect of the climatic variables on the system. It can be roughly said that photovoltaic systems perform with greater efficiency in conditions of lower irradiance levels. This is due to the great influence of the irradiance on the operating module temperature and the negative effect of the latter on the system performance.

To study more carefully the effects of the climatic conditions on the generated power and system efficiency another simulation is carried out. In this last case, the effect of each climatic variable is studied independently and the generated power and system efficiency results are presented as graphs in Figure 4.15. The reference values for temperature, wind speed and irradiance are 5 ºC, 6 m/s and 600 W/m^2, respectively. In each case study the following range of the variables has been used: temperature from -5 to +15 ºC, wind speed from 1 to 12 m/s and irradiance from 200 to 1200 W/m^2.

As expected, the increasing ambient temperature has a negative influence on the generated power and the system efficiency being inverse proportional to both of them. On the other hand, both characteristics parameters increase as the wind speed increases. These two performances are rather expected, because the operating module temperature depends on those climatic variables and, therefore, they influence the system efficiency and generated power.

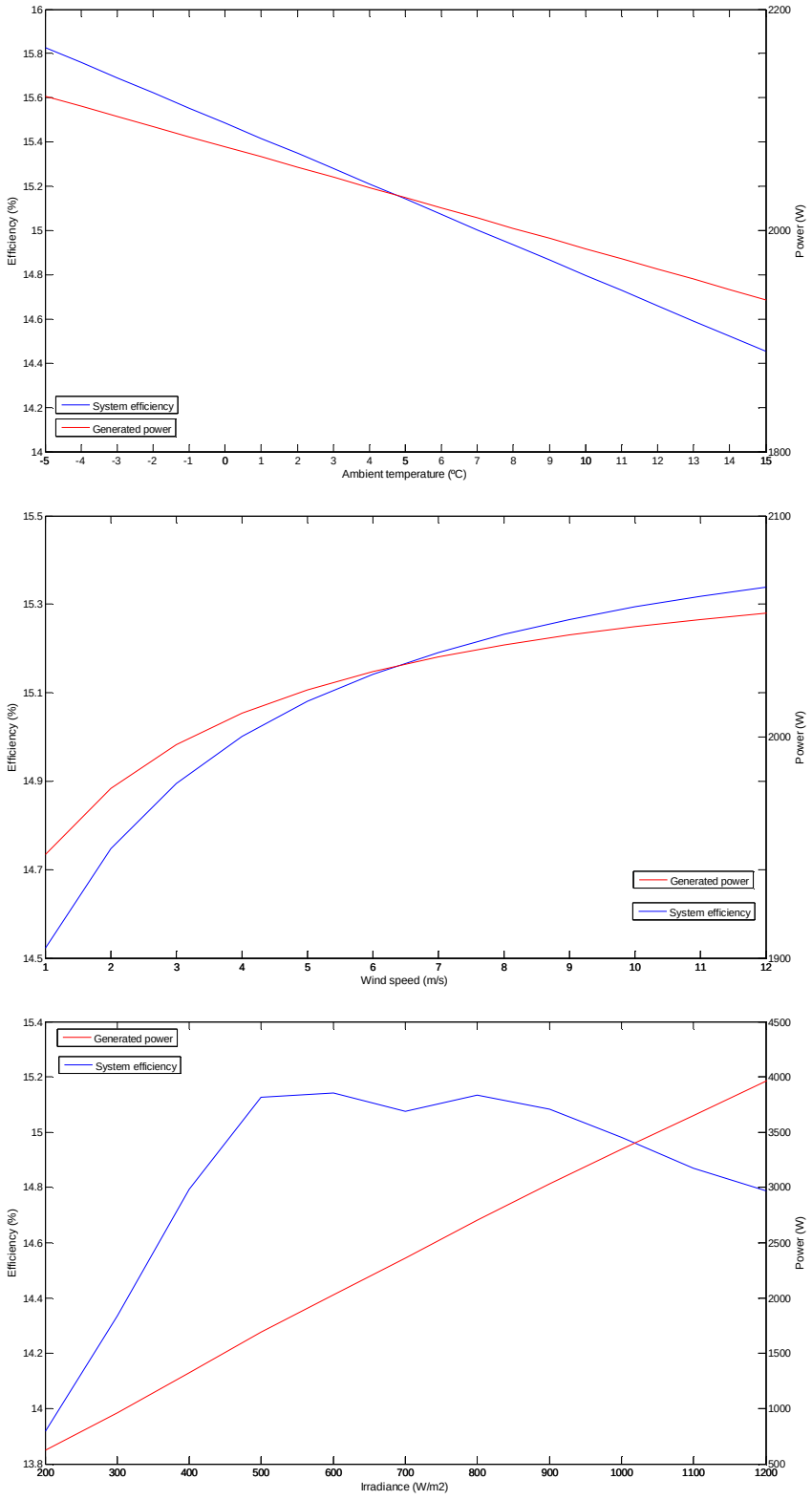

***Figure 4.14**. Generated power and system efficiency as function climatic parameters affecting the performance of 17-PV modules string.*

The effect of irradiance on the system efficiency and generated power is more complex to analyze. Regarding to the generated power, it is directly proportional to the irradiance received by the photovoltaic modules. The system efficiency, although,

presents greatest values for intermediate values of irradiance. This is due to the effect of irradiance on the module temperature and the generated power. On one hand, with increasing level of irradiance the operating temperature increases; which, as known, has a negative influence on the efficiency. On the other hand, since the generated power is directly proportional to irradiance, it leads the system efficiency to increase. Thus, as conclusion, an agreement between the operating temperature and generated power is found for values of irradiance around 600-800 W/m^2, leading to the greatest values of system efficiency.

5. TUT CLIMATIC MEASUREMENT SYSTEM

5.1. Introduction

The aim of this chapter is to describe the designing process of the TUT climatic measurement system and to present the final design of it. This measurement system must accomplish different goals. Accurate measurement of the climatic conditions that affect to the photovoltaic modules performance are required, especially regarding the solar radiation measurements of global, direct and diffuse radiation. On the other hand, it is also essential to measure the operation conditions of the PV modules and strings.

The former requirement is meant for several purposes such as obtaining the climatic condition parameters that affect to the PV panels performance, generating a yearly climatic conditions database, estimating the energy yield of the system, sharing the actual climatic conditions in the department's website or knowing the accurate values of solar radiation received by the system for PV module performance studies. The latter is intended to lead the characterization, calibration and testing of the photovoltaic systems under real operating conditions, as well as to make the testing of several electronic devices such as inverters and interfacing devices possible. The chapter is organised as following.

Section 2 describes the main features of the solar photovoltaic power test plant built on the rooftop of the Department of Electrical Energy Engineering of TUT. Section 3 presents the measurement system considerations and the designing process carried out, summarizing the studied literature for each system and the deeply extensive study of the market need to select the most suitable sensors for the measurements. Later on, the selected components and accessories needed by them are described in detail in Sections 4, 5 and 6. Also technical and mounting issues are discussed in these sections. Finally, in Section 7, a budget summary of the climatic measurement system is presented.

5.2. TUT solar PV power station test plant

The TUT solar PV power station test plant, built during spring of 2010, is composed of 69 solar panels and mounted on the rooftop of the Department of Electrical Energy Engineering in Tampere University of Technology. The plant was meant to be a grid connected system with research purposes. The main lines of research intended are, for instance, to study the influence of different connection of the strings on the generated power, to test and evaluate different power electronic components or systems, such as inverters and to study the effects of environmental parameters in the performance of the generator.

The built system consists of a 69 NP190GKg panels provided by Naps Systems Oy. The total nominal power of the test plant is 12.7 kWp. Modules are based on 54 polycrystalline Si solar cells connected in series. The module electrical performance under STC and dimensions are shown in Table 5.1. [29] For more details see Figure B.2 in Appendix B.

Table 5.1. *Electrical performance and dimensions of the module NP1906Kg. [29]*

Quantity	
Power at max power point (P_{MPP})	190 W
I_{MPP}	7.33 A
V_{MPP}	25.9 V
I_{SC}	8.02 A
V_{OC}	33.1 V
Dimensions (length, width, thickness)	1475 mm x 986 mm x 35 mm
Weight	19.5 kg

The panels are located as shown in Figure B.1 in Appendix B avoiding shadows from other buildings and panels and connected in 6 strings. There are 3 strings of 17 panels and 3 strings of 6 panels with voltage differences of 440 V and 155 V between terminals, respectively. Figure 5.1 shows a picture taken of the photovoltaic station.

Figure 5.1. *Part of the modules of the TUT PV power station test plant.*

Thus, several different outputs are available for numerous power system configurations. String connexions are illustrated in Figure B.3 and Figure B.4 in Appendix B. Basically, there are two configurations which have been already considered to be studied, a four-output and a 3-output configurations. The former consists of 3 strings of 17 panels and another string of 18 modules. The latter consists of 3 strings of 23 modules. The electrical features of both configurations are illustrated in

Table 5.2. However, in principle and also in practise, all the configurations with 69 panels can be connected. The control panel for crossed connections is located in the laboratory in the second floor of the Department, as indicated in Figure B.1 in Appendix B.

Table 5.2. *Electrical features of different string configurations in STC conditions.*

4-outputs configuration			**3-outputs configuration**		
17-panels string:			23-panels string:		
	P_{MPP}	3.1 kW		P_{MPP}	4.2 kW
	U_{MPP}	440 V		U_{MPP}	596 V
	U_{OC}	563 V		U_{OC}	761 V
18-panels string:					
	P_{MPP}	3.3 kW			
	U_{MPP}	466 V			
	U_{OC}	596 V			

Regarding the environmental operating conditions, the specific characteristics of the Finnish climate must be taken into account. Finland is located between the latitudes 60N and 70N in the Northern Europe. Its climate is, despite the location, very favourable to living conditions due to the warming effect of the Gulf Stream. The mean temperature for July in Helsinki is 17 ºC and that for January -6 ºC, which are anomalously high for the latitude belt concerned.

Hence, modules and measurement systems must be prepared to operate under extreme climatic conditions. They may operate at temperatures lower than -25 ºC and without almost any solar radiation during winter. While, during summer, it is possible to reach temperatures greater than +25 ºC and irradiance levels of 1000 W/m^2. This issue is especially important regarding the sensors characteristics performance. For more details about the TUT PV power station test plant see Appendix B.

5.3. Climatic measurement system design

5.3.1. System considerations

As presented in Chapter 3, the Guide to Meteorological Instruments and Methods of Observation defines an automatic weather station (AWS) as a “meteorological station at which observations are made and transmitted automatically”. [42] This guide also establishes the meteorological and climatologic requirements that any AWS must accomplish, as well as the measurement methods to follow and the standards references.

After studying several weather stations designed by the Finnish Meteorological Institute as the Joikonen observatory or the ones located in Taivalkoski Kk Kauppatie and Espoo Sepänkylä, or the AEMET’s weather station located in Zaragoza’s airport; [1] it is possible to assume that the most commonly measured climatic parameters are

temperature, humidity, visibility, wind speed, wind direction, precipitation, etc. Regarding the sunshine duration and solar radiation, stations like the Helsinki Kumpula's one mostly measure ultraviolet, global and diffuse radiation. [9]

However, according to the objectives described in the previous section, the designed system has to be focused on measuring the climatic parameters that affect to the solar module's performance. These ones are ambient temperature, humidity, wind speed, wind direction and solar radiation (global, direct and diffuse). They have been described more closely in Chapter 3.

On the other hand, diverse literature [16, 10, 21, etc.] bases the characterization of photovoltaic modules and strings mostly on the knowledge of irradiance received by the solar panels, the operating module temperature and power characteristic parameters. Nevertheless, some other parameters that influence the performance of the photovoltaic systems as wind speed and ambient temperature are usually measured too. [7, 18]

The most important difference between the described sensors needed for both purposes is that the required quality for the weather station's sensors is well established and higher than the quality of the sensors needed to perform the characterization of the modules. In addition, to study the PV panels' characteristics, a precise knowledge about the shadowing conditions of the strings is needed, as well as the operating temperature of each string of the plant. Thus, several solar and module temperature sensors must be carefully located to control all the solar PV power station test plant's strings and modules. This, in case of using the accurate and more expensive sensors required for the weather station, would mean an unaffordable expensive system.

It is apparent to reach the conclusion that both systems must be designed separately, focusing on the requirements needed to satisfy each case. The result is an accurate weather station that measures the global climatic conditions of the plant, including ambient temperature, humidity, wind speed and direction and global and diffuse solar radiation; and a climatic monitoring system to lead the characterization of the photovoltaic generator. However, conditions such as wind speed and direction or humidity are not needed to be measured by the latter system since they are not changing in the small area where the power plant is located (within a diameter of 50 m).

Regarding the data-acquisition system, as commented in Section 3.6, a computer-based DAQ system is the most suitable and desirable option. [18] Several references [10, Beng10, and 32] base the data-acquisition system on microcontrollers, but for a system acquiring so many signals it is not the best and most efficient solution. Besides of that, synchronization processes are needed to match the climatic measurements with the power measurements of the system in order to allow analyzing the PV systems performance.

The following subsections present the state-of-the-art of the measurement systems design, as well as of the DAQ-systems related to the climatic monitoring systems.

5.3.2. Automatic weather station

When facing the designing of a state-of-the-art weather station meant to accomplish some general high-quality measurements and to satisfy some particular measurement needs at the same time, the first stage consist in studying the literature available, as well as other projects already designed with similar purpose and defining the criteria to attend. Hence, after reading several references as Garrison [11], van der Bos [38], the Guide to Meteorological Instruments and Methods of Observation [42], etc.; Chapter 3 gathered the most important aspects leading to design an automatic weather station based on numerous measurement variables. Table 5.3 summarizes the sensor types described in Chapter 3 for the different climatic variables that the AWS must measure.

Table 5.3. *Sensor types for the different climatic variables measured in the weather station.*

Climatic variable	**Sensor type**
Temperature	Electrical resistance thermometer (RTD)
	Thermistor
	Thermocouple
Humidity	Chilled mirror meters
	Psychometric meters
	Capacitance sensors
Wind speed and direction	Cup and propeller sensors
	Wind direction vanes
	Sonic anemometers
Solar radiation	Pyranometers
	Pyrheliometers

The second stage of the designing process is to carry out a deeply extensive study of the market according to the criteria established in Chapter 3. The most suitable sensors and interfaces are selected, also regarding to the availability and delivering conditions of the providers. It is important to empathise that all the sensors must be able to operate under the extreme conditions that the Finnish climate presents. This market study is shown in Appendix A of this document. In it, several sensors for each climatic variable are presented and an operational budget in Section A.4 is included as well.

It must be said that not just the described sensors in Appendix A were sought but some other companies were contacted asking for interesting sensors. From some of them, even from some companies of the presented sensors, the answer was unfavourable due to the delivery extra costs and timing. Also the contacts and associations of the Tampere University of Technology with national and international companies as Vaisala and National Instruments were an important matter to take into consideration during the designing process.

After gathering all the information and knowing the different available options, it is time to make an assessment to decide the sensors that make the weather station. The following lines describe the procedure carried out.

For the ambient temperature a digital resistance thermometer is the chosen option. Platinum RTD provides the most accurate measurement even in most extreme conditions. This issue is especially important for the relative humidity sensor due to the fact that, under these environmental conditions, it must be heated for a proper operation. The closest sensors to these conditions are the Climatronics P/N 101812 G2 and the Vaisala HMP155. However, due to the already commented relation between the TUT and Vasiala and to the fact that it was impossible to contact a suitable provider of Climatronics for Finland, the Vaisala HMP155 is the selected one. The HMP155 are shown in Table A.2, in Section A.1.

The first idea for the wind speed and direction sensors was to utilize a high-quality cup and vane wind measurement station adapted for the environmental conditions with heating systems. It seemed the most accurate solution and also very trustable since many currently operating weather stations use this type of sensors. Though, after discussing the topic with some sale manager engineers, it came to light that a cup and vane wind station would need yearly maintenance due to the environmental conditions. Therefore, using an ultrasonic wind sensor which does not need almost any maintenance is the most suitable option for the weather station. Since Vaisala offers a fitting sensor and it is already decided to order the ambient temperature and relative humidity sensors to this company, the WS425 ultrasonic wind sensor is the chosen option. The WS425 features are shown in Table A.8 (Section A.2).

The quality and accuracy requested to the solar radiation measurements entails using secondary standard instruments or first class, in case of using a pyrheliometer. This condition already excludes most of the instruments of the market due to the fact that most of the commercial pyranometers are not designed for research applications but for applied purposes. Hence, just the Kipp&Zonnen instruments are suitable for the solar radiation measurements (for more detailed information, see Section A.3).

As commented in Chapter 3, there are two possible methods to measure the global, direct and diffuse radiation: using a pyrheliometer mounted on a sun-tracker and a pyranometer or using two pyranometers, one mounted with a shadowing ring. After studying the two options, it is easy to prove that the first option is the most accurate solution but much more expensive due to the cost of the sun-tracker (for detailed information, see Table A.18). Thus, it is decided to build a system composed by a CMP22 and a CMP21 pyranometers. These instruments are respectively chosen to operate measuring the solar global radiation reaching the area and to be mounted with a shadowing ring measuring the diffuse radiation.

5.3.3. Operating conditions monitoring system

As commented in previous sections, characterization of photovoltaic modules is based on the observation and measurement of the current operation conditions. They generally may be separated in two groups: power operation and climatic conditions. The latter is a collection of variables that affect the operating performance of the modules and include irradiance received by the panels, ambient temperature, wind speed and direction and

operating module temperature, among others. King [16] provides several test methods and analytical procedures for characterizing the electrical performance of PV modules and arrays.

Just a few literature sources are available that established the criteria to design this type of systems but there is large specific literature that provides numerous solutions. Hence the first stage to design the monitoring system is to study several different articles learning the solutions proposed by the authors for their own systems. The following lines describe in detail the main purpose of the studied monitoring systems as well as the sensors and interfaces used.

Forero et al. [10] develop a novel data acquisition system designed and implemented with facilities for monitoring the operation of a stand-alone solar PV plant and for measuring, acquiring and statistically evaluating the environmental variables. Their system provides facilities to get information through measurements of environmental and system variables. The measurements of the solar radiation are taken using a SP Lite pyranometer of the firm Kipp&Zonen. The ambient temperature measurements are taken with a NTC thermistor.

Durisch et al. [6] develop, test and put into operation a flexible test stand for outdoor characterisation of single cells and modules at the Paul Scherrer Institute (PSI). A sun tracker provides precise solar alignment for the probes. Six pyranometers CM21 of Kipp&Zonen and two reference cells of Siemens are mounted on the tracking system. The direct irradiance is measured using pyrheliometers Eppley mounted on separate sun trackers developed by PSI. The ambient temperature is measured using a ventilated radiation-shield Pt-100 sensor. A surface-temperature probe Pt-100 is arranged on the back of the modules to measure their temperature.

Martínez Bohórques et at. [23] design, construct and test a complete temperature-measuring instrumentation system based on precision Pt-100-type analogue sensors. They attach the sensors to the back-side of the solar modules to measure their operating temperature.

Koutroulis et al. [18] propose a computer-based data-acquisition system for monitoring both meteorological data and renewable energy source system operational parameters. The ambient temperature and humidity are measured using the Rotronic MP100A hygrometer and the global irradiance is measured using the Delta-T GS1 pyranometer. The wind speed and direction parameters are measured with the A100R anemometer and W200P type wind vane of Vector Instruments.

Benghanem [5] develops a low cost, autonomous remote weather data acquisition system, using readily and easily available equipment to collect and transfer local data to any PC equipped with an Internet connection. The measurement of solar irradiation is dedicated to a solar cell calibrated with a pyranometer of Kipp&Zonen. For the humidity measurement a Humirel HS1101 capacitive sensor is taken and the temperature measurements are made with a thermistor. The wind speed and direction are measured using the A100R anemometer and W200P wind vane of Virtual

Instruments. Table 5.4 gathers the different sensors used in the previous studied systems.

Table 5.4. *Sensors used in the different studied systems.*

Parameter	Forero [10]	Durisch [6]	Martínez [23]	Koutroulis [18]	Benghanem [5]
Ambient temp.	Thermistor	Pt-100		MP100A	Thermistor
Humidity				MP100A	HS1101
Wind speed				A100R	A100R
Wind direction				W200P	W200P
Global radiation	Sp Lite	CM21		GS1	
Direct radiation		Eppley			
Module temp.		Pt-100	Pt-100		

In the matter of our system, the measurements of ambient temperature, humidity, wind speed and direction are already provided by the sensors of the weather station. The WS also provides accurate solar radiation data hence just the measurement of the temperature of modules is missing. However, an accurate knowledge about the shadowing conditions of each string is need, thus comprehensive mesh of solar radiation sensors and module temperature sensors is the objective of this system.

Regarding the module temperature sensing, as well as in Durisch et al. [6] and Martínez et al. [23], the best option is selecting an adhesive Pt-100 temperature sensor to measure the operating temperature.

To measure the irradiance conditions of the strings, as Forero et al. [10] and Durisch et al. [6], a Kipp&Zonen pyranometer is the chosen option. However, due to the fact that several radiation sensors are need to provide information about the irradiance and shadowing conditions of all the strings of the plant, a lower cost Sp Lite 2 photodiode-based pyranometer is the selected one (for more detailed information, see Section A.3 in Appendix A).

5.4. Automatic weather station

This section is meant to describe in detail the selected sensors that compose the weather station including the optional systems and accessories that they need to operate such as radiation shields, ventilation units, mounting brackets, power sources, etc. A scheme of the global system is shown in Figure 5.2.

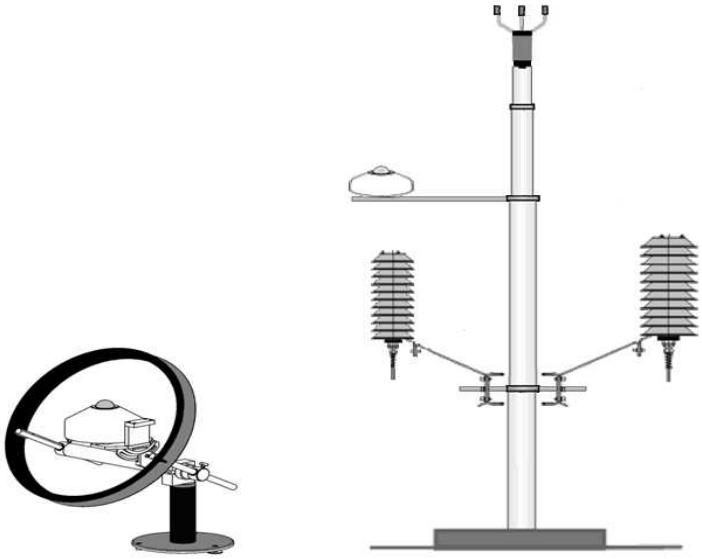

Figure 5.2. *Scheme of the designed weather station including the ambient temperature and relative humidity, wind speed and direction and global and diffuse solar radiation sensors.*

The sensor used for ambient temperature and relative humidity is a calibrated HMP155. It is an instrument composed by a humidity sensor that needs to be heated so an extra temperature probe is needed to measure the ambient temperature. Figure 5.3 shows the humidity sensor and the extra temperature probe. The sensor is ordered with an analogical output from 0 to 10 mA. To protect both probes several radiation shields are need, the DTR503A for the humidity sensor and the DTR502 for the temperature probe (both shields during the mounting process are shown in Figure 5.4.) Finally, a power supply of 16 to 28 V and 150 mA is need for the heating system. However, instead of ordering it also from Vaisala, this power supply is provided by local providers.

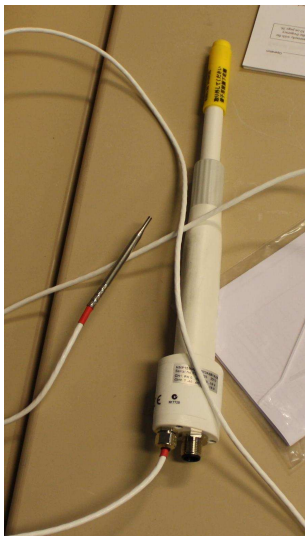

Figure 5.3. *HMP155 sensor with the extra temperature probe during the mounting process.*

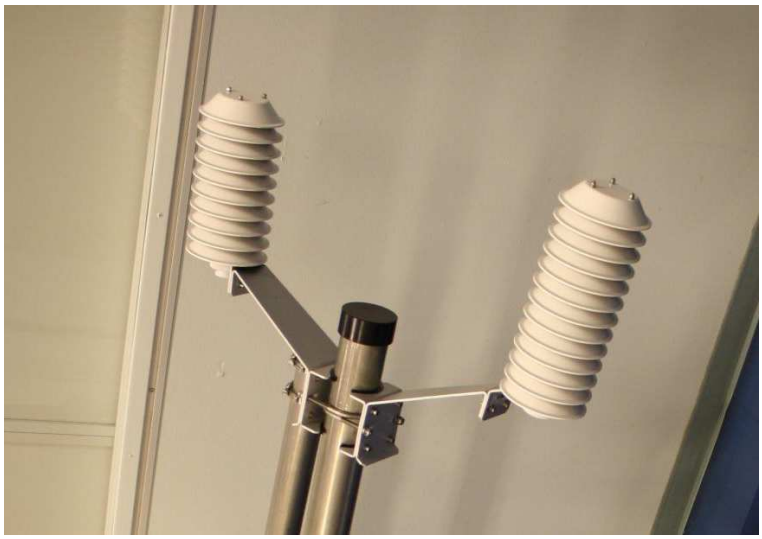

Figure 5.4. *Radiation shields DTR503 and DTR502 joined to the pole during the mounting process.*

WS425 ultrasonic wind sensor is the chosen sensor to measure the wind speed and direction. Figure 5.5 shows the WS425 sensor during the mounting process in the laboratory. It provides a digital output and needs a specific interface to produce an analogical output. A more economical model of the serial to analog converter is ordered from Nokeval. WS425 also needs two power supplies, one to operate and another one for the heating system. This heating system prevents from snow accumulation and freezing of the emitters. The main features of the power supplies are voltage range from 10 to 15 V and current of 12 mA and 36 V, 0.7 mA, respective. As in the previous case, these power supplies are from local providers.

Figure 5.5. *WS425 ultrasonic wind sensor during the mounting process.*

Regarding the solar radiation sensors, as described in Section 5.2.4, CMP22 and CMP21 pyranometers from Kipp&Zonen are used to measure the global and diffuse radiation. These sensors need a ventilation unit to be able to operate under the environmental conditions of the location so 2 CV3 ventilation units were ordered as well. Figure 5.6 shows a CMP22 pyranometer mounted with the cover of the ventilation unit and Figure 5.7 shows the heating system of the ventilation unit itself. Pyranometers are passive sensors that do not need powering, but the ventilation units need. So another two power supplies are need, the voltage and current of them are 12 V and 1.3 A, respectively. Concerning the mounting issues, the pyranometer CMP22 needs a mounting bracket and plate to be located on, while the pyranometer CMP21 is mounted on the shadowing ring CM121C as shown in Figure 5.8.

The shadowing ring keeps the pyranometer in the shade during the entire day, preventing the direct solar radiation to reach the sensor. As a result only the diffuse solar radiation is measured. A regular schedule of maintenance would require manual adjustment of the sliding bars that are connected to the actual shadow ring. Naturally, the shadow ring intercepts also a proportion of the diffuse sky radiation. A correction factor for this effect is recommended to be used as a refinement of the measurement. A table of correction factors is combined with the table for sliding bar setting.

Figure 5.6. *Kipp&Zonen's pyranometer CMP22 mounted under the cover of the CV3 ventilation unit.*

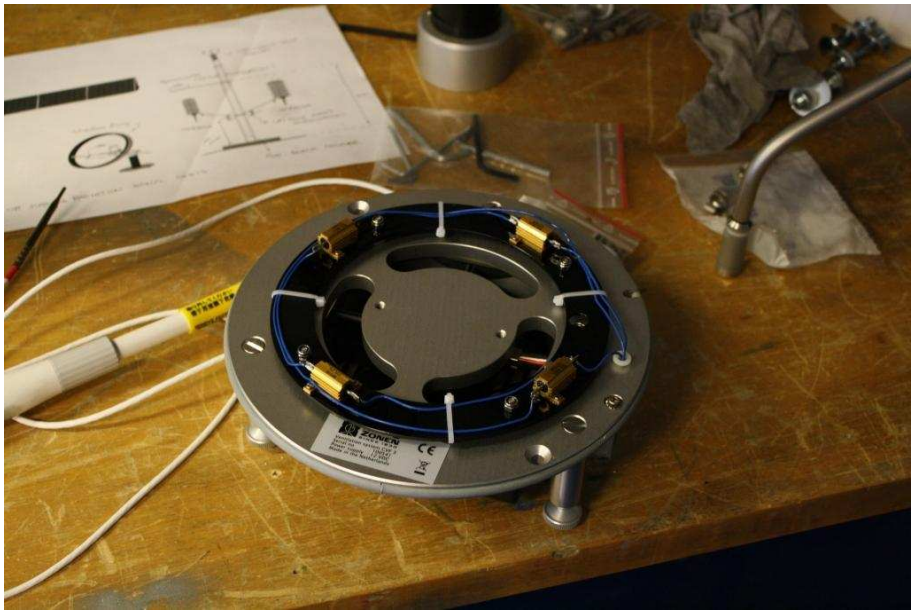

Figure 5.7. *Kipp&Zonen's CV3 ventilation unit system during the mounting process.*

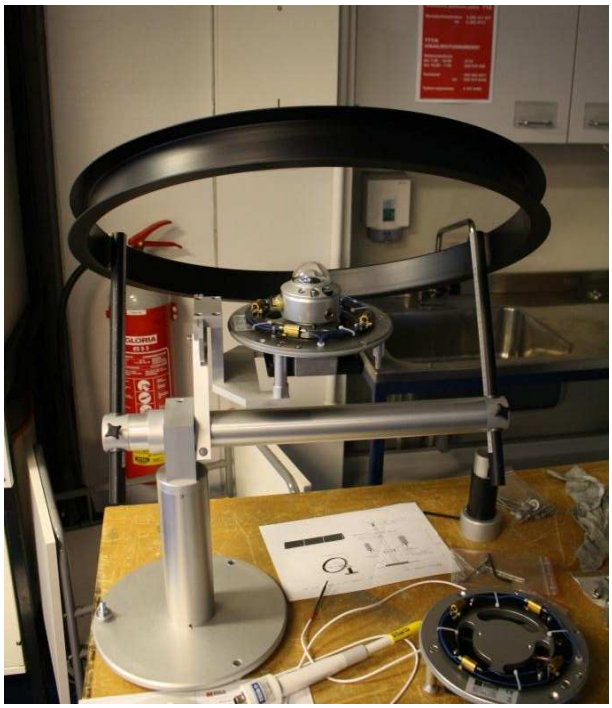

Figure 5.8. *Pyranometer CMP21 mounted on the CM121C shadow ring with the CV3 ventilation unit during the mounting process in the laboratory.*

The first idea was to mount all the sensors, except the pyranometer mounted on the shadowing ring, on a vertical pole as shown in the scheme in Figure 5.1. However, after discussing with the technicians of the laboratory, it was decided that the best choice is to use two different poles to reduce the height and make easier the mounting process. One pole will be for the ambient temperature and relative humidity sensors with their radiation shields and another one for the CMP22 and the ultrasonic wind sensor located on the top of it. The location of the poles is decided to be set on the highest point of the

top-roof of the Department of Electrical Energy Engineering. On the other hand, the CMP21 pyranometer and the shadow ring are decided to be located on a more accessible point on the top-roof due to the need to adjust the position of the shadow ring periodically in every two weeks.

5.5. Irradiance and temperature measurement system for modules

The comprehensive mesh of solar radiation and module temperature sensors to provide measurements of the operating conditions through the whole solar power plant facility is decided to be built using photodiode-based pyranometers SP Lite 2 of the firm Kipp&Zonen and temperature sensors Pt-100-type RTDs.

SP Lite 2 sensors are passive sensors that do not need powering or any extra instrumentation or interfacing. They provide an analogical output and can be directly connected to the data-acquisition system. These sensors are decided to be mounted with the same tilt as the PV strings so they can provide the exact irradiance yielded on the modules. A pair of sensors is mounted for each string to provide information when the string starts and ends to be under solar radiation. In this way it is also possible to interpolate when a cloud is partially covering the string. Figure 5.9 shows a SP Lite 2 during the mounting process.

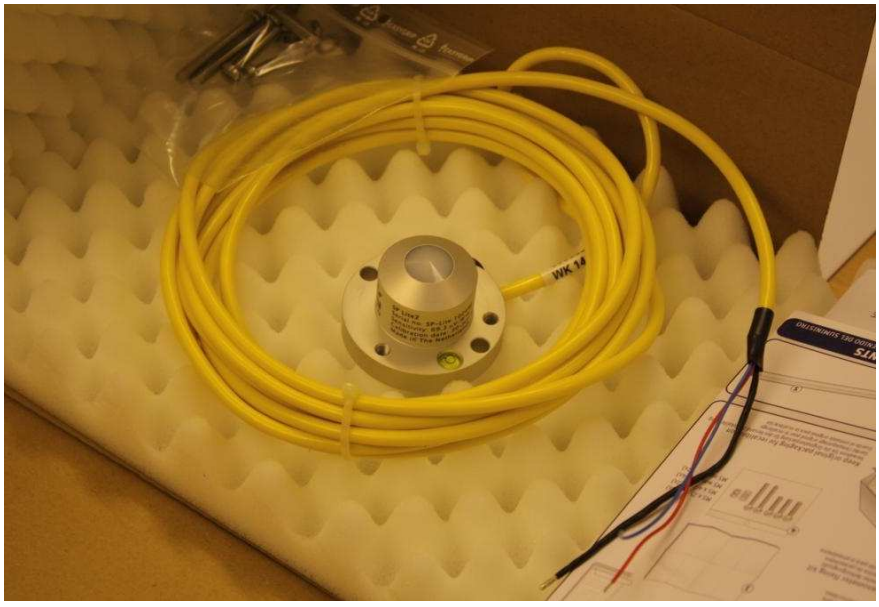

Figure 5.9. *Photodiode-based pyranometer SP Lite 2 during the mounting process in the laboratory.*

The temperature Pt-100 sensors are provided by National Instruments. A 3-wires connection is chosen to improve the measurement accuracy and to reduce the noise. These sensors are attached to the back-side of the photovoltaic modules so they measure quite closely the operating temperature of the solar cells. It has been decided to install a

temperature sensor jointly with each photodiode to obtain couples of irradiance and module temperature measurements.

The available space on the rooftop of the department and the different obstacles for the solar radiation made necessary to split the solar strings according to the possibilities as can be seen in Figure 5.1. Due this matter, more than two couples of irradiance and module temperature sensors (I-M) are needed per string. The main idea is to know the operating conditions of each PV module. Hence two couples I-M sensors are decided to be located for each group of solar panels. However, in case the irradiance condition of several groups is the same there is no need to set extra I-M sensor couples. Therefore, 17 couples of I-M sensors are needed to satisfy the objective of the system and they make the so called Temperature-Irradiance System.

There are still four solar modules that are meant to operate alone (the "Extra" modules). The purpose of these modules is to serve prototyping and testing at low voltages save for personnel. It was decided to install an extra I-M couple of sensors for each of these panels: the Extra Modules System.

Thus 21 SP Lite 2 and Pt-100 sensors are respectively ordered from Kipp&Zonen and National Instruments. Figure 5.10 shows a scheme with the location of the 21 couples of sensors through the TUT solar PV power test plant.

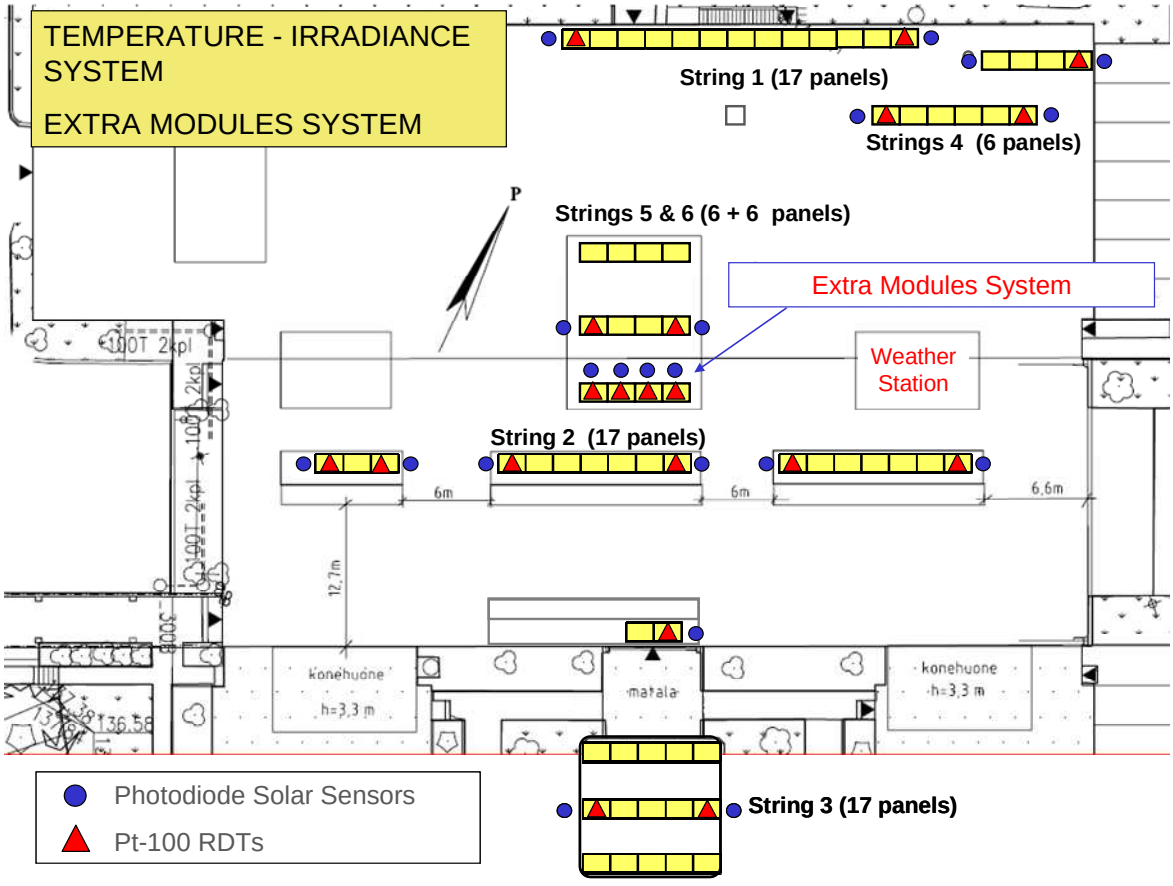

Figure 5.10. *Scheme of the location of the SP Lite 2 and Pt-100 sensors over the TUT PV solar power test plant.*

5.6. Data acquisition system

After studying several possible data acquisition system architectures, as explained in Section 3.7, a computer-based data-acquisition system is the chosen option to acquiesce and digitalize the data provided by the sensors as shown in Figure 5.11. Due to the current agreement of the TUT with National Instruments (NI) and that the TUT already has the licence for the software Laibview, it was decided to use data-acquisition systems of this firm. The next stage is to study the different solutions provided by NI for such a system.

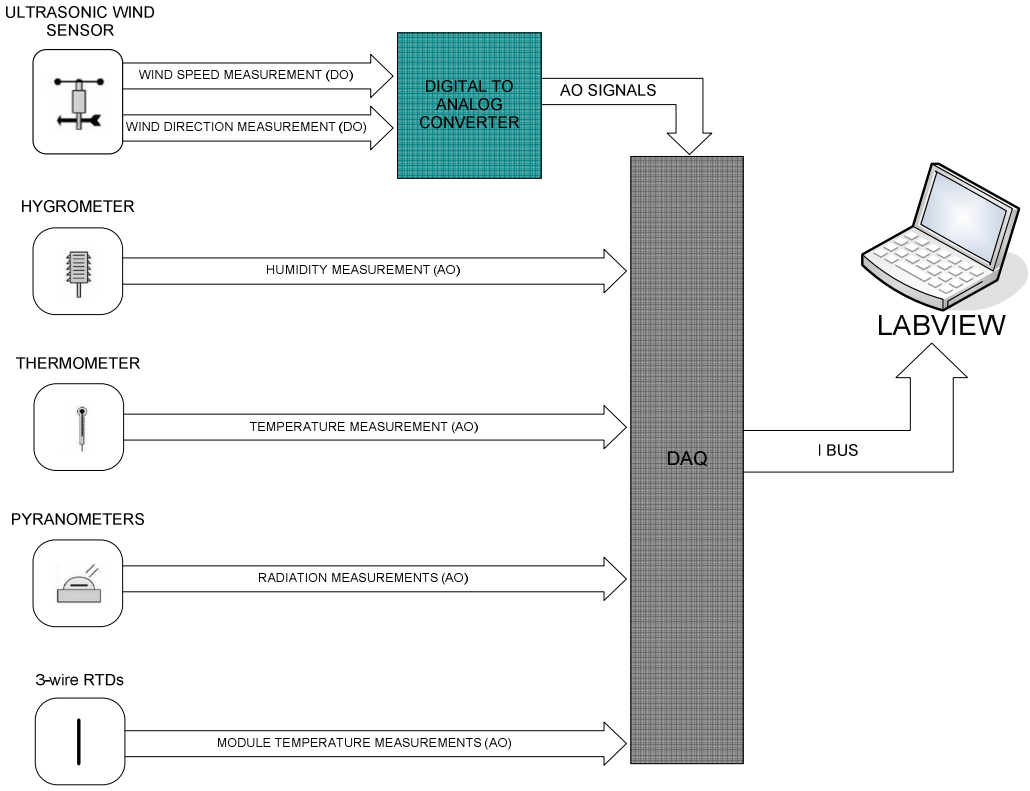

Figure 5.11. *Block diagram of the TUT Measurement System.*

National Instruments offers a PC-based measurements and large variety of PC-buses and form factors, including USB, PCI, PCI Express, PXI, PXI Express, wireless, and Ethernet. [30] According to the sampling needs of a climatic measurements system, the first approach was using CompactDAQs and several swappable I/O modules connected to the PC by USB connection. This suitable solution leaded to a very flexible and economical system that allowed using specific modules to connect the sensor outputs. However, after presenting the designed sensor system and discussing the matter with a sales manager from NI it came up that a better solution may be using an Ethernet connection. For this, a CompactRio data-acquisition card is needed and it perfectly suits to the measurement system, satisfying all the requirements. The swappable I/O modules are the same for both CompactDAQ and CompactRio systems.

Thus, a master and slave system is decided to be used to acquire and transmit the signals provided by the sensors. Both RIO units are acquiring and the slave unit transmits the already digitalized data to the master. This master transmits all the information to a PC through an Ethernet cable without interference and noise problems. This type of acquisition system allows to locate the units to the nearest possible to the sensors decreasing the needed cable lengths. Another benefit of using two units is that possible future extensions of the system are allowed, just changing the I/O modules or including more is need. The CompactRIO units and part of the I/O modules used are shown in Figure 5.12.

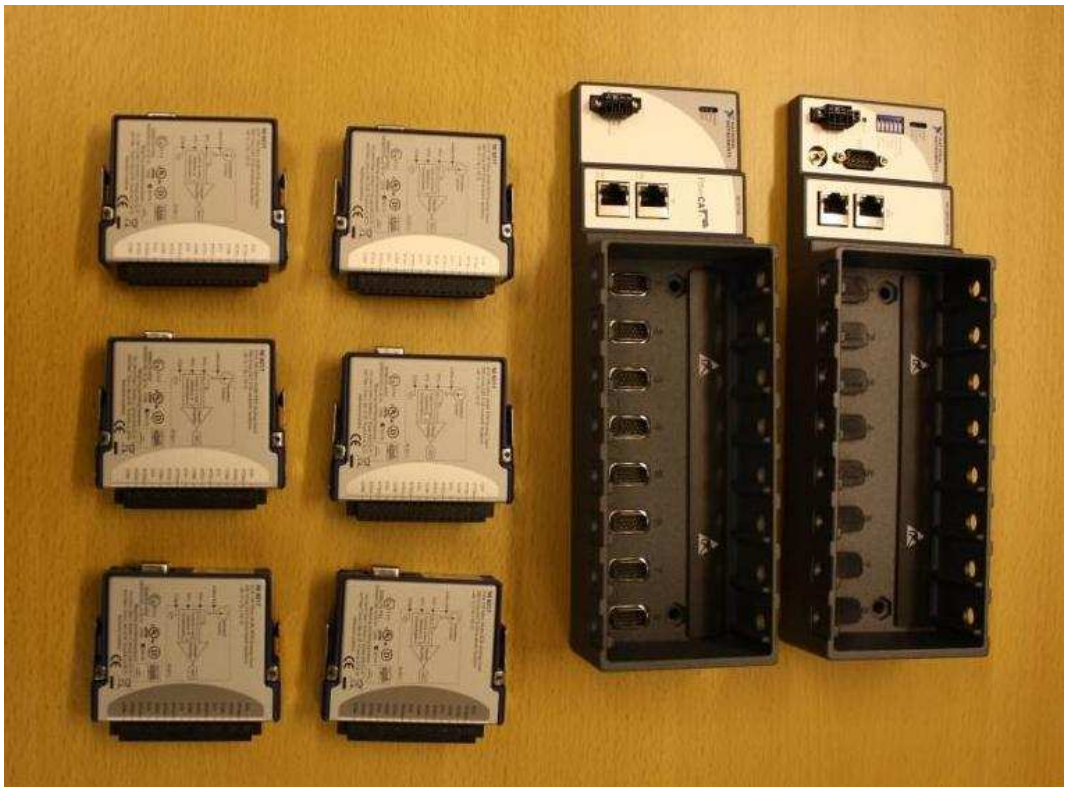

Figure 5.12. *Components of the data-acquisition system during the mounting process.*

Regarding the selection of the necessary I/O modules to acquire the signals coming from the sensors, it is the basic need to gather all the signals and signal types to manage them. The measurement system provides 6 analogical signals of 0 – 1 V from the weather station, 21 analogical signals in the range of mV from the photodiodes and measurements from the 21 Pt-100 3-wire sensors. Hence, the 28 analogical voltage signals are acquired using 2 NI9205 I/O modules with 32 inputs each of them, one module per CompactRIO unit. And the 21 signals from the 3-wire type Pt-100 sensors are acquired using specific I/O modules of NI for this type of sensors. Therefore, 6 NI9217 modules with 4 channels per module are ordered form National Instruments.

5.7. Budget summary

Finally, Table 5.5 presents information about the cost of the different components of the system divided by the supplying companies. It is important to mention that NI offered important discounts in all the ordered devices. In this way, Vaisala's bill reaches 5.658 €, Perel Oy's (provider in Finland of Kipp&Zonen) one 23.694 € and NI's one 6.262 €. The total amount of the TUT climatic measurement system purchase price reaches 35.614 €. For more detailed information, the ordering bills can be found in Appendix C.

Table 5.5. *Budget summary of the climatic measurement system.*

Company	**Device**	**Units**	**Price**		**Total**
Vaisala	HMP115A	1	1,137.00 €		1,137.00 €
	DTR503A	1	312.00 €		312.00 €
	DTR502B	1	300.00 €		300.00 €
	WS425	1	2,889.00 €		2,889.00 €
	VAT			22%	1,020.36 €
				Subtotal 1:	**5,658.36 €**
Kipp&Zonen	SP Lite 2	21	316.00 €		6,636.00 €
	CMF2	1	294.00 €		294.00 €
	CVF3	2	941.00 €		1,882.00 €
	CM121C	1	2,436.00 €		2,436.00 €
	CMP21	1	2,638.00 €		2,638.00 €
	CMP22	1	5,535.00 €		5,535.00 €
	VAT			22%	4,272.62 €
				Subtotal 2:	**23,693.62 €**
National Instruments	CRIO-9074	1	2,399.00 €	-70%	719.70 €
	NI 91444	1	879.00 €	-10%	791.10 €
	NI 9205	2	699.00 €	-10%	1,258.20 €
	NI 9217	6	419.00 €	-25%	1,885.50 €
	Pt-100	21	29.00 €	-25%	456.75 €
	VAT			22%	1,129.21 €
				Subtotal 3:	**6,261.96 €**
				Total:	**35,613.94 €**

6. PV MODULES AND SENSORS TESTING

6.1. Introduction

The aim of this chapter is to present the obtained results after testing the photovoltaic modules and sensors. First the irradiance and module temperature measurement system built is presented, followed by a description of the power measurement system design. As explained in the previous chapter, this system is composed by pairs of irradiance and module temperature sensors at the ends of each string of the power testing plant. In Figure 6.1 a photodiode-based pyranometer can be seen mounted next to a solar module. The pyranometers are mounted with the same tilt as the modules in order to receive the same amount of solar radiation than the strings. Figure 6.2 shows a module temperature sensor attached to the back-side part of the same PV module. To achieve it, the RTDs are stuck with special glue and pushed against the module.

Figure 6.1. SP Lite 2 pyranometer mounted next to a photovoltaic string.

Figure 6.2. Platinum RTD attached to the back-side of a PV module.

Regarding the automatic weather station and the solar radiation sensors, they must be mounted as explained in Chapter 5. The ultrasonic wind sensor is located on the top of a pole that also supports the pyranometer that measures the global solar radiation received by the plant. The ambient temperature and relative humidity sensors are located on another pole, protected by individual radiation shields that also support the sensors. Finally, the pyranometer meant to measure the diffuse solar radiation is mounted on the shadowing ring support.

The measurements are carried out in close collaboration within the power electronics part of the research group. They are researching on systems to measure the electrical performance of the photovoltaic modules. So far, they have developed a measurement method that utilizes IGBT switch channels as electronically variable resistors. The goal is to find a simple and reliable solution to measure the *I-V* curve in laboratory conditions quickly and accurately. A scheme of the connection is shown in Figure 6.3.

The measuring device is composed of a 1 GHz digital oscilloscope, a DC power source, and plug-in power and voltage probes of the oscilloscope. The oscilloscope stores in desired intervals the currents and voltages of the solar modules. Where necessary, a traditional presentation of current-voltage curve can be plotted. Data in the oscilloscope's memory may be stored for later analysis. Figure 6.4 shows a picture of the power measurement system.

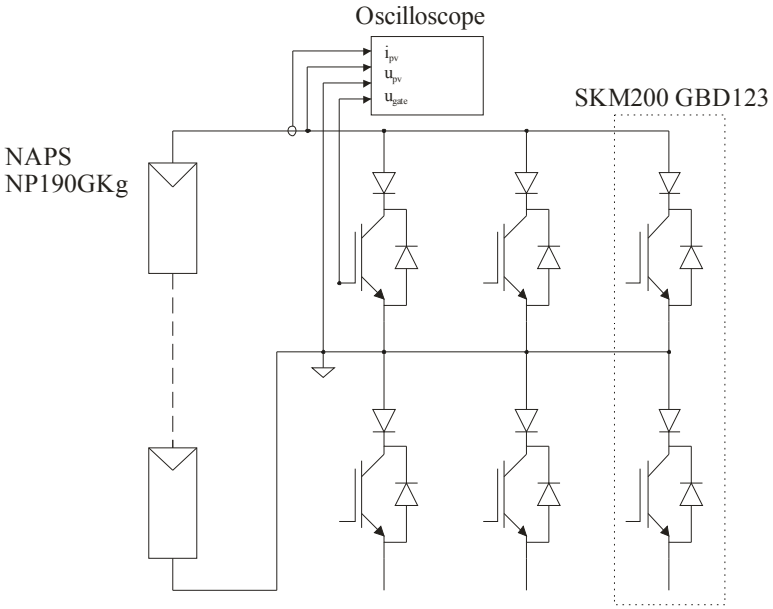

Figure 6.3. Scheme of the I-V curve measurement method for PV power systems.

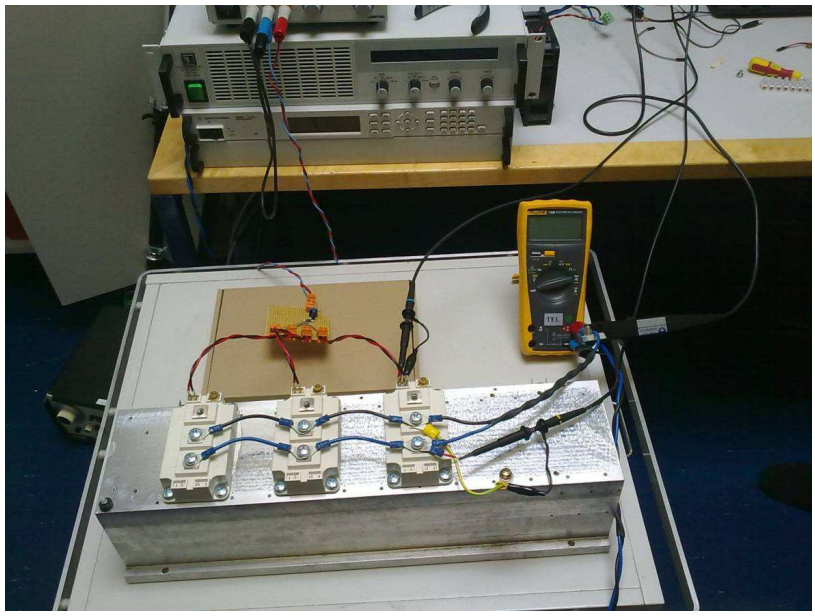

Figure 6.4. IGBT modules, cooler and power measuring connections.

The initial idea was to test the PV modules and the designed measuring system after finishing building the climatic measuring system, always considering this objective as a secondary objective of the project due to the delivering and mounting stages. Eventually, it has been impossible to build the system in time to carry out a proper testing of it for this thesis. This was due to the timescales of goods delivery and installation, which were not part of this thesis project. It turned out that also partial testing of the measurement system was not feasible within the timescale. Therefore, the electrical performance of the PV power plant was measured utilizing the climatic data measured using the facilities of the Department of Electronics.

String voltage and current are measured to obtain the electrical performance of the strings and their I-V curves. On the other hand, the Department of Electronics' facility provides ambient temperature, relative humidity, wind speed, irradiance and module temperature data of the whole measuring days. Next sections present the measurements and simulations carried out based on the described systems. The measurements of the different quantities have been made at the same time thus, it is possible to match them.

6.2. Operating conditions measurements

Several power measurements have been taken during two days with very different climatic conditions. The first measurements were taken in August, when climatic conditions were still warm and with high amount of irradiance. The second measurements were taken in September in a cloudy day with clear sky at some points and at lower temperatures.

Weather measurement data from the Department of Electronics are completely available only for the first measurement day, because the data was partially corrupted during the second day. Particularly, the corrupted data includes the time from 6 h to 13 h. Thus the irradiance and module temperature for the second day are not available. Hence, the irradiance received by the string is obtained by simulating the string's electrical performance for different irradiance values and comparing it with the measured electrical values. Since the irradiance has a great influence on the power generated and short-circuit current, these are the parameters that must be compared to find the approximated irradiance received by the string.

In the first measuring day, two different strings are measured: a 17-panels string and a 6-panels string. The latter day, this last string is measured several times with different climatic conditions. Table 6.1 shows the dates and times when the power measurements took place. Figures 6.5 and 6.6 show the measured irradiance (red line) and module temperature (blue line) during the days where the measurements were carried out. The exact moments when the power measurements take place are specified with a cyan coloured circle.

Table 6.1. Times of the power measurements.

Measurement	Date	Time
M1 (6 panels)	26/08/2010	09:48
M2 (17 panels)	26/08/2010	11:20
M3 (6 panels)	06/09/2010	08:58
M4 (6 panels)	06/09/2010	12:48
M5 (6 panels)	06/09/2010	12:53

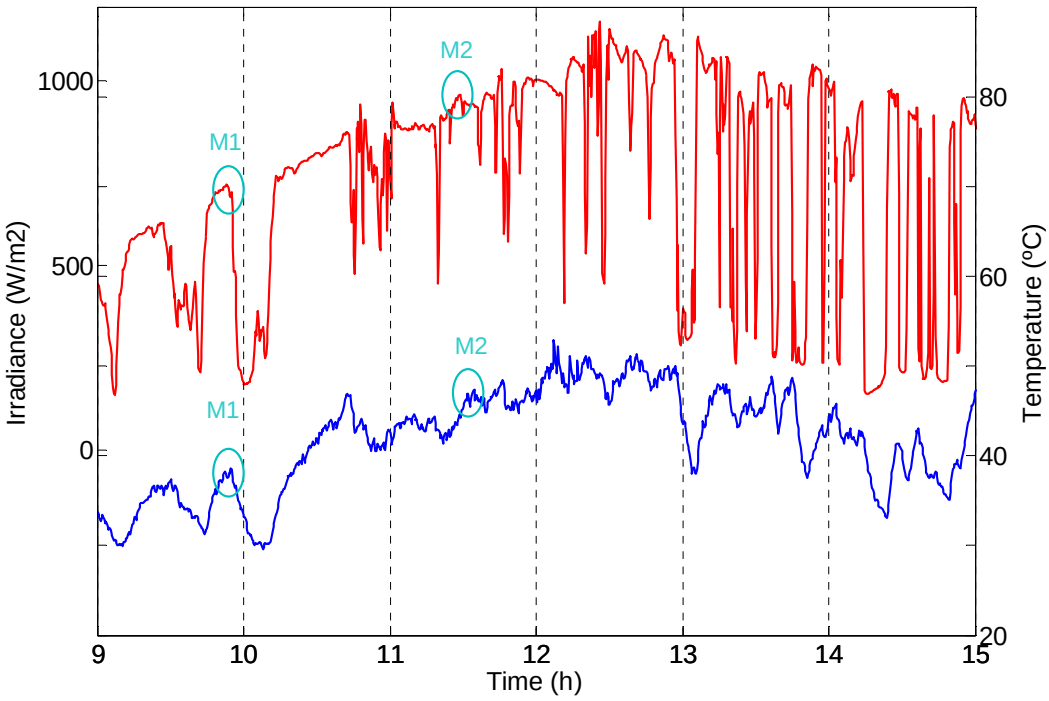

Figure 6.5. Irradiance and module temperature measured in August 26th 2010.

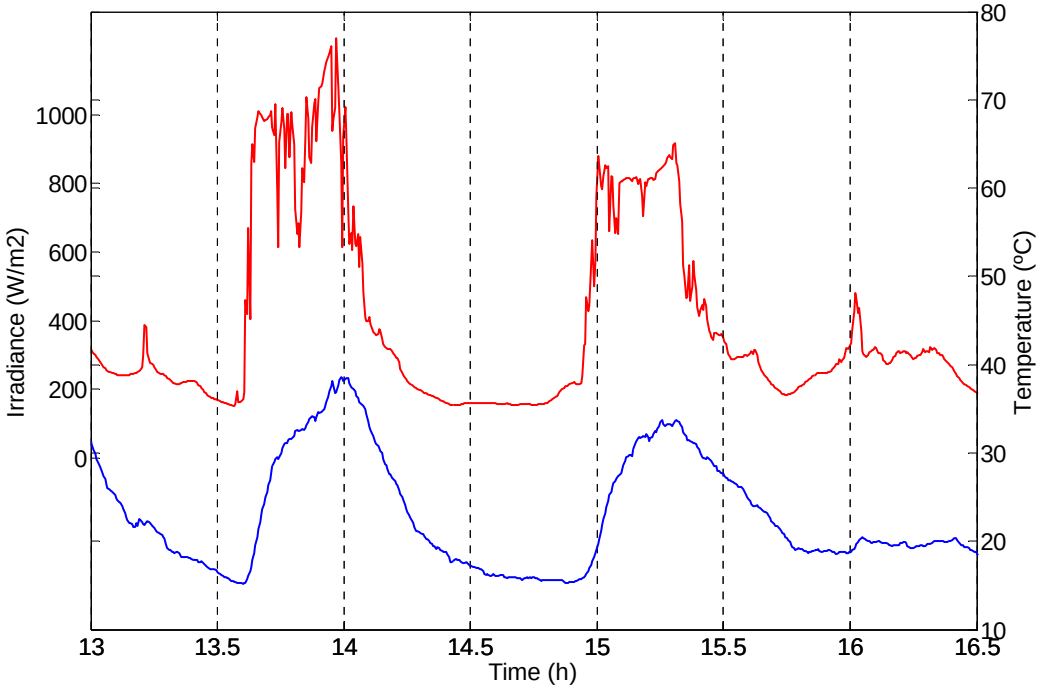

Figure 6.6. Irradiance and module temperature measured in September 6th 2010.

Table 6.2 shows the measured climatic conditions at the specified times. As can be checked in Figure 6.6 and Table 6.2, the calculated irradiance levels of the measurements 4 and 5 are perfectly possible according to the irradiance level 10

minutes after the measurements took place. The measured and simulated module temperatures are shown in Table 6.3. These simulated module temperatures are calculated at the climatic conditions given in Table 6.2 using the thermal model presented in Chapter 4.

Table 6.2. Climatic conditions at the measurement times.

Measurement	Irradiation	Temperature	Wind speed	Humidity
M1 (6 panels)	712.30 W/m^2	25.6 ºC	2.90 m/s	64 %
M2 (17 panels)	932.10 W/m^2	25.6 ºC	2.90 m/s	64 %
M3 (6 panels)	669.00 W/m^2 (app.)	15.0 ºC	5.00 m/s	62 %
M4 (6 panels)	161.70 W/m^2 (app.)	15.0 ºC	5.00 m/s	62 %
M5 (6 panels)	289.30 W/m^2 (app.)	15.0 ºC	5.00 m/s	62 %

Table 6.3. Measured and simulated module temperatures at the measurement times.

Measurement	Measured T_{MOD}	Simulated T_{MOD}	Error
M1 (6 panels)	35.61 ºC	38.09 ºC	1.45 ºC
M2 (17 panels)	44.21 ºC	42.76 ºC	2.48 ºC
M3 (6 panels)	-	23.90 ºC	-
M4 (6 panels)	-	17.17 ºC	-
M5 (6 panels)	-	18.88 ºC	-

There is an important thermal inertia at the modules. Sudden changes in the irradiance do not affect too much the module temperature. In this way, the module temperature curves are always smoother than the irradiance ones. Another aspect of this thermal inertia is that a delay between the irradiance and module temperature appears when the former starts changing after a long period of high or low irradiance level. As can be seen in Figure 6.6, at around 14 h the maximum module temperature is reached when the irradiance is already decreasing. The delay is even more important earlier, when the irradiance increases from less than 200 to almost 1000 W/m^2 relatively fast. This phenomenon produces differences between the measured and simulated module temperatures as seen in Table 6.3. Similar delay happens when the irradiance suddenly drops after the maximum point.

This issue produces the errors between the measured and simulated module temperature but also will produce errors between the string performance results. The problem is that the thermal model is meant to predict the module temperature in stationary state without caring about the previous instant. Hence, taking into consideration the previous temperature in calculating the influence of the climatic parameters on the module temperature may be an improvement for the model.

6.3. String performance measurements

For each moment specified in Table 6.1 the string voltages and currents are stored for further analysis. During the first day, August 26th 2010, two different strings were tested: a 6-panels string and a 17-panels string. However, the first measurements of the 17-panels string presented problems continuosly due to the heating of the IGBTs. Thus, during the second day, on September 6th 2010, just a 6-panels string is measured. The stored electrical and climatic data are matched to analyse the measurements and to compare them with the theoretical results. Several I-V and P-V curves represent the electrical and simulated string performance in Figures 6.7, 6.8, 6.9 and 6.10. Table 6.4 gathers the electrically measured parameters for the 5 measurements and Table 6.5 presents the corresponding simulated results for both climatic situations.

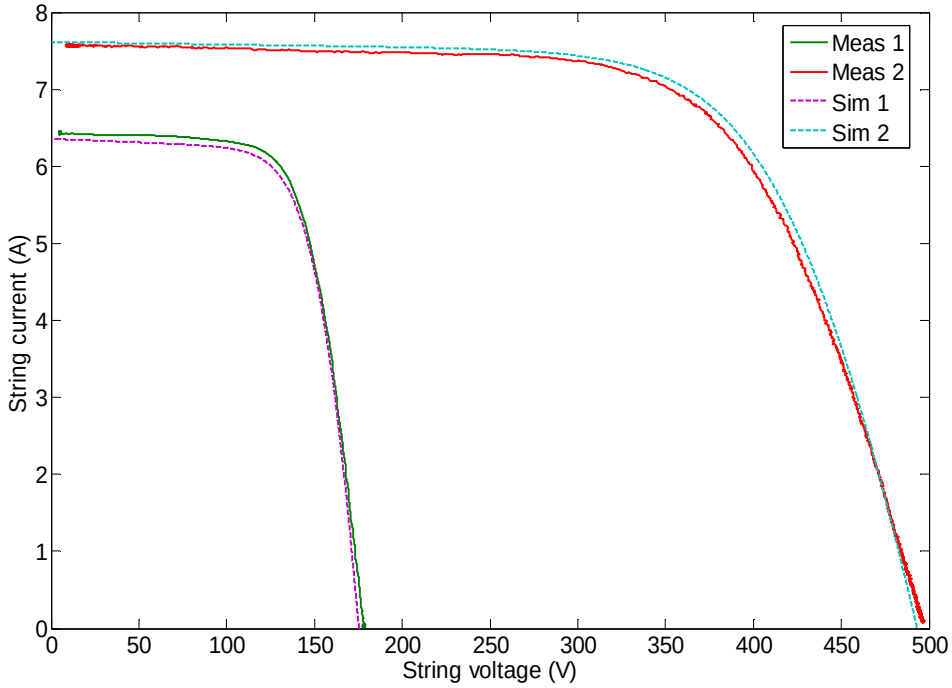

Figure 6.7. Measured and simulated I-V curves of the 6 modules string and 17 modules string from August 26th 2010.

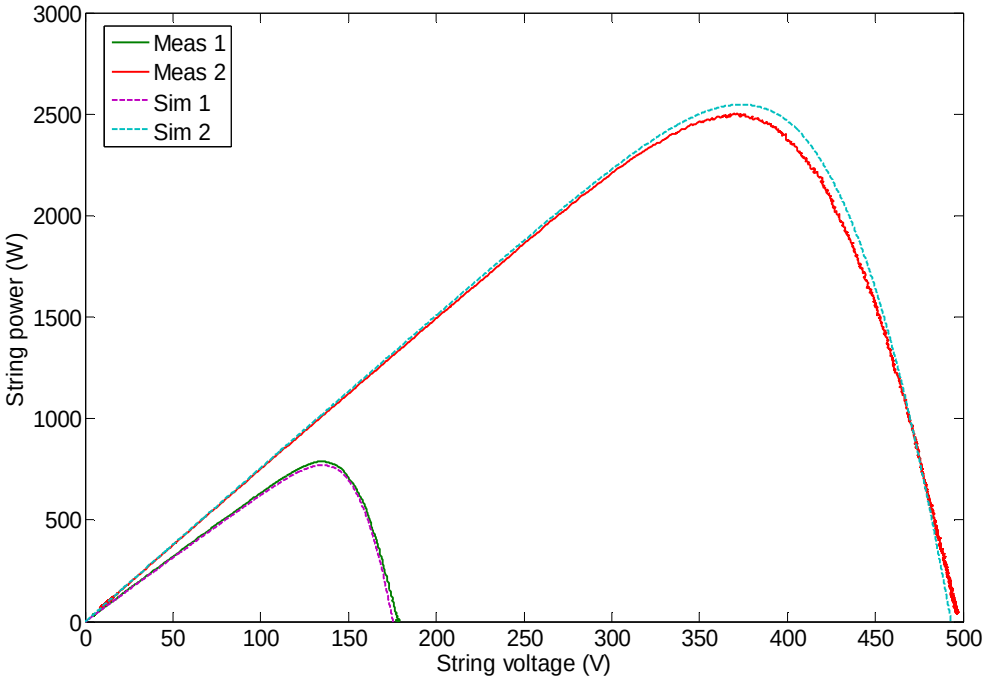

Figure 6.8. Measured and simulated P-V curves of the 6 modules string and 17 modules string from August 26th 2010.

I-V and P-V curves of measurements M1 and M2 show clearly the difference between the conditions of each measurement. On one hand, the short circuit current is highly influenced by the irradiance received by the strings. For M1, the irradiance level is lower (712.3 W/m^2) than for M2 (932.1 W/m^2), hence the I_{SC} is also lower for M1 (6.5 A) than for M2 (7.8 A). On the other hand, the difference of the open circuit voltage is due to the number of modules connected in series in each string. The measured V_{OC} is 178 V for M1 and 499 V for M2. The maximum generated power is also affected by this issue and the measurements show values of 779.4 W and 2527.2 W, respectively.

The simulated curves corresponding to measurements M1 and M2 show a appropriate reasonable behaviour of the thermal module and PV generator models. The differences between the simulated and experimental curves are relatively small, being the greatest for the maximum power in M2. However, due to the time mismatch between the measurements, it is difficult to evaluate them more closely.

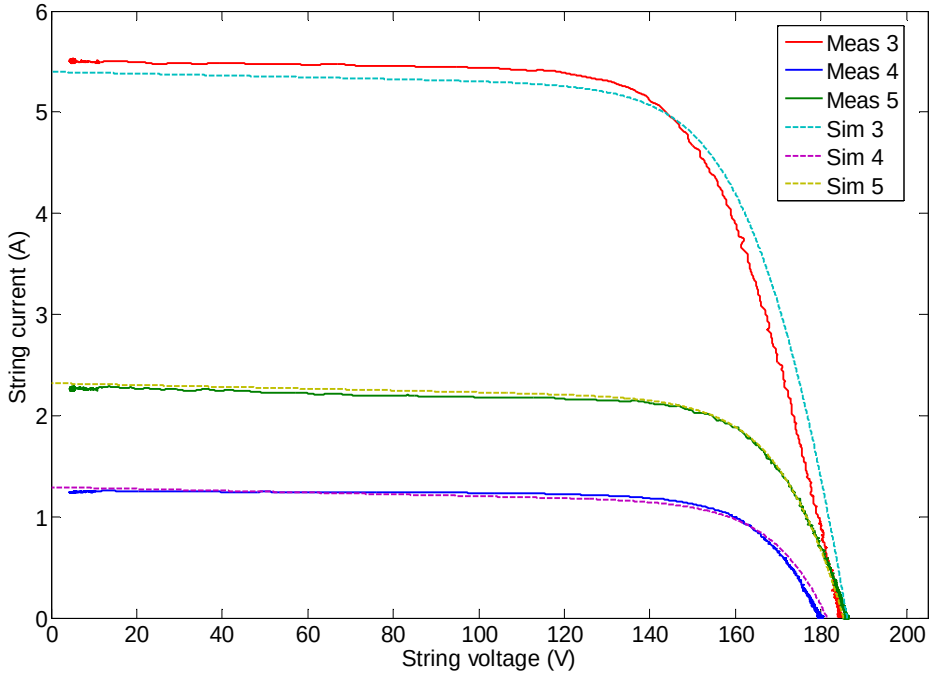

Figure 6.9. Measured and simulated I-V curves of the 6 modules string from September 6th 2010.

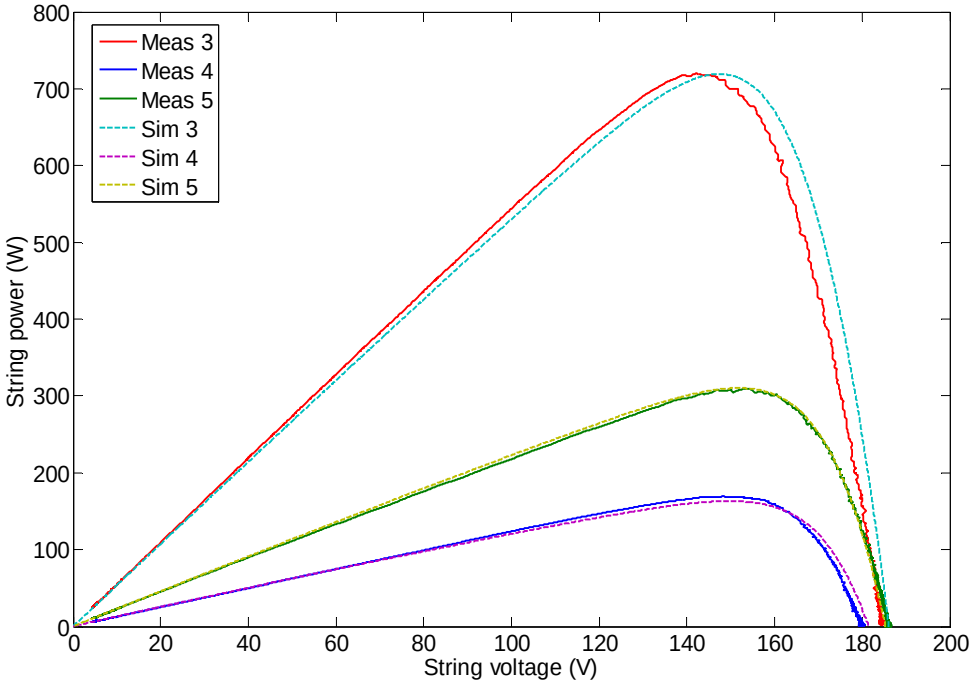

Figure 6.10. Measured and simulated P-V curves of the 6 modules string from September 6th 2010.

I-V and P-V curves of measurements M3, M4 and M5 show better the performance of a PV string under different operating conditions. Measurements were taken during a

partially cloud day, hence the irradiance level was constantly changing. The rest of climatic parameters kept approximately constant; hence irradiance is the most significant parameter to compare the results. Change of irradiance produced difference of 4.4 A in the short circuit current and 550.5 W in the maximum power between measurements M3 and M4. The irradiance received by the string also affects the efficiency of the string, which increases with increasing irradiance. This behaviour was expected for such irradiance levels according to the results obtained in Chapter 4.

Simulations corresponding to measurements M4, M5 and M6 do not offer any information due to the fact that the irradiance level taken for these cases was obtained by approximating the simulated curves to the measured ones.

Table 6.4. Measured electrical performance of the strings under different climatic conditions.

Measurement	P_{MAX}	I_{SC}	V_{OC}	Efficiency
M1 (6 panels)	779.4 W	6.50 A	178.00 V	13.58 %
M2 (17 panels)	2527.2 W	7.80 A	499.00 V	11.87 %
M3 (6 panels)	719.4 W	5.60 A	185.00 V	13.34 %
M4 (6 panels)	168.9 W	1.20 A	180.00 V	12.96 %
M5 (6 panels)	309.3 W	2.30 A	187.00 V	13.27 %

Table 6.5. Simulated electrical performance of the strings under different climatic conditions.

Simulation	P_{MAX}	I_{SC}	V_{OC}	Efficiency	Error
M1 (6 panels)	768.4 W	6.20 A	175.00 V	13.38 %	0.19 %
M2 (17 panels)	2540.2 W	7.60 A	491.80 V	11.93 %	0.06 %
M3 (6 panels)	718.9 W	5.40 A	186.10 V	13.33 %	0.01 %
M4 (6 panels)	167.2 W	1.24 A	181.46 V	12.53 %	0.13 %
M5 (6 panels)	310.2 W	2.32 A	185.25 V	13.30 %	0.04 %

As can be seen in the figures 6.7 to 6.10 and especially in the tables 6.4 and 6.5 there are small differences in the results. These are produced mainly due to the poor precision of the taken data since they could not be measured by the same system at the same exact times. They are matched approximately afterwards, during processing of the data. On the other hand, the already commented problem of the thermal module affects to the results but it looses significance after taking into consideration this issue. However, it is possible to confirm that the measured climatic and electric data approximately match since the errors are small and the errors in efficiency are under 0.20 %.

7. CONCLUSIONS

Photovoltaic is the most elegant way to convert solar energy into electricity and it will necessarily play a significant role in any sustainable future for energy production. This leads to numerous studies focusing on the performance of different PV technologies and interfacing devices related to them. Hence, the knowledge of PV module and array performance characterization under standard and actual operating conditions becomes essential. For these reasons, the Department of Electrical Energy Engineering of the Tampere University of Technology has designed and built a Solar PV Power Test Plant composed by 69 PV modules on the rooftop of the department's building.

The main objective of this Thesis was to design a climatic measurement system to measure the climatic and operating conditions of the power test plant with several purposes. On one hand, it was desired to measure accurately the climatic conditions of the plant to be able to gather historical climatic information or to share it in real time on the web site of the department. On the other hand, it was necessary to measure the operating conditions of the PV modules and strings of TUT's plant, especially regarding to the global, direct and diffuse solar radiation yields to the panels and to the shadowing conditions of each string. To accomplish it, an accurate automatic weather station and a radiation and temperature measurement system have been designed. The weather station measures the ambient temperature, relative humidity, wind speed and direction and global and diffuse solar radiation of the plant with high precision. On the other hand, the radiation and temperature measurement system measures the operating string temperatures and the irradiance received by each string of the plant.

The climatic measuring system contains a state-of-the art automatic weather station and, in parallel, a mesh of irradiance and module temperature measurements. The weather station design is based on specific literature such as the Guide to Meteorological Instruments and Methods of observation from the World Meteorological Organization among others, several operating facilities and a deeply extensive market study of the available sensors, instruments and data-acquisition systems. Regarding the irradiance and temperature measurements, literature about operating facilities and previous studies have been studied expensively in order to design a suitable system that satisfy the knowledge of the operating conditions of the modules need. The data acquisition system is based on using CompactRio data acquisition cards from National Instruments. This leads to a very flexible and economical system that allows using specific swappable I/O modules to connect the sensor outputs. After collecting the data provided by the sensors, these data-acquisition cards transmit the information to a PC through an Ethernet cable without interference or noise problems.

A thermal model based on the climatic conditions for the PV modules has been programmed using Matlab™ Simulink. The intention was to study the influence of the climatic conditions on the operating module temperature and to complete the existing photovoltaic generator model in order to study the influence of these climatic conditions on the performance and efficiency of the solar panels as well. Simulations show a clear dependence of the module temperature on the ambient temperature, wind speed and irradiance conditions, while the relative humidity and the wind direction do not affect much to the solar panels. Regarding the generated power and string efficiency, increasing ambient temperature and wind speed causes a negative and positive influence, respectively. However, the practical combinations of irradiance, temperature and wind speed in real outdoor environment cause that the system has an optimum efficiency somewhere in the mid values of these parameters. This happens regardless the basic fact that the higher the irradiance is, the more power is generated by the modules.

As a last reason of the thermal model, the intention was to allow the comparison of the real and simulated string performances by measuring on the PV system once the measuring systems were installed. Eventually, it has been impossible to build the system in time to carry out a proper testing of it for this thesis. This was due to the timescales of goods delivery and installation, which were not part of this thesis project. It turned out that also partial testing of the measurement system was not feasible within the timescale. Therefore, the electrical performance of the PV power plant was measured utilizing the climatic data measured using the facilities of the Department of Electronics. Measurements of module temperature and irradiance show the appearance of a delay between the curves caused by the thermal inertia of the modules. This phenomena was not considered in the model, which is meant to predict the module temperature in a stationary state, thus a small error appears between the measured module temperature and the simulated one. The same happens with the string performance results, small errors are exposed between the measured and simulated efficiency and generated power. However, the results still confirm the right performance of the thermal model and measuring system.

This thesis was limited on the investigation of the climatic and operating conditions influence on the operating module temperature and electrical performance and to the measurement of these conditions. In order to study the electrical performance of the strings, matching the data with the data provided by the designed climatic system, a Labview program must be further developed to acquire the whole set of signals, process and present it in an understandable manner. Also a power measuring system that can be continuously operating must be completed. Once everything is carried out, further studies over the PV systems and interfaces performance, for example, under different shadowing conditions will be able to be conducted.

REFERENCES

[1] Agencia Estatal de Meteorología. [WWW]. [2010]. Available at: http://www.aemet.es/es/portada

[2] Alonso García, M. C. and Balenzategui, J. L. Estimation of photovoltaic module yearly temperature and performance based on Nominal Operation Cell Temperature calculations. Renewable Energy, 29, 2004, pp. 1997-2010.

[3] Amy de la Breteque, E. Thermal aspects of c-Si photovoltaic module energy rating. Solar Energy, 83, 2009, pp. 1425-1443.

[4] Archer, M.D. and Hill, R. Clean Electricity from photovoltaics. Imperial College Press, 2001.

[5] Benghanem, M. Measurement of meteorological data based on wireless data acquisition system monitoring. Applied Energy 86, 2009. pp 2651-2660.

[6] Durisch, W., Tille, D., Wörz, A. and Plapp, W. Characterisation of photovoltaic generators. Applied Energy, 65, 2000, pp. 273-284.

[7] Durish, W., Urban, J. and Smestad, G. Characterisation of solar cells and modules under actual operating conditions.WREC, 1996.

[8] Dzimano, G. Modeling of Photovoltaic Systems, Doctoral Thesis. The Ohio State University, 2008.

[9] Finnish Meteorological Institute. Weather Stations in Finland. [WWW]. [2010]. Available at: http://ilmatieteenlaitos.fi/weather/stations.html

[10] Forero, N., Hernández, J., Gordillo., G. Development of a monitoring system for a PV solar plant. Energy Conversion and Management 47, 2006. pp 2329-2336.

[11] Garrison, J. D., et. al.. Environmental Measurement. CRC Press LLC, 2000.

[12] Goswami, D. Y. Energy Conversion. Chapter 5. Taylor & Francis Group, LLC, 2007.

[13] Guasch Murillo, D. Modelado y análisis de sistemas fotovoltáicos, Doctoral Thesis. Universitat Politècnica de Catalunya (UPC), 2003.

[14] Jones, A. D., and Underwood, C. P. A Thermal Model For Photovoltaic Systems. Solar Energy, 4, 2001, pp. 349-359.

[15] Khalil, S. A. Parameterization models for solar radiation and solar technology applications. Energy Conversion and Management 49, 2008. pp 2384–2391.

[16] King, D. L. Photovoltaic Module and Array Performance Characterization Methods for All System Operating Conditions. Sandia National Laboratoties, AIP Press, 1997.

[17] Kjaer, S.B., Pederson, J. K. & Blaabjerg, F. A review of single-phase grid-connected inverters for photovoltaic modules. IEEE transactions on industry applications vol. 41 no. 5, 2005, pp. 1292-1306.

[18] Koutrouilis, E., Kalaitzakis., K. Development of an integrated data-acquisition system for renewable energy sources systems monitoring. Renewable Energy 28, 2003. pp 139-152.

[19] Luque, A. & Hegedus, S. Handbook of photovoltaic science and engineering. Jonh Wiley & Sons, 2003.

[20] Mäki, A. Topology of a Silicon-Based Grid-Connected Photovoltaic Generator. Master of Science Thesis. Tampere University of Technology, 2010.

[21] Malik, A. Q., Damit, S. J. B. H. Outdoor testing of simple crystal silicon solar cells. Renewable Energy, 28, 2003, pp. 1413-1445.

[22] Markvart, T. Solar electricity 2nd ed. UK 2000, John Wiley & Sons. p. 280.

[23] Martínez Bohórquez, M. A., Enrique Gómez, J. M., and Andújar Márquez, J. M. A new and inexpensive temperature-measuring system: Application to photovoltaic solar facilities. Solar Energy, 83, 2009, pp. 883-890.

[24] Mattei, M., Notton, G., Cristofari, C., Muselli, M., Poggi, P. Calculation of the polycrystalline PV module temperature using a simple method of energy balance. Renewable Energy, 31, 2006, pp. 553-567.

[25] Messenger, R. and Ventre, J. Photovoltaic Systems Engineering, Third Edition. CRC Press, 2010.

[26] Morton, O. Solar energy: A new day dawning?: Silicon Valley sunrise. Nature 443, 2006.

[27] Mukaro, R., Francis, X. C. A Microcontroller-Based Data Acquisition System for Solar Radiation and Environmental Monitoring. IEEE Transactions on Instrumentation and Measurement 48, 1999. pp 1232-1238.

[28] Nagae, S. et. al. Evaluation of the impact of solar spectrum and temperature variations on output power of silicon-based photovoltaic modules. Elsevier, 2006.

[29] NAPS Systems. Technical Description of Photovoltaic module NP190GKg. [WWW]. [Cited 14/09/2009]. Available at: http://www.napssystems.com/stc/attachments/NP190GKg%20TD140909P.pdf

[30] National Instruments, 2010. [WWW]. At: http://www.ni.com.

[31] Patel, M. R. Spacecraft power systems. CRC Press, 2005, pp. 133-194.

[32] Rosiek, S. and Batlles, F.J. A microcontroller-based data-acquisition system for meteorological station monitoring.

[33] Sera, D., Teodorescu, R. and Rodriguez, P. PV panel model based on datasheet values. IEEE Xplore, 2007.

[34] Skoplaki, E., Boudouvis, A.G. and Palyvos, J.A., A simple correlation for the operating temperature of photovoltaic modules of arbitrary mounting. Solar energy materials & solar cells, 92, 2008, pp. 1393-1402.

[35] Skoplaki, E., Palyvos., J. A. On the temperature dependence of photovoltaic module electrical performance: A review of efficiency/power correlations. Elsevier, 2008.

[36] Skoplaki, E. and Palyvos, J. A. Operating temperature of photovoltaic modules: A survey of pertinent correlations, Renewable Energy, 34, 2009, pp. 23-29.

[37] Tamizhmani, G., Ji, L., Tang, Y., Petacci, L. and Osterwald, C. Photovoltaic Module Thermal/Wind Performance: Long-Term Monitoring and Model Development For Energy Rating. NCPV and Solar Program Review Meeting, 2003, pp. 936-939.

[38] van den Bos, C. J., van den Bos, A. Solar Radiation Sensors: Applications. New Detector Development, Characterization and Classification According to ISO 9060. IEEE Xplore, 1995.

[39] Villalva, M. G., Gazoli, J. R. & Filho, E. R. Comprehensive approach to modelling and simulation of photovoltaic arrays. IEEE transactions on power electronics vol. 24 no. 5, 2009, pp.1198-1208.

[40] Webster, J. G. The measurement, instrumentation, and sensors handbook. CRC Press LLC, 1999.

[41] Wilshaw, A., Pearshall, N., Hill, R. Installation and operation of the first city center PV monitoring station in the United Kingdom. Solar Energy 59, 1997. pp 19-26.

[42] World Meteorological Organization. Guide to Meteorological Instruments and Methods of Observation. WMO-No. 8, 2008.

[43] Young, H. D. & Freedman, R. A. Sears and Zemansky's university physics: with modern physics 12th ed. USA 2008, Pearson Addison-Wesley. p 1551.

APPENDIX A: MARKET STUDY

A.1. Ambient temperature and humidity sensors

Climatronics sensors P/N 102669 and P/N 101812 G2

Climatronics' relative humidity and temperature sensors use a capacitive relative humidity transducer and is specifically designed for industrial meteorological monitoring systems.

Features:

- Low power consumption.
- Up to interfacing with data acquisition systems.
- Linear outputs: 0-20 mA or 0-1 VDC.
- Electronic temperature compensation of the humidity element: keeps the humidity accuracy at conditions close to condensation.
- P/N 101812 includes a Class A 100 Ohm platinum resistance thermometer.

Table A.1. *Specifications of the Climatronics' sensors PN/ 102669 and P/N 101812 G2.*

Climatronics - Sensor P/N 102669		
	Humidity sensor (Capacitive)	Temperature sensor
Operating Range	0 – 100 %	-40 to +60 ºC
Accuracy	< ± 1.5 % @ 23 ºC	± 0.2 ºC
Repeatability	± 0.5 % RH	± 0.1 ºC
Excitation Power	3.6… 35 VDC, 10 mA	3.6… 35 VDC, 10 mA
Output Range	0 – 100 % = 0 – 1 VDC / 0–20mA	- 40 to +60 ºC = 0 – 1 VDC/ 0-20mA
Active Output Load	>1 kOhm for Vout	>1 kOhm for Vout

Climatronics - Sensor P/N 101812 G2		
	Humidity sensor (Capacitive)	Temp. sensor (100 Ohm platinum RTD)
Operating Range	0 – 100 %	-40 to +70 ºC
Accuracy	± 1 % RH	± 0.3 ºC
Repeatability	± 0.3 % RH	± 0.1 ºC
Excitation Power		0.1 ºC
Output Range	4.8… 26.5VDC, 10mA	Resistive 4-wire connection
Active Output Load	0 – 100 % = 0 – 1 VDC / 0-20mA	-40 to +70 ºC = 0 – 1 VDC/ 0-20mA

Vaisala sensor HMP155

The Vaisala's new Humicap Humidity and Temperature Probe HMP155 provides reliable humidity and temperature measurements. Measuring humidity reliably is challenging in environments where humidity is near saturation.

Measurements may be corrupted by fog, mist, rain, and heavy dew. A wet probe may not give an accurate measurement in the ambient air. This is an environment to which Vaisala has designed a patented, warmed probe for reliable measuring. As the sensor head is warmed continuously, the humidity level inside it stays below the ambient level. Thus, it also reduces the risk of condensation forming on the probe.

The HMP155 is especially designed for use in meteorological applications, such as synoptic and hydrological weather stations, aviation, and road weather. It is also suitable in a wide range of instrumentation, for example, recorders, data loggers, and laboratory equipment and monitoring.

Features:

- Low power consumption.
- Designed for a wide range of instrumentation (e.g. laboratory equipment).
- Different output possibilities: voltage, RS-485, resistive Pt-100.

Table A.2. *Specifications of the Vaisala's sensor HMP155.*

Vaisala – HMP155		
	Humidity sensor (Humicap 180R(C))	Temperature sensor (Pt 100 RTD)
Operating Range	0.8 – 100 %	-80 to +60 ºC
Accuracy	± 1 % RH @ 20 ºC	± 0.2 ºC (approx)
Excitation Power	7… 28 VDC	7… 28 VDC
Output Range	0 - 100 % = 0 -1/5/10 VDC	-80 to +60 ºC = 0 – 1/5/10 VDC

Rotronic sensor MP101A

The MP101A is a combined humidity and temperature probe designed for out-door applications. Sensor operates from a DC voltage and presents low power consumption. The linear output signals are consistent with the requirements of most data acquisition systems.

Features:

- Low power consumption, no warm-up time.
- Durable, stable sensor with low maintenance requirements.
- Linear outputs.
- High accuracy over full range of humidity and temperature.
- Special compensation permits up to 100m cable length.

Table A.3. *Specifications of the Rotronics's sensor MP101A.*

Rotronic – MP101A		
	Humidity sensor (Hygromer C94)	Temperature Sensor (Pt100 RTD)
Operating Range	0.8 – 100 %	-40 to +60 ºC
Accuracy	± 1 % RH @ 20 ºC	± 0.2 ºC
Repeatability	± 0.3 % RH	± 0.1 ºC
Excitation Power	4.8… 30 VDC	4.8… 30 VDC
Output Range	0 – 100 % = 0 – 1 VDC	-40 to +60 ºC = 0 – 1 VDC
Active Output Load	> 1 kOhm for Vout	> 1 kOhm for Vout

Delta-T sensor Rht2nl

Table A.4. *Specifications of the Delta-T's sensor Rht2nl.*

Delta-T - Sensor Rht2nl		
	Humidity sensor (Capacitive)	Temperature sensor (Thermistor)
Operating Range	0 - 100 %	-30 to +70 ºC
Accuracy	< ± 2 % @ 23ºC	± 0.1 ºC
Excitation Power	5… 32 VDC, 2 mA	-
Output Range	Different. Volt. / 0 – 1 VDC	"3 wires" - resistance

Rainwise sensors RH/T Standard or Precision

The RH/T sensor combines a temperature sensor with a relative humidity sensor. The compact mounting unit provides accurate, responsive measurements wit a minimum of hysteresis.

The temperature sensor is available in several configurations, including RTDs, thermistors and thermocouples depending upon the requirements. The standard sensor includes a built-in operational amplifier which provides consistency against cable length variation and resistance to electrical noise problems. The humidity sensor is a thin film polymer capacitor.

With the proper Rainwise interface, the RH/T can be furnished with either a RS-232, digital or analogue output.

Table A.5. *Specifications of the Rainwise's sensors RH/T standard and precision.*

Rainwise - Sensor RH/T		
	Humidity sensor (Thin film polymer capacitor)	
Operating Range	-40 to +85 ºC	
Accuracy	± 2 % RH @ 25 ºC (10 – 90 % RH)	
Output Range	0 - 1 VDC	
	Temperature sensor (standard)	Temperature sensor (precision)
Operating Range	-40 to +65 ºC	-50 to +65 ºC
Resolution	0.1 ºC	0.1 ºC
Accuracy	± 0.1 ºC	± 0.1 ºC

A.2. Wind speed and direction sensors

Climatronics WM-III

Climatronics' Wind Mark III (WM-III) Wind Sensors combine accuracy and reliability. Wind speed is sensed by a three-cup anemometer and converted to an electrical signal by a solid-state photo chopper. A counter balanced wind vane coupled to a precision low torque potentiometer senses wind direction. Almost any data acquisition systems currently available on the market can be interfaced with the WM-III sensor. The WM-III sensor can be obtained with a current loop output of 4 – 20 mA.

Features:

- Non-freezing, high performance wind set.
- Accurate wind speed and direction measurement.
- Low measurement starting threshold.
- Excellent linearity.

- Fast response.

Possible analogue output signal for the wind speed sensor with Current Loop Wind Sensors P/N 101908 is available.

Table A.6. *Specifications of the Climatronics' sensor WM-III.*

Specifications		
	Wind Speed Sensor	Wind Direction Sensor
Accuracy	± 0,11 m/s or 1.5 %	± 3 degrees
Threshold	< 0,45 m/s	< 0.45 m/s
Distance Constant	< 2,4 / 4.6 m	< 2. 4 / 4.6 m
Damping Ratio	N/A	>0.4 to 0.6 at 10º
Operating Range	0 to 75 m/s	0 to 360º
Signal Output	Frequency proportional	Analogue
Power Requirements	5 – 15 VDC (1 mA)	Max 5 mA (2 Kohms)
Operating Temperature	-40 to +60 ºC	
Sensor Heater	20 W	

Vaisala WA25 Wind Set

The Vaisala Wind Set WA25 is a high-quality cup and vane wind measurement station designed for arctic conditions. It consists of an anemometer WAA252, a wind vane WAV252, an optional cross arm, a power supply and cabling.

Most of the heating power is consumed where it is needed most – in the cups and vane. Foil heaters, integrated into the cups and vane, prevent snow buildup and ice formation. Heating power is also supplied to the sensor shafts, bearings and bodies.

The WAA252 is a fast-response, low-threshold anemometer. The output pulse rate is directly proportional to wind speed. However, for the highest accuracy, the characteristic transfer function should be used to compensate for starting inertia.

The WAV252 is a counterbalanced, low threshold, optoelectronic wind vane providing a 6-bit GRAY-coded message.

Features:

- Non-freezing, high performance wind set.
- Accurate wind speed and direction measurement.
- Low measurement starting threshold.
- Excellent linearity.
- Fast response.

Vaisala Wind Transmitter WAT12 is an economic solution to a standard interface between Vaisala's wind sensor and computer with analogue inputs. The transmitter

converts the wind speed and direction data measured into two analogue current loop signals respectively. The power to the sensors is also supplied through the WAT12 unit.

Table A.7. *Specifications of the Vaisala's WA25 wind set sensors.*

Specifications		
	Wind Speed Sensor	Wind Direction Sensor
Accuracy	± 0.17 m/s	< ± 3 deg.
Threshold	< 0.5 m/s	< 0.4 m/s
Distance Constant	2.7 m	2.7 m
Damping Ratio	N/A	0,3
Operating Range	0.4 to 75 m/s	0 to 360º
Signal Output	Frequency proportional	6-bit GRAY
Power Requirements	24 VDC ± 10 % (3.2 A max.)	24 VDC ± 10 % (2.1 A max.)
Operating Temperature	-55 to +55 ºC	

Vaisala WS425

The Vaisala Ultrasonic Wind Sensor WS425 gives meteorologists an alternative to the cup and vane mechanical sensors. The WS425 has no moving parts, and is resistant to contamination and corrosion. In addition to improving accuracy and the reliability of data in all wind conditions and climates, the WS425 eliminates on-demand and periodic maintenance.

The WS425 uses ultrasound to determine horizontal wind speed and direction. The measurement is based on transit time, the time it takes for the ultrasound to travel from one transducer to another, depending on the wind speed. The heated model has thermostatically controlled heaters in the transducer heads to prevent freezing rain or snow build- up. The standard model operates with a low current 10 ... 15 V supply. For the heated model, an additional 36 V supply is used for heating.

Features:

- Superior data availability and accuracy in all wind directions due to the patented three transducer layout.
- No maintenance needed.
- Effects of temperature, humidity and pressure fully compensated.
- Large transducer heads are insensitive to rain.
- RS232/485/422, SDI-12 and analogue outputs.
- Operates with 10 ... 15 VDC, additional 36 VDC required for heated model.
- Stainless steel as standard sensor material.

Table A.8. *Specifications of the Vaisala's sensor WS425.*

Specifications		
	Wind Speed Sensor	Wind Direction Sensor
Accuracy	± 0.135 m/s	± 2 deg.
Threshold	0 m/s	0 m/s
Distance Constant	0 m	0 m
Resolution	0.1 m/s	1 deg.
Operating Range	0 to 65 m/s	0 to 360º
Signal Output	Digital / Analogue	Digital / Analogue
Power Requirements	10 – 15 VDC (12 mA typ.)	
Heating Power Requirements	36 VDC (0.7 A)	
Operating Temperature	-55 to +55 ºC	

Delta-T Anemometer AN1 and Wind Vane WD1

Table A.9. *Specifications of the Delta-T's sensor wind vane WD1.*

Specifications		
	Wind Speed Sensor	Wind Direction Sensor
Accuracy	± 1 %	0.3 deg.
Operating Range	0.2 to 75 m/s	0 to 358º
Signal Output	Digital (0-60Hz) / Analogue	Resistive (0-1000Ohm)
Power Requirements	None	None
Operating Temperature	-30 to +50 ºC	-50 to +70 ºC

Rainwise Aervane

The WeatherLog Aervane is designed to meet or exceed the EPA guidelines for regulatory modelling applications. The direction is obtained through an optical resolver with no "dead band". The resolution and accuracy are ± 1 deg.

A Rainwise interface can provide an RS-232 output or any desired analogue output including 4-20 mA, 0 – 1 VDC, etc.

Features:

- Accuracy traceable to NIST.
- No direction dead band.

Table A.10. *Specifications of the Rainwise's Aervane.*

Specifications		
	Wind Speed Sensor	Wind Direction Sensor
Accuracy	± 1 %	1 deg.
Threshold	< 0,36 m/s	< 0,5 m/s
Distance Constant	3 m	3 m
Damping Ratio	N/A	0,53
Operating Range	0 to 75 m/s	0 to 360º
Signal Output	Analogue	Analogue

A.3. Solar sensors

Climatronics solar radiation sensor

Suitable for the measurement of solar irradiance on a plane surface, the solar radiation sensor is designed to output a mV signal that is directly proportional to the incoming solar irradiance. This high accuracy pyranometer incorporates a radial 64 thermocouples sensing element, imprinted on a thick-film substrate, housed under Schott glass domes.

Features:

- First-class Pyranometer (WMO).
- Good cosine/directional response.
- Excellent long-term stability.
- Good linearity.
- Fast response.
- Low dome thermal offset error.

Table A.11. *Specifications of the Climatronics' solar radiation sensor.*

Specifications			
ISO Classification	First Class	Sensitivity	9 to 15 uV/W/m^2
Response (95%)	18 s	Impedance	70 to 100 Ohm
Zero offsets		Level accuracy	0.5 º
thermal radiation (200W/m2)	± 15 W/m^2	Operating temperature	-40 to +80 ºC
Temperature change (5K/hr)	± 4 W/m^2	Spectral range (50 % points)	305 to 2800 nm
Non-stability (change/year)	± 1 %	Typical signal output	0 to 25 mV
Non-linearity (0 - 1000 W/m^2)	± 1.2 %	Maximum irradiance	2000 W/m^2
Directional error (at 1000W/m^2 beam)	± 20 W/m^2	Expected daily accuracy	± 1 %
Temperature dependence of sensitivity	± 2 % (-10 to +40ºC)	Tilt error (at 1000 W/m^2)	± 1.5 %

Delta-T Sunshine Sensor BF3

The BF3 Sunshine Sensor measures global (total) and diffuse radiation, and sunshine duration. It uses an array of photodiodes with a unique computer-generated shading pattern to measure incident solar radiation. A microcontroller calculates the global and diffuse components of the radiation and the sunshine state. Direct beam is calculated from Total minus Diffuse.

Two analogue voltage outputs are provided for the Global and Diffuse radiation. The sunshine state is represented by a digital output. Power for the sensor comes from internal alkaline batteries or alternatively from external excitation.

Features:

- Measures Global and Diffuse radiation.
- No routine adjustment or polar alignment.
- Works at any altitude.
- No moving parts, no shade rings and no motorised tracking needed.
- Outputs can be set to Energy (W/m^2), PAR (umol/m/s) or Lux.
- Second class pyranometer.
- Optional heated version.

Table A.12. *Specifications of the Delta-T's sunshine sensor BF3.*

Specifications	
ISO Classification	Second Class
Operating Temperature	-20 to 70 ºC
Temperature coefficient	± 0.15 % /ºC
Input Voltage	5 - 15 VDC
Accuracy: Total radiation	± 12 %
Accuracy: Diffuse radiation	± 15 %
Resolution	0.3
Spectral Response	400 - 700 nm
Signal Output	0 - 1250 W/m^2 = 0-2500 mV
Heater power	18W at 12 VDC, 1.5 A

Delta-T Sunshine Pyranometer SPN1

The Sunshine Pyranometer is a patented, meteorological class instrument, with a built-in heater, designed for long-term outdoor exposure. It is an affordable alternative to shade-rings pyranometers, pyrheliometers and sunshine recorders.

Pyranometer SPN1T needs no routine adjustment or polar alignment and works at any latitude. It uses an array of seven miniature thermopile sensor and a computer-generated shading pattern to measure the direct and diffuse components of incident solar radiation. The shading pattern and thermopiles are arranged so that at least one thermopile is always fully exposed to the solar beam, and at least one is fully shaded from it, regardless of the position of the sun in the sky.

The Sunshine Pyranometer provides 2 analogue voltage outputs for global and diffuse radiation, and a digital output for sunshine duration. An internal heater keeps the dome clear of dew, ice and snow down to -20 ºC (in still air conditions), ensuring reliable readings in difficult climatic conditions.

Features:

- Measures Global and Diffuse radiation.
- No routine adjustment or polar alignment.
- No moving parts, no shade rings and no motorised tracking needed.
- Precision ground glass dome
- Wideband thermopile sensors.
- Near ideal spectral and cosine response.
- Good quality pyranometer (first class).

Table A.12. *Specifications of the Delta-T's sunshine pyranometer SPN1.*

Specifications			
ISO Classification	First Class	Sensitivity	9 to 15 uV/W/m^2
Response (95%)	< 200 ms	Impedance	70 to 100 ohm
Zero offsets		Operating temperature	-40 to +70 ºC
dark reading	< 3 W/m^2	Spectral range	400 to 2700 nm
temperature change (5K/hr)	< 3 W/m^2	Typical signal output	0 to 2500 mV
Non-stability (change/year)	± 1 %	Maximum irradiance	> 2000 W/m^2
Non-linearity	< 1 %	Expected daily accuracy	± 5 %
Temperature dependence of sensitivity	± 0,02 % (-20 to +70 ºC)	Power requirement	5 to 15 VDC
Tilt error	Negligible	Heater control	20 W

Kipp & Zonen Pyranometers

Pyranometers are radiometers designed for measuring the irradiance on a plane surface resulting from radiant fluxes in the wavelength range from 300 to 3000 nm. Kipp & Zonen supplies a full range of pyranometers and accessories, according to the ISO 9060 and World Meteorological Organization (WMO) standards. Common characteristics of the pyranometers are robustness, and good weather performance.

The instruments do not require power and are all supplied with calibration certificates that are traceable to WRR (Word Radiometric Reference). The combination of a pyranometer and shadow ring CM 121B offers a simple solution to the problem of measuring diffuse radiation from the sky. The shadow from the ring covers the pyranometer dome completely. The ring will not need adjustment for several days. Some pyranometers may include a Pt-100 temperature probe.

Table A.13. *Specifications of the Kipp & Zonen's pyranometers.*

Specifications				
	CMP 22	CMP 21	CMP 11	CMP 6
ISO Classification	Secondary Standard	Secondary Standard	Secondary Standard	First Class
Response (95%)	5 s	5 s	5 s	18 s
thermal radiation (200W/m^2)	± 3 W/m^2	± 7 W/m^2	± 7 W/m^2	± 15 W/m^2
temperature change (5K/hr)	± 1 W/m^2	± 2 W/m^2	± 2 W/m^2	± 4 W/m^2
Non-stability (change/year)	± 0.5 %	± 0.5 %	± 0.5 %	± 1 %
Non-linearity (0 - 1000 W/m^2)	± 0.2 %	± 0.2 %	± 0.5 %	± 1 %
Directional error (at 80º with 1000W/m^2 beam)	± 5 W/m^2	± 10 W/m^2	± 10 W/m^2	± 20 W/m^2
Temperature dependence of sensitivity	± 0.5 % (-20 to +50 ºC)	± 1 % (-20 to +5 ºC)	± 1 % (-10 to +40 ºC)	± 4 % (-10 to +40 ºC)
Tilt error (at 1000 W/m^2)	± 0.2 %	± 0.2 %	± 0.2 %	± 1 %
Sensitivity	7 to 14 uV/W/m^2	7 to 14 uV/W/m^2	7 to 14 uV/W/m^2	5 to 16 uV/W/m^2
Impedance	10 to 100 Ohm	10 to 100 Ohm	10 to 100 Ohm	20 to 200 Ohm
Level accuracy	0.1 º	0.1 º	0.1 º	0.5 º
Operating temperature	-40 to +80 ºC	-40 to +80 ºC	-40 to +80 ºC	-40 to +80 ºC
Spectral range (50 % points)	200 to 3600 nm	310 to 2800 nm	310 to 2800 nm	210 to 2800 nm
Typical signal output	0 to 15 mV	0 to 15 mV	0 to 15 mV	0 to 15 mV

Maximum irradiance	4000 W/m2	4000 W/m2	4000 W/m2	2000 W/m2
Expected daily accuracy	± 1 %	± 2 %	± 2 %	± 5 %
Recommended applications	Scientific research requiring the highest level of measurement accuracy and reliability	Meteorological networks, reference measurements in extreme climates, polar or arid	Meteorological networks, PV panel and thermal collector testing, materials testing	Good quality measurements for hydrology networks, greenhouse climate control

Kipp & Zonen Pyrheliometer CHP1

CHP 1 is a new pyrheliometer that builds on the legacy of the CH 1, offering the reliability and durability of its predecessor together with important improvements. The detector is similar to that used in the CMP 21 and 22 pyranometers, which minimizes the influence of ambient temperature fluctuations and provides a fast response time. Both Pt-100 and 10 k thermistor temperature sensors are fitted as standard, to allow use of the individual temperature response data supplied with each CHP 1. Due to the signal cable connector and screw-in desiccant cartridge the new design is easy to install and maintain. The specifications exceed ISO and WMO performance criteria for First Class Normal Incidence Pyrheliometers. Every CHP 1 is supplied with a calibration certificate traceable to the World Radiometric Reference.

CHP 1 is the best all-weather pyrheliometer available for continuous measurements of direct solar radiation and exceeds the specifications for high end solar radiation networks, such as the Baseline Surface Radiation Network (BSRN). For research into photovoltaic systems and materials, accurate direct solar irradiance data is needed.

A pyrheliometer needs to be pointed at the sun at all times so that the solar disk always falls within the field of view of the instrument. Kipp & Zonen sun trackers provide a stable mounting to keep the pyrheliometer pointing at the sun to accurately measure the direct solar radiation.

Table A.14. *Specifications of the Kipp & Zonen's pyrheliometer CHP1.*

Specifications			
Maximum irradiance	4000 W/m^2	Sensitivity	7 to 14 $uV/W/m^2$
Response time	5 s	Impedance	10 to 100 Ohm
Non-stability (change/year)	0.5 %	Level accuracy	-
Non-linearity (0 - 1000 W/m^2)	0.2 %	Operating temperature	-40 to +80 ºC
Directional error (at 80º with 1000W/m^2 beam)	< 10 W/m^2	Spectral range (50 % points)	200 to 4000 nm
Temperature dependence	0.5 % (-20 to +50 ºC)	Typical signal output	0 to 15 mV

Kipp & Zonen Photodiode SP-Lite2

SP Lite2 is designed for all-weather measurement of solar radiation. It has a specially shaped Teflon diffuser that gives very good directional response and is largely self-cleaning. The detector is a silicon photo-diode, so the spectral response is not as broad or flat as in CMP series pyranometers with thermopile detectors. The standard cable length is 5 m with an option of 15 m. The mounting flange incorporates a bubble level and 3 adjustment screws for easy levelling. A threaded hole takes the accessory screw-in mounting rod for fitting to masts and poles.

Table A.15. *Specifications of the Kipp & Zonen's photodiode SP Lite 2.*

Specifications			
ISO Classification	First class	Sensitivity	60 to 100 uV/W/m^2
Response time	<< 1 s	Impedance	50 Ohm
Non-stability (change/year)	< 2 %	Level accuracy	-
Non-linearity (0 - 1000 W/m^2)	< 1 %	Operating temperature	-30 to +70 ºC
Directional error (at 80º with 1000W/m^2 beam)	< 10 W/m^2	Spectral range (50 % points)	400 to 1100 nm
Temperature dependence	- 0.15 % (-30 to +70 ºC)	Typical signal output	0 to 100 mV
Maximum irradiance	2000 W/m^2	Detector	Silicon photo-diode

A.4. Operating budget

Table A.16. *List of prices of the temperature and relative humidity sensors.*

Temperature / Humidity Sensors	
Climatronics P/N 102669	-
Climatronics P/N 101812 G2	-
Vaisala HMP155	1,137.00 €
Vaisala DTR503A (radiation shield)	312.00 €
Rotronix MP101A	-
Delta-T RHT2nl	882.00 €
Rainwise RH/T	695.50 €

Table A.17. *List of prices of the wind speed and direction sensors.*

Wind Speed and Direction Sensors	
Climatronics WM-III	-
Vaisala WA25	4,489.00 €
Vaisala WS425	2,889.00 €
Vaisala DTR503A (radiation shield)	312.00 €
Delta-T AN1-03 (anemometer)	910.00 €
Delta-T WD1-03 (wind direction)	1,032.00 €
Rainwise Aervane	1,906.00 €

Table A.18. *List of prices of the solar radiation sensors.*

Solar radiation Sensors		
Climatronics	Solar Radiation Sensor	-
Delta-T	BF3	1,586.00 €
	SPN1	4,022.00 €
Kipp & Zonen	SP Lite 2 Photodiode	381.84 €
	CMP6 - 25 m cable	1,406.37 €
	CMP11 - 25 m cable	2,066.82 €
	CMP21 - 25 m cable	2,638.47 €
	CMP21 - 10 m - Pt100	2,669.55 €
	CMP22 - 10 m cable	5,439.00 €
	CMP22 - 25 m cable	5,535.57 €
	CMP22 - 10 m - Pt100	5,566.65 €
	CM121C (Shadow Ring)	2,436.45 €
	CHP1 Pyrheliometer	2,608.50 €
	Solys 2 Sun Tracker	10,545.00 €

APPENDIX B: TUT SOLAR PV POWER STATION TEST PLANT

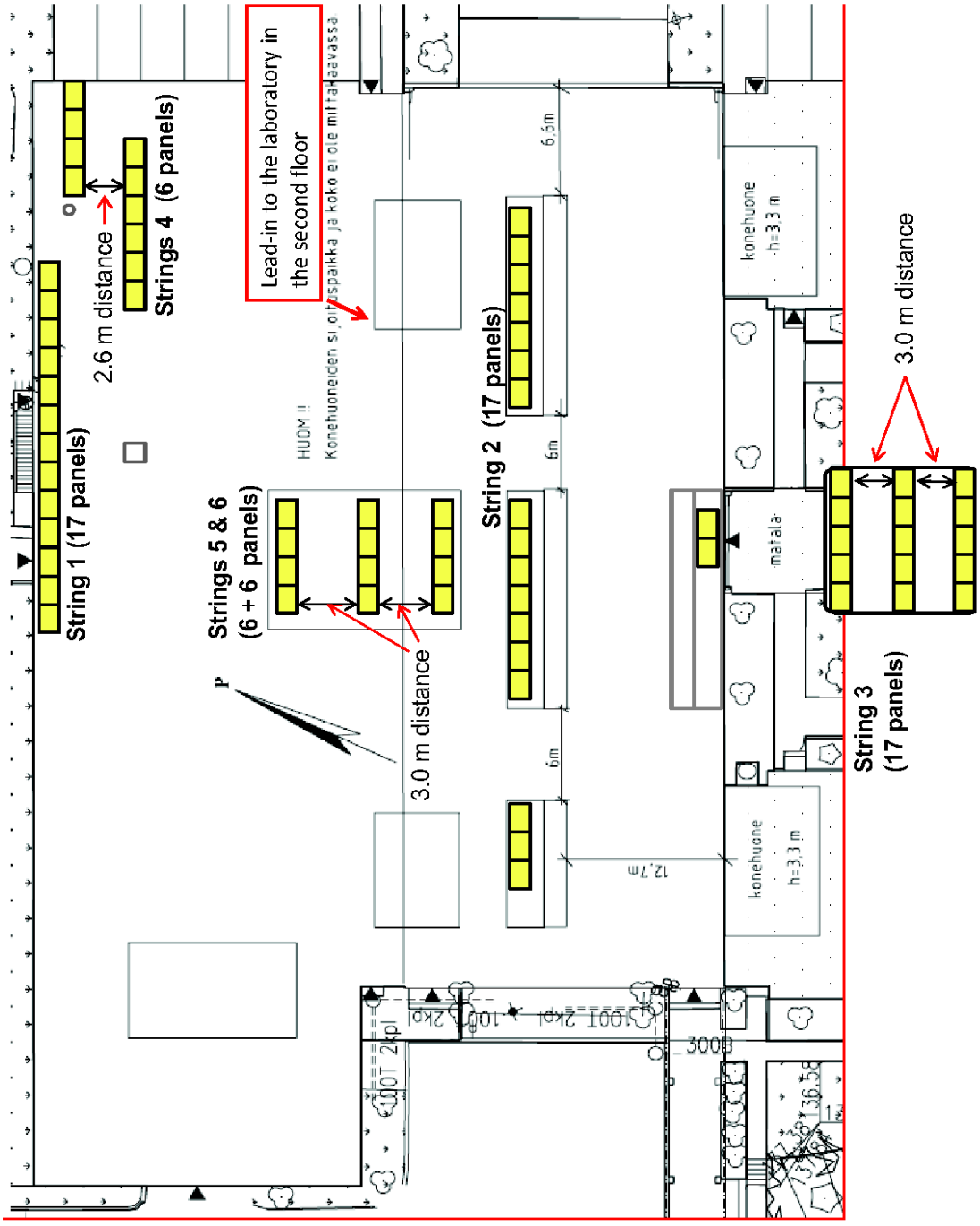

***Figure B.1**. TUT solar PV power station test plant layout.*

Technical Description

Photovoltaic Module NP190GKg
Product Code: 13189

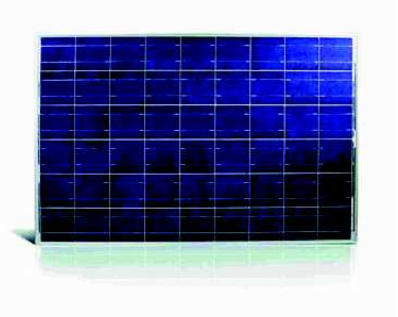

54 polycrystalline Si solar cells
Main application: grid PV systems

Module Electrical Performance under Standard Test Conditions
Refers to standard test conditions of 1000 Wm^{-2} solar irradiance, 25°C cell temperature, Air Mass 1.5.
Note: Maximum power point is subject to +5W/-0W variation. All other values are typical and for guidance only.
Maximum Power Point: 190 Watts, 7.33 Amps at 25.9 Volts.
Short Circuit: 8.02 Amps. Open circuit: 33.1 Volts.

Dimensions and Weight *all dimensions +/- 2mm, weight approximately +/-0.3kg*
Length: 1475mm. Width: 986mm. Thickness at edge: 35mm. Weight: 19.5kg

Construction
Top cover material: low iron tempered glass 4mm
Encapsulant (lamination material): EVA
3 factory-fitted bypass diodes
2 x 1m cables 4 sq mm
Rear cover material: PVDF-PET-PVDF
Frame: anodised aluminium
1 junction box type S1410-2

Integral mounting holes
4 holes, size 7mm.
Along length: 790mm centre to centre, 342.5mm centre to module edge.
Across width: 943mm centre to centre, 21.5mm centre to module edge.

Cell circuit
Cell dimensions: Length (tab direction) 156mm. Width: 156mm.
Electrical circuit: 54 cells in series
Cell layout: 6 rows, each row is 9 cells long.

Normal Operating Cell Temperature (NOCT)
46°C *error in measurement around +/- 2°C*
Cell temperature at 800Wm^{-2} solar irradiance, 20°C ambient temperature, wind speed <=1ms^{-1}, free air access to rear.

Efficiencies based on Standard Test Conditions Rating
Module: 13.1% Laminated area: 13.2% Cells alone: 14.5%
Note: Standard Test Conditions efficiency figures should only be used to compare one module with another. These efficiency figures do not apply to actual field perfomance, for which a careful analysis of operating conditions is necessary to determine the effects of module temperature and other factors.

Specifications may change due to Naps policy of continuous product improvement.
Please check current specification before purchasing.
Information last updated: 14-Sep-09

Naps Systems Oy, Pakkalankuja 7A, FIN-01510 Vantaa, Finland
Tel +358 20 7545 666, Fax +358 20 7545 660, www.napssystems.com

***Figure B.2**. PV module NP190GKg from Naps Systems technical description. [29]*

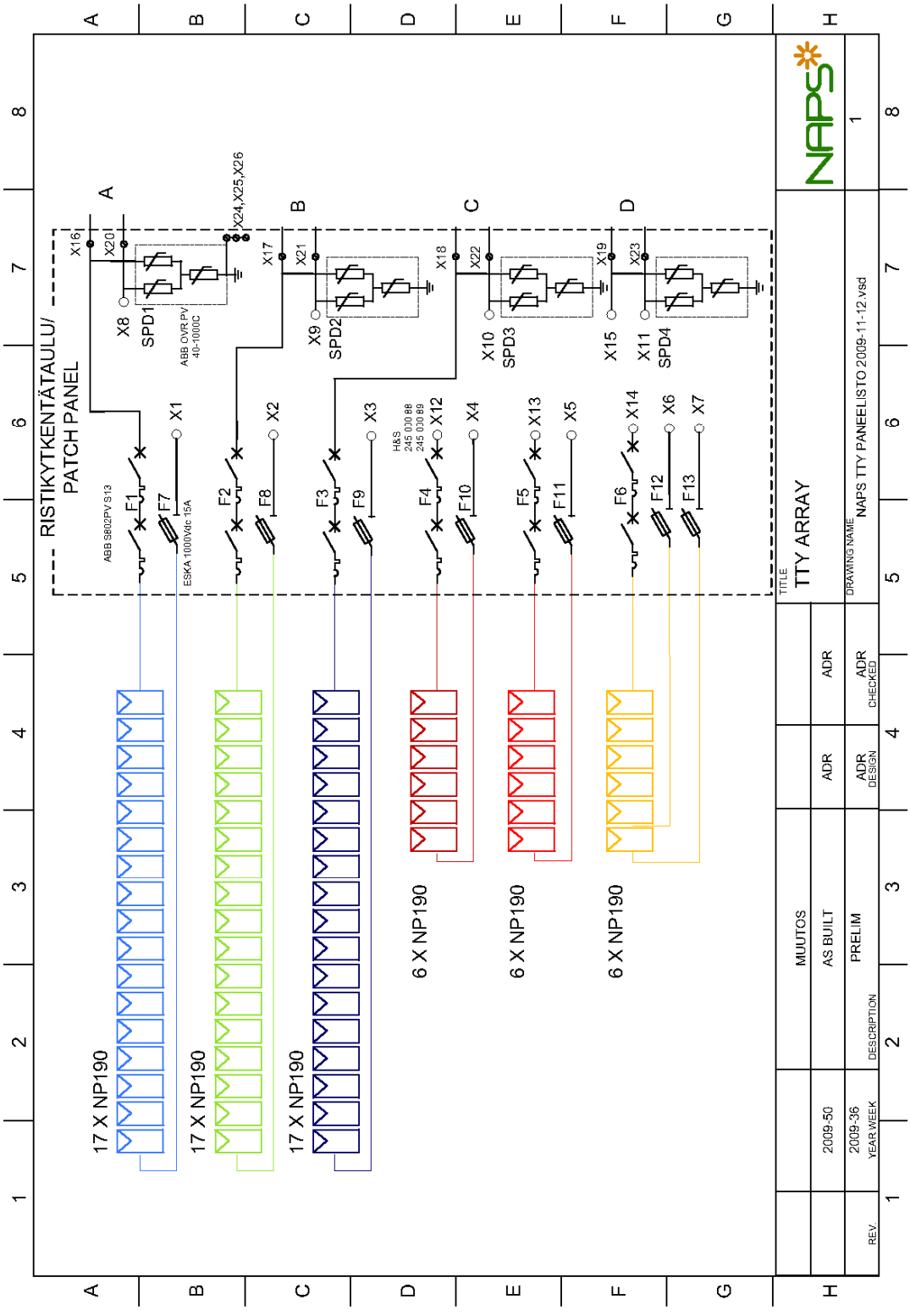

Figure B.3. *Photovoltaic strings electrical connection.*

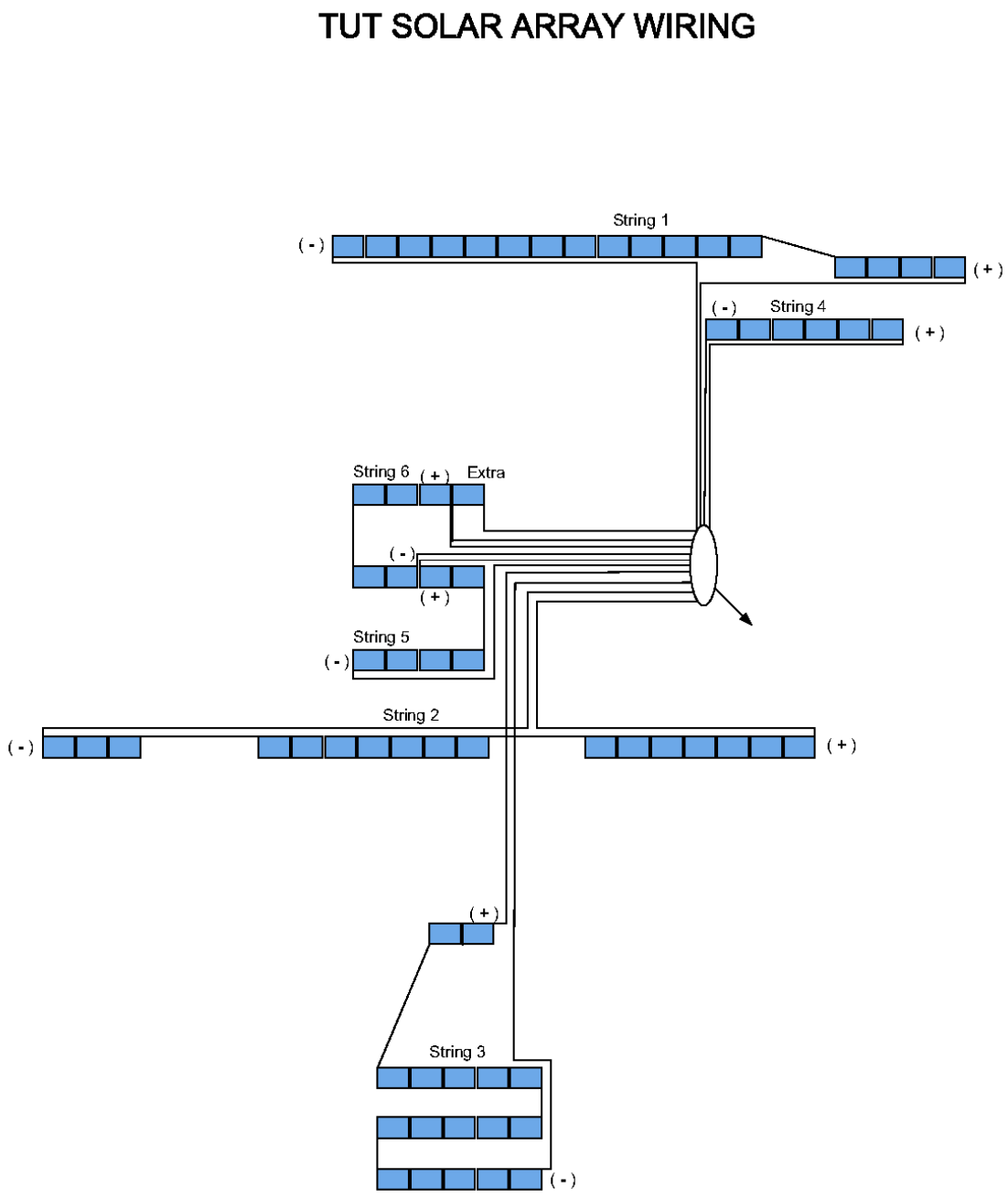

Figure B.4. *Photovoltaic strings connection scheme.*

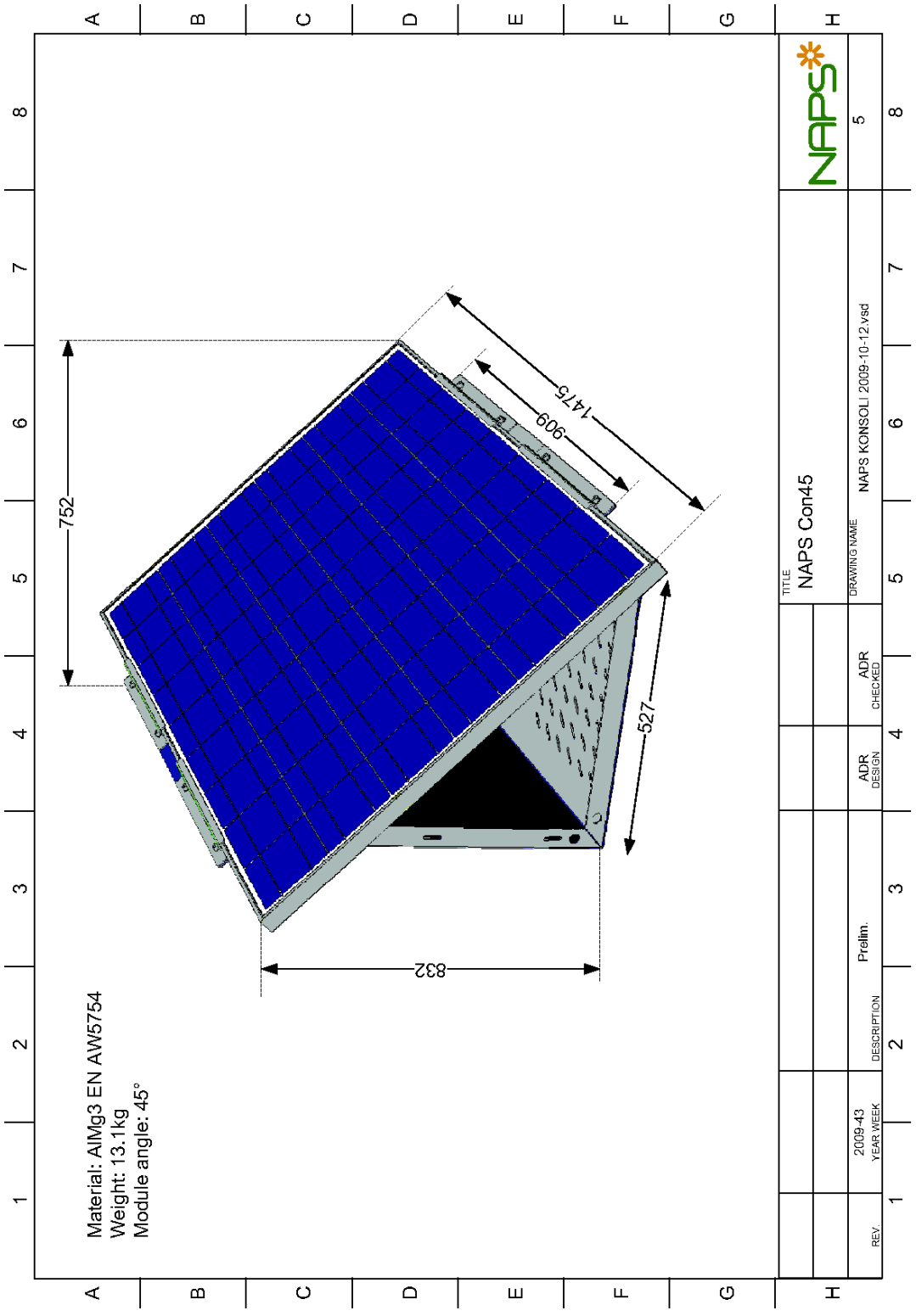

***Figure B.5**. Photovoltaic module position scheme.*

***Figure B.6**. TUT solar PV power station test plant I.*

Figure B.7*. TUT solar PV power station test plant II.*

Figure B.8. TUT solar PV power station test plant III.

APPENDIX C: ORDERING BILLS

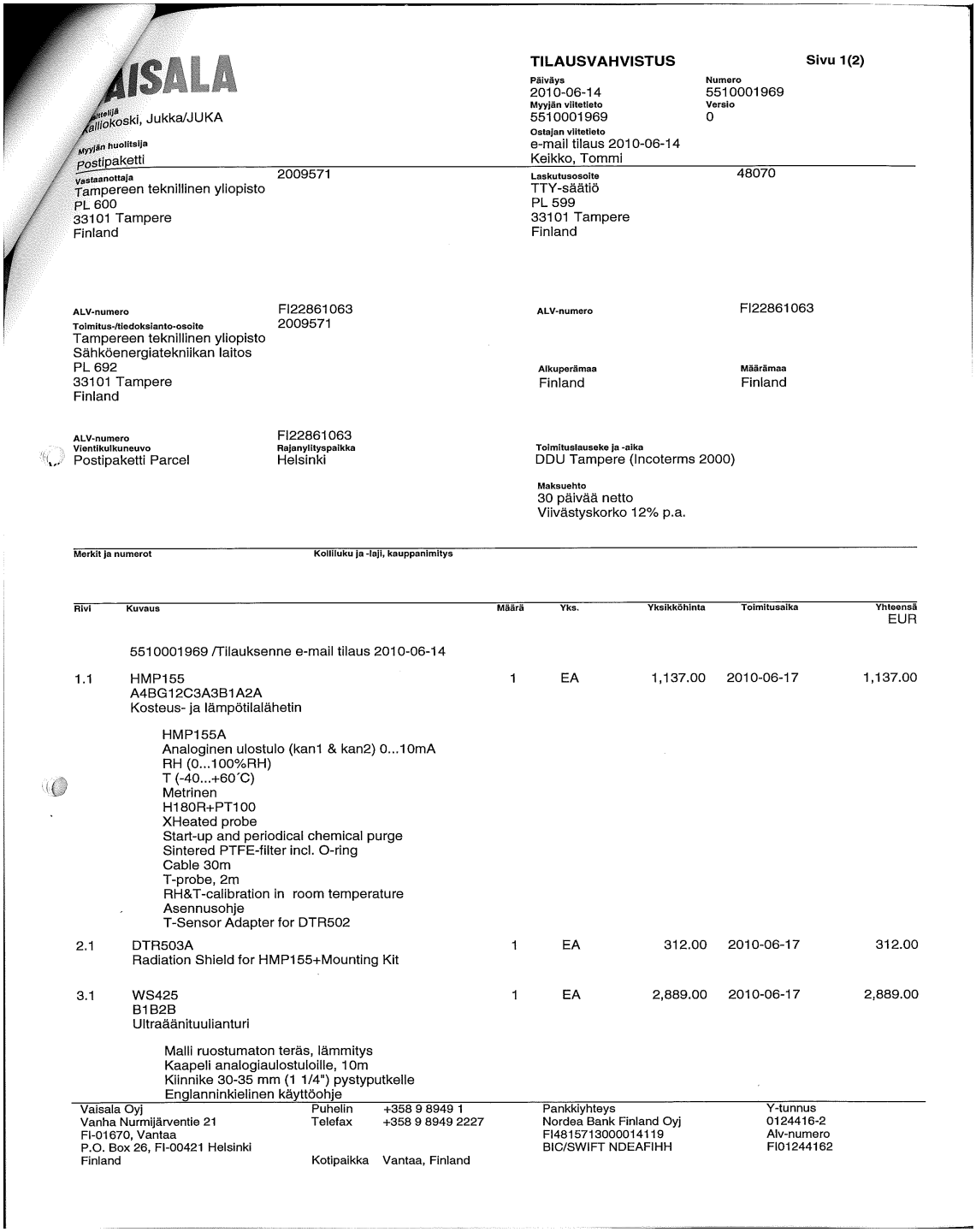

VAISALA

Käsittelijä
Kalliokoski, Jukka/JUKA

Myyjän huoltsija
Postipaketti

TILAUSVAHVISTUS **Sivu 1(2)**

Päiväys
2010-06-14
Myyjän viitetieto
5510001969
Ostajan viitetieto
e-mail tilaus 2010-06-14
Keikko, Tommi

Numero
5510001969
Versio
0

Vastaanottaja
Tampereen teknillinen yliopisto
PL 600
33101 Tampere
Finland
2009571

Laskutusosoite
TTY-säätiö
PL 599
33101 Tampere
Finland
48070

ALV-numero
FI22861063
Toimitus-/tiedoksianto-osoite
2009571
Tampereen teknillinen yliopisto
Sähköenergiatekniikan laitos
PL 692
33101 Tampere
Finland

ALV-numero
FI22861063

Alkuperämaa
Finland

Määrämaa
Finland

ALV-numero
FI22861063
Vientikulkuneuvo
Postipaketti Parcel
Rajanylityspaikka
Helsinki

Toimituslauseke ja -aika
DDU Tampere (Incoterms 2000)

Maksuehto
30 päivää netto
Viivästyskorko 12% p.a.

Merkit ja numerot
Kolliluku ja -laji, kauppanimitys

Rivi	Kuvaus	Määrä	Yks.	Yksikköhinta	Toimitusaika	Yhteensä EUR
	5510001969 /Tilauksenne e-mail tilaus 2010-06-14					
1.1	HMP155 A4BG12C3A3B1A2A Kosteus- ja lämpötilalähetin HMP155A Analoginen ulostulo (kan1 & kan2) 0...10mA RH (0...100%RH) T (-40...+60°C) Metrinen H180R+PT100 XHeated probe Start-up and periodical chemical purge Sintered PTFE-filter incl. O-ring Cable 30m T-probe, 2m RH&T-calibration in room temperature Asennusohje T-Sensor Adapter for DTR502	1	EA	1,137.00	2010-06-17	1,137.00
2.1	DTR503A Radiation Shield for HMP155+Mounting Kit	1	EA	312.00	2010-06-17	312.00
3.1	WS425 B1B2B Ultraäänituulianturi Malli ruostumaton teräs, lämmitys Kaapeli analogiaulostuloille, 10m Kiinnike 30-35 mm (1 1/4") pystyputkelle Englanninkielinen käyttöohje	1	EA	2,889.00	2010-06-17	2,889.00

Vaisala Oyj
Vanha Nurmijärventie 21
FI-01670, Vantaa
P.O. Box 26, FI-00421 Helsinki
Finland

Puhelin +358 9 8949 1
Telefax +358 9 8949 2227

Kotipaikka Vantaa, Finland

Pankkiyhteys
Nordea Bank Finland Oyj
FI4815713000014119
BIC/SWIFT NDEAFIHH

Y-tunnus
0124416-2
Alv-numero
FI01244162

***Figure C.1**. Ordering confirmation from Vaisala I.*

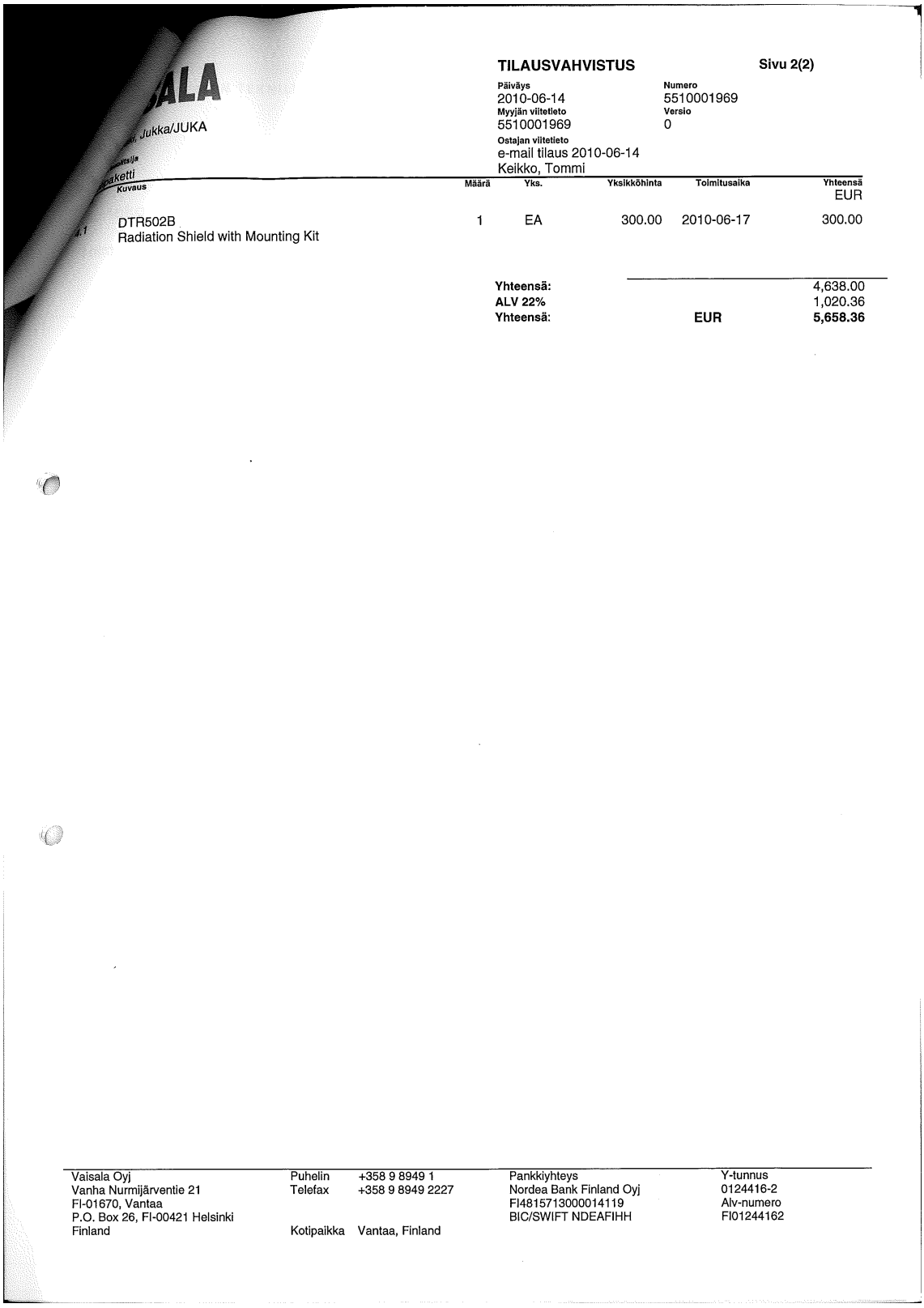

TILAUSVAHVISTUS Sivu 2(2)

Päiväys 2010-06-14
Numero 5510001969
Myyjän viitetieto 5510001969
Versio 0
Ostajan viitetieto e-mail tilaus 2010-06-14 Keikko, Tommi

Kuvaus	Määrä	Yks.	Yksikköhinta	Toimitusaika	Yhteensä EUR
DTR502B Radiation Shield with Mounting Kit	1	EA	300.00	2010-06-17	300.00

Yhteensä:		4,638.00
ALV 22%		1,020.36
Yhteensä:	**EUR**	**5,658.36**

Vaisala Oyj	Puhelin	+358 9 8949 1	Pankkiyhteys	Y-tunnus
Vanha Nurmijärventie 21	Telefax	+358 9 8949 2227	Nordea Bank Finland Oyj	0124416-2
FI-01670, Vantaa			FI4815713000014119	Alv-numero
P.O. Box 26, FI-00421 Helsinki			BIC/SWIFT NDEAFIHH	FI01244162
Finland	Kotipaikka	Vantaa, Finland		

***Figure C.2**. Ordering confirmation from Vaisala II.*

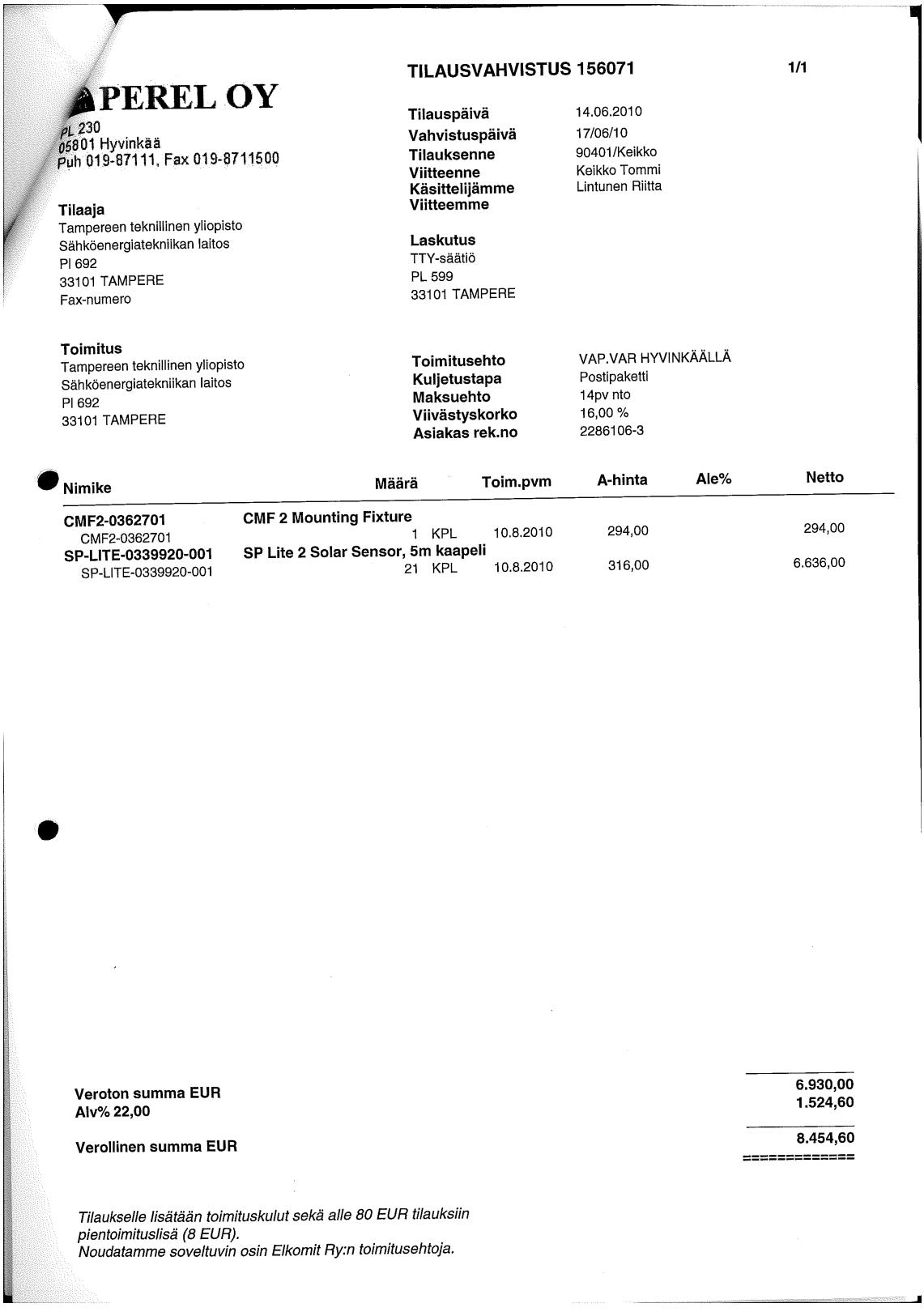

PEREL OY
PL 230
05801 Hyvinkää
Puh 019-87111, Fax 019-8711500

TILAUSVAHVISTUS 156071 1/1

Tilauspäivä	14.06.2010
Vahvistuspäivä	17/06/10
Tilauksenne	90401/Keikko
Viitteenne	Keikko Tommi
Käsittelijämme	Lintunen Riitta
Viitteemme	

Tilaaja
Tampereen teknillinen yliopisto
Sähköenergiatekniikan laitos
PI 692
33101 TAMPERE
Fax-numero

Laskutus
TTY-säätiö
PL 599
33101 TAMPERE

Toimitus
Tampereen teknillinen yliopisto
Sähköenergiatekniikan laitos
PI 692
33101 TAMPERE

Toimitusehto	VAP.VAR HYVINKÄÄLLÄ
Kuljetustapa	Postipaketti
Maksuehto	14pv nto
Viivästyskorko	16,00 %
Asiakas rek.no	2286106-3

Nimike	Määrä	Toim.pvm	A-hinta	Ale%	Netto
CMF2-0362701	**CMF 2 Mounting Fixture**				
CMF2-0362701	1 KPL	10.8.2010	294,00		294,00
SP-LITE-0339920-001	**SP Lite 2 Solar Sensor, 5m kaapeli**				
SP-LITE-0339920-001	21 KPL	10.8.2010	316,00		6.636,00

Veroton summa EUR	**6.930,00**
Alv% 22,00	**1.524,60**
Verollinen summa EUR	**8.454,60**

Tilaukselle lisätään toimituskulut sekä alle 80 EUR tilauksiin pientoimituslisä (8 EUR).
Noudatamme soveltuvin osin Elkomit Ry:n toimitusehtoja.

***Figure C.3**. Ordering confirmation from Perel Oy (Finnish Kipp&Zonen's provider) I.*

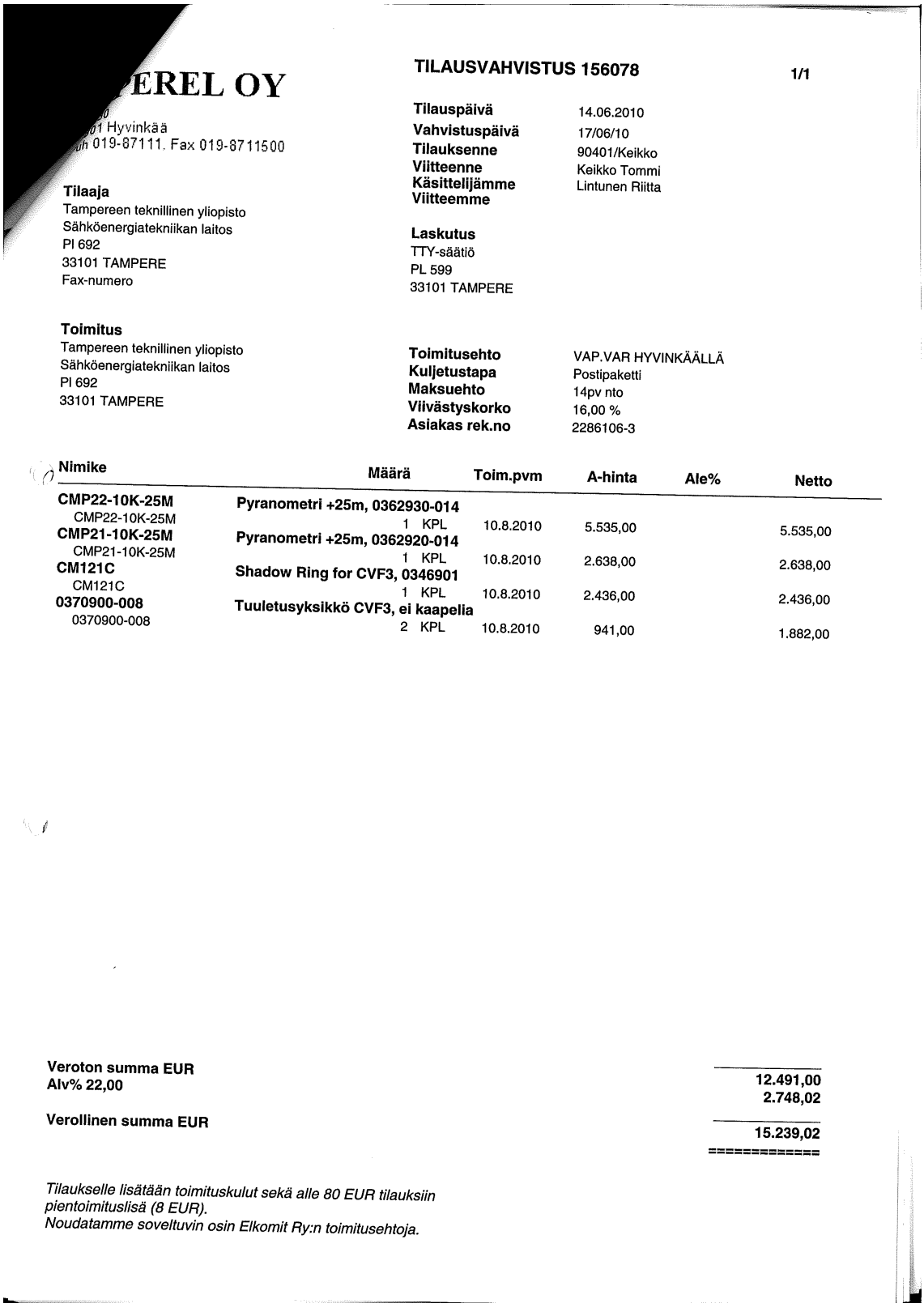

PEREL OY

01 Hyvinkää
puh 019-87111, Fax 019-8711500

TILAUSVAHVISTUS 156078 1/1

Tilauspäivä	14.06.2010
Vahvistuspäivä	17/06/10
Tilauksenne	90401/Keikko
Viitteenne	Keikko Tommi
Käsittelijämme	Lintunen Riitta
Viitteemme	

Tilaaja
Tampereen teknillinen yliopisto
Sähköenergiatekniikan laitos
PI 692
33101 TAMPERE
Fax-numero

Laskutus
TTY-säätiö
PL 599
33101 TAMPERE

Toimitus
Tampereen teknillinen yliopisto
Sähköenergiatekniikan laitos
PI 692
33101 TAMPERE

Toimitusehto	VAP.VAR HYVINKÄÄLLÄ
Kuljetustapa	Postipaketti
Maksuehto	14pv nto
Viivästyskorko	16,00 %
Asiakas rek.no	2286106-3

Nimike	Määrä	Toim.pvm	A-hinta	Ale%	Netto
CMP22-10K-25M	**Pyranometri +25m, 0362930-014**				
CMP22-10K-25M	1 KPL	10.8.2010	5.535,00		5.535,00
CMP21-10K-25M	**Pyranometri +25m, 0362920-014**				
CMP21-10K-25M	1 KPL	10.8.2010	2.638,00		2.638,00
CM121C	**Shadow Ring for CVF3, 0346901**				
CM121C	1 KPL	10.8.2010	2.436,00		2.436,00
0370900-008	**Tuuletusyksikkö CVF3, ei kaapelia**				
0370900-008	2 KPL	10.8.2010	941,00		1.882,00

Veroton summa EUR	**12.491,00**
Alv% 22,00	**2.748,02**
Verollinen summa EUR	**15.239,02**

Tilaukselle lisätään toimituskulut sekä alle 80 EUR tilauksiin pientoimituslisä (8 EUR).
Noudatamme soveltuvin osin Elkomit Ry:n toimitusehtoja.

***Figure C.4**. Ordering confirmation from Perel Oy (Finnish Kipp&Zonen's provider) II.*

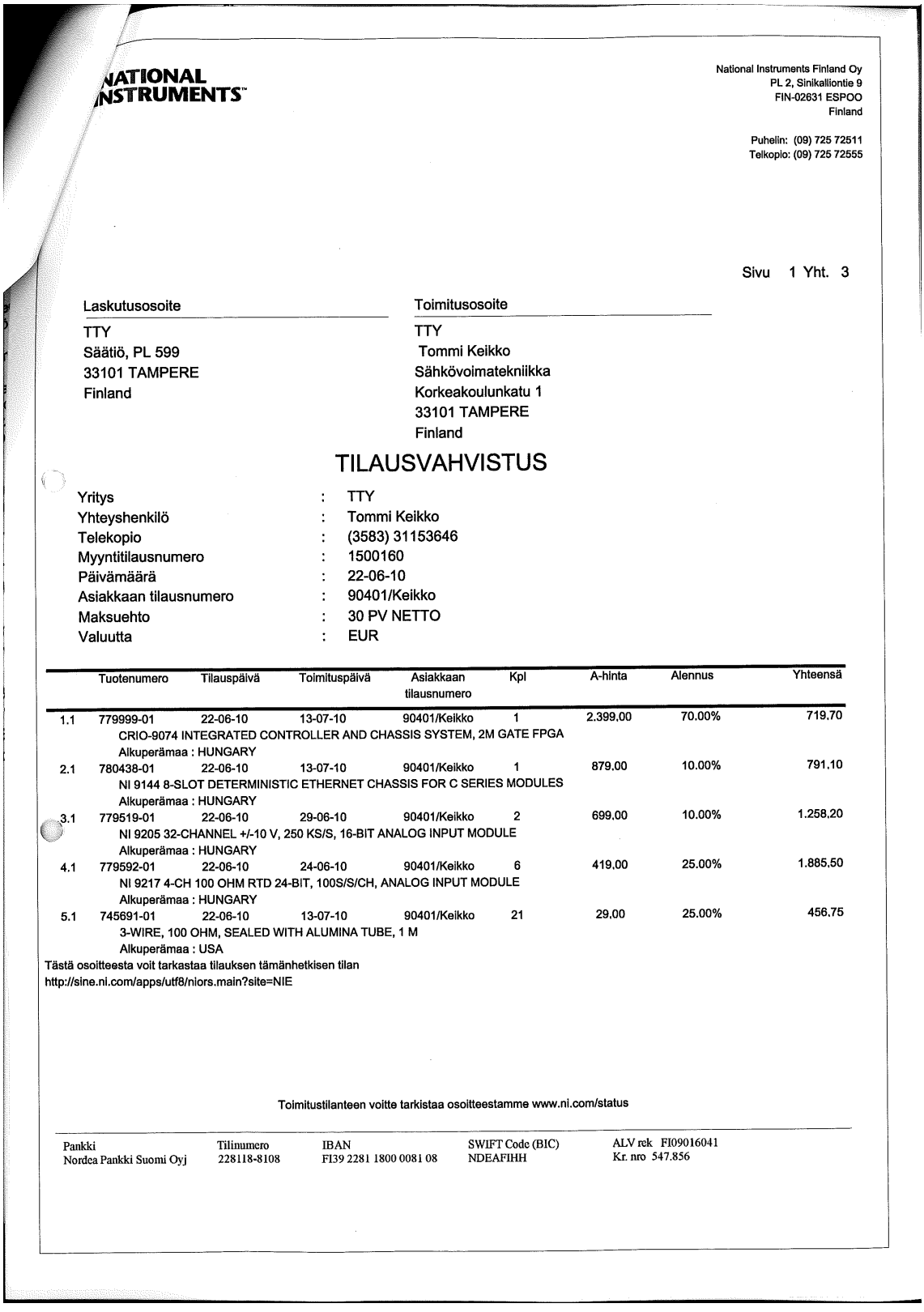

NATIONAL INSTRUMENTS™

National Instruments Finland Oy
PL 2, Sinikalliontie 9
FIN-02631 ESPOO
Finland

Puhelin: (09) 725 72511
Telkopio: (09) 725 72555

Sivu 1 Yht. 3

Laskutusosoite

TTY
Säätiö, PL 599
33101 TAMPERE
Finland

Toimitusosoite

TTY
Tommi Keikko
Sähkövoimatekniikka
Korkeakoulunkatu 1
33101 TAMPERE
Finland

TILAUSVAHVISTUS

Yritys	:	TTY
Yhteyshenkilö	:	Tommi Keikko
Telekopio	:	(3583) 31153646
Myyntitilausnumero	:	1500160
Päivämäärä	:	22-06-10
Asiakkaan tilausnumero	:	90401/Keikko
Maksuehto	:	30 PV NETTO
Valuutta	:	EUR

	Tuotenumero	Tilauspäivä	Toimituspäivä	Asiakkaan tilausnumero	Kpl	A-hinta	Alennus	Yhteensä
1.1	779999-01	22-06-10	13-07-10	90401/Keikko	1	2.399,00	70.00%	719,70
	CRIO-9074 INTEGRATED CONTROLLER AND CHASSIS SYSTEM, 2M GATE FPGA							
	Alkuperämaa : HUNGARY							
2.1	780438-01	22-06-10	13-07-10	90401/Keikko	1	879,00	10.00%	791,10
	NI 9144 8-SLOT DETERMINISTIC ETHERNET CHASSIS FOR C SERIES MODULES							
	Alkuperämaa : HUNGARY							
3.1	779519-01	22-06-10	29-06-10	90401/Keikko	2	699,00	10.00%	1.258,20
	NI 9205 32-CHANNEL +/-10 V, 250 KS/S, 16-BIT ANALOG INPUT MODULE							
	Alkuperämaa : HUNGARY							
4.1	779592-01	22-06-10	24-06-10	90401/Keikko	6	419,00	25.00%	1.885,50
	NI 9217 4-CH 100 OHM RTD 24-BIT, 100S/S/CH, ANALOG INPUT MODULE							
	Alkuperämaa : HUNGARY							
5.1	745691-01	22-06-10	13-07-10	90401/Keikko	21	29,00	25.00%	456,75
	3-WIRE, 100 OHM, SEALED WITH ALUMINA TUBE, 1 M							
	Alkuperämaa : USA							

Tästä osoitteesta voit tarkastaa tilauksen tämänhetkisen tilan
http://sine.ni.com/apps/utf8/niors.main?site=NIE

Toimitustilanteen voitte tarkistaa osoitteestamme www.ni.com/status

Pankki	Tilinumero	IBAN	SWIFT Code (BIC)	ALV rek FI09016041
Nordea Pankki Suomi Oyj	228118-8108	FI39 2281 1800 0081 08	NDEAFIHH	Kr. nro 547.856

***Figure C.5**. Ordering confirmation from National Instruments I.*

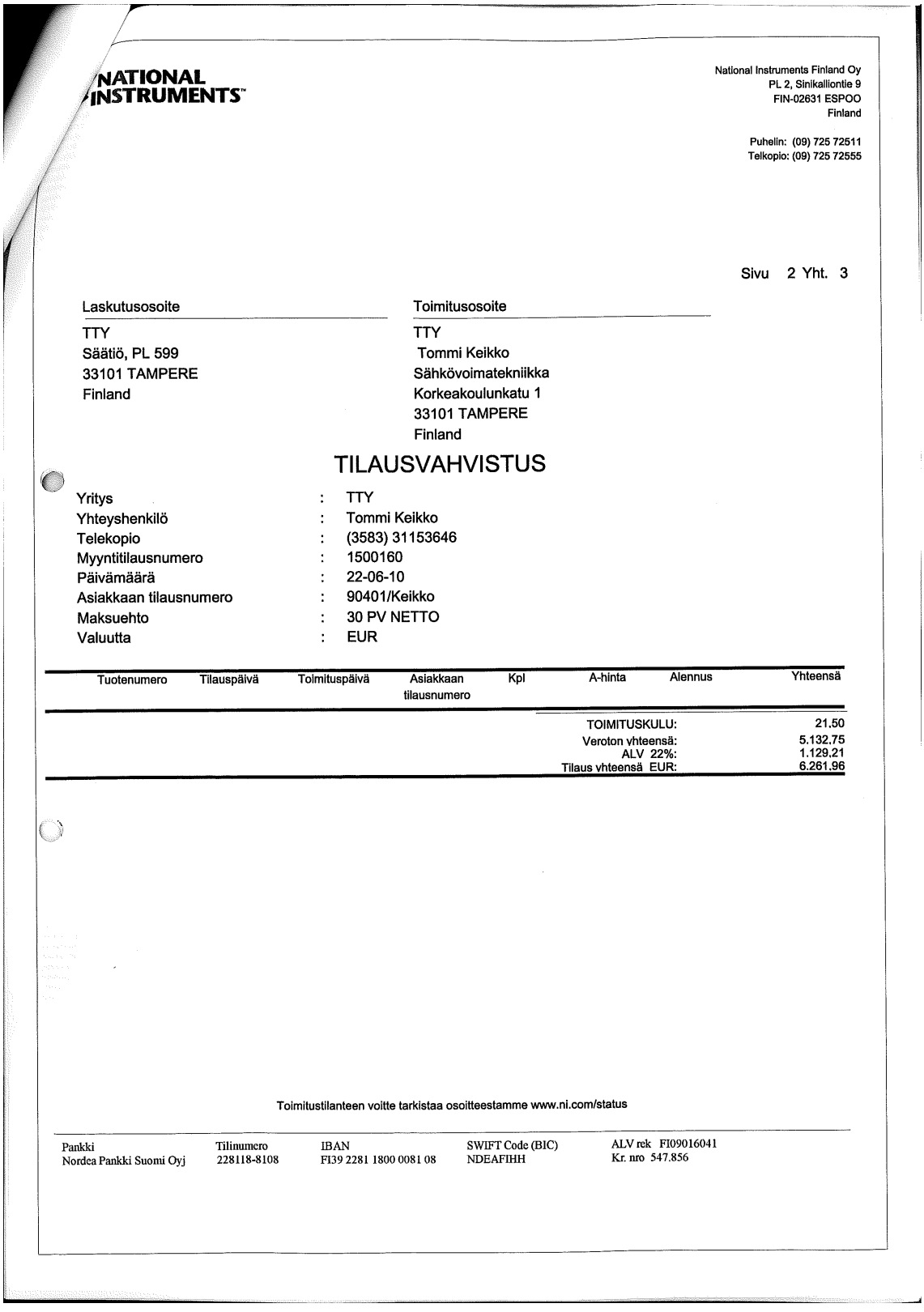

NATIONAL INSTRUMENTS™

National Instruments Finland Oy
PL 2, Sinikalliontie 9
FIN-02631 ESPOO
Finland

Puhelin: (09) 725 72511
Telkopio: (09) 725 72555

Sivu 2 Yht. 3

Laskutusosoite	Toimitusosoite
TTY	TTY
Säätiö, PL 599	Tommi Keikko
33101 TAMPERE	Sähkövoimatekniikka
Finland	Korkeakoulunkatu 1
	33101 TAMPERE
	Finland

TILAUSVAHVISTUS

Yritys	:	TTY
Yhteyshenkilö	:	Tommi Keikko
Telekopio	:	(3583) 31153646
Myyntitilausnumero	:	1500160
Päivämäärä	:	22-06-10
Asiakkaan tilausnumero	:	90401/Keikko
Maksuehto	:	30 PV NETTO
Valuutta	:	EUR

Tuotenumero	Tilauspäivä	Toimituspäivä	Asiakkaan tilausnumero	Kpl	A-hinta	Alennus	Yhteensä
					TOIMITUSKULU:		21.50
					Veroton yhteensä:		5.132,75
					ALV 22%:		1.129,21
					Tilaus yhteensä EUR:		6.261,96

Toimitustilanteen voitte tarkistaa osoitteestamme www.ni.com/status

Pankki	Tilinumero	IBAN	SWIFT Code (BIC)	ALV rek FI09016041
Nordea Pankki Suomi Oyj	228118-8108	FI39 2281 1800 0081 08	NDEAFIHH	Kr. nro 547.856

***Figure C.6**. Ordering confirmation from National Instruments II.*